

Mechanistic Investigation of Chlorinated Ethylene Degradation using Chlorine and Carbon Isotope Fractionation

Dissertation

der Mathematisch-Naturwissenschaftlichen Fakultät
der Eberhard Karls Universität Tübingen
zur Erlangung des Grades eines
Doktors der Naturwissenschaften
(Dr. rer. nat.)

Vorgelegt von
Stefan Anton Cretnik
aus München

Tübingen
2013

Tag der mündlichen Qualifikation:

11.11.2013

Dekan:

Prof. Dr. Wolfgang Rosenstiel

1. Berichterstatter:

Dr. Martin Elsner

2. Berichterstatter:

Prof. Dr. Stefan Haderlein

Table of Contents

1	GENERAL INTRODUCTION.....	1
1.1	IMPORTANCE OF CHLOROETHENES AND DECHLORINATION REACTIONS	1
1.2	ASSESSMENT OF DECHLORINATION REACTIONS AND COMPOUND SPECIFIC ISOTOPE ANALYSIS (CSIA)	2
1.2.1	<i>Studies of reductive dehalogenation: State of the art.....</i>	2
1.2.2	<i>Concept and application of CSIA.....</i>	3
1.2.3	<i>Masking effects and the need for dual isotope plots.....</i>	5
1.2.4	<i>Recent developments in compound-specific chlorine isotope analysis of chloroethenes.....</i>	5
1.3	CHALLENGES TO ASSESS REACTIONS OF CHLOROETHENES IN REDUCTIVE DECHLORINATION	6
1.4	REFERENCES.....	8
2	CHLORINE ISOTOPE EFFECTS FROM ISOTOPE RATIO MASS SPECTROMETRY SUGGEST INTRAMOLECULAR C-CL BOND COMPETITION IN TRICHLOROETHENE (TCE) REDUCTIVE DEHALOGENATION.....	11
2.1	ABSTRACT	12
2.2	INTRODUCTION	13
2.3	EXPERIMENTAL SECTION	17
2.4	MATHEMATICAL APPROACH (I): COMPOUND AVERAGE ISOTOPE EFFECTS	17
2.4.1	<i>Fitting Substrate and Product Isotope Ratios: Compound-Average Isotope Effects.....</i>	17
2.4.2	<i>Compound-Average Isotope Effects from Reactant Values.....</i>	18
2.4.3	<i>Expressions for Product Isotope Values.....</i>	19
2.4.4	<i>Carbon Isotope Effects from Product Values.....</i>	20
2.4.5	<i>Chlorine Isotope Effects from Product Values.....</i>	20
2.5	MATHEMATICAL APPROACH (II): PRIMARY AND SECONDARY ISOTOPE EFFECTS	20
2.5.1	<i>Case 1—PCE: Indistinguishable Molecular Positions.....</i>	20
2.5.2	<i>Case 2—TCE: Distinguishable Molecular Positions.....</i>	22
2.5.3	<i>Interpretation of the Product Curve Enrichment Trends $\epsilon_{TCE \rightarrow \text{chloride}}$ and $\epsilon_{TCE \rightarrow \text{cis-DCE}}$ for TCE</i>	24
2.5.4	<i>Contributions from α-Positions to $\epsilon_{TCE \rightarrow \text{chloride}}$ and $\epsilon_{TCE \rightarrow \text{cis-DCE}}$.....</i>	25
2.5.5	<i>Interpretation of Intercepts K for the TCE Case.....</i>	26
2.6	RESULTS AND DISCUSSION	27
2.6.1	<i>Compound-Specific Carbon Isotope Effects in Reductive Dehalogenation of PCE to TCE by Desulfitobacterium sp. Strain Viet1 and of TCE to cis-DCE by Geobacter Lovleyi Strain SZ.....</i>	27
2.6.2	<i>Compound-Specific and Position-Specific Chlorine Isotope Effects in Reductive Dehalogenation of PCE to TCE by Desulfitobacterium sp. Strain Viet1</i>	28
2.6.3	<i>Compound-Specific and Position-Specific Chlorine Isotope Effects in Reductive Dehalogenation of TCE to cis-DCE by Geobacter lovleyi Strain SZ.....</i>	31
2.7	CONCLUSIONS	36
2.8	ACKNOWLEDGEMENTS.....	38
2.9	REFERENCES	39

3	REDUCTIVE DECHLORINATION OF TCE BY CHEMICAL MODEL SYSTEMS IN COMPARISON TO DEHALOGENATING BACTERIA: INSIGHTS FROM DUAL ELEMENT ISOTOPE ANALYSIS.....	43
3.1	ABSTRACT	44
3.2	INTRODUCTION	45
3.3	MATERIALS AND METHODS	47
3.4	RESULTS AND DISCUSSION	53
3.5	ENVIRONMENTAL SIGNIFICANCE	58
3.6	ACKNOWLEDGMENTS	58
3.7	REFERENCES	59
4	CL AND C ISOTOPE ANALYSIS TO ASSESS THE EFFECTIVENESS OF CHLOROETHENE DEGRADATION BY ZERO-VALENT IRON: EVIDENCE FROM DUAL ELEMENT AND PRODUCT ISOTOPE VALUES.....	65
4.1	ABSTRACT	66
4.2	INTRODUCTION	67
4.3	MATERIALS AND METHODS	70
4.4	CONCENTRATION AND ISOTOPE ANALYSIS.....	72
4.5	EVALUATION OF C AND CL ISOTOPE FRACTIONATION	74
4.6	RESULTS AND DISCUSSION	76
4.7	RAYLEIGH FITS OF ISOTOPE FRACTIONATION.....	77
4.8	DUAL ISOTOPE APPROACH	81
4.9	PRODUCT RELATED ISOTOPE FRACTIONATION.....	82
4.10	CONCLUSIONS	83
4.11	ACKNOWLEDGEMENTS.....	84
4.12	REFERENCES	85
5	GENERAL CONCLUSIONS	89
	APPENDIX A1: COMPOUND-SPECIFIC CHLORINE ISOTOPE ANALYSIS: A COMPARISON OF GC-IRMS AND GC-QMS METHODS IN AN INTERLABORATORY STUDY	I
	APPENDIX A2: SUPPORTING INFORMATION OF CHAPTER 2	XIII
	A2.1 MATERIALS AND METHODS	XIV
	A2.2 EQUATIONS	XVII
	A2.3 VISUALISATION OF FIGURE 4 WITH DIFFERENT CONTRIBUTIONS OF PRIMARY AND SECONDARY ISOTOPE EFFECTS	XXI
	APPENDIX A3: SUPPORTING INFORMATION OF CHAPTER 3	XIV
	APPENDIX A4: SUPPORTING INFORMATION OF CHAPTER 4	XVIII

Dank

Allen voran möchte ich meinem Doktorvater Dr. Martin Elsner für die spannende und hochaktuelle Themenstellung danken. Sein Engagement und Optimismus trugen wesentlich zum Gelingen der Arbeit bei. Die Laborausstattung und das von ihm geschaffene Forschungsumfeld ließen keine Wünsche offen.

Bei Herrn Prof. Dr. Stefan Haderlein möchte ich mich herzlich für die Zweitbetreuung und das Interesse an der vorliegenden Arbeit bedanken. Ihm und seiner Gruppe Dr. Christine Laskow, Karin Ebert und Daniel Buchner danke ich für deren Beitrag bei den Bioabbau-Experimenten.

I am very grateful to Prof. Dr. Kristopher McNeill for his creative ideas and helpful advice in my thesis committee. Very special thanks to him and Dr. Sarah Kliegman for the warm welcome in Zürich and our inspiring collaboration.

A big thank you goes to Dr. Kristen Thoreson for the practical support with the model reactions and the good times in the synthesis-lab.

Sincere thanks to Dr. Anat Bernstein for her kind introduction into isotope analysis and the cultivation of anaerobic microorganisms.

Mein besonderer Dank gilt Prof. Dr. Frank Löffler für den freundlichen Kontakt und die Bereitstellung von mikrobiologischen Kulturen.

Ein herzliches Dankeschön geht an unsere Techniker Harald Lowag, Martina Höche, Günther Hinreiner für diverse Spezialanfertigungen und die umfassende Unterstützung im Isotopenlabor.

Vielen Dank an meine Laborkollegen und Freunde Shiran, Michael, Emmanuel, Riad, Kathrin, Heide, Juliane - für die nötige Portion Humor bei aller Ernsthaftigkeit.

Aus tiefstem Herzen möchte ich meinen Eltern Angelika und Martin und meinen Geschwistern Anja und Philipp für euren unerschöpflichen Rückhalt danken. Carolin danke ich für ihre Liebe und ihre Unterstützung in Studium, Doktorarbeit und darüber hinaus.

Zusammenfassung

Chlorierte Ethene sind großtechnische chemische Produkte und werden häufig als Grundwasserschadstoffe erfasst. Deren Abbau durch reduktive Dechlorierung wird in Sanierungsmaßnahmen genutzt, und wurde in zahlreichen Studien mit biotischen und abiotischen Modellsystemen untersucht. Trotz allem sind die Prozesse zur Bildung von teils toxischen und teils harmlosen Produkten nur unvollständig verstanden, was sich in Widersprüchen zwischen den erhobenen mechanistischen Hypothesen äußert. Der nötige Zugang zu elementaren Schritten dieser Reaktionen wurde in dieser Arbeit durch eine neu entwickelte Methode zur substanzspezifischen Messung von stabilen Chlor Isotopen erreicht.

Zunächst wurden Bioabbau-Experimente mit dieser Messmethode untersucht um die grundlegende Fragestellung zu beantworten, wie sich Chlor-Isotopeneffekte in den Produkten einer Abbaureaktion äußern. Daraus konnte ein mathematischer Ansatz entwickelt werden der erste Einblicke in positions-spezifische Chlor-Isotopeneffekte gewährt. Aus deren Interpretation konnte die Regioselektivität im Bioabbau von Trichlorethene (TCE) an zwei Chlorsubstituenten abgeleitet werden. Dieses Ergebnis ist systematisch im Abgleich mit den mechanistischen Hypothesen diskutiert.

Mit dem Ansatz einer kombinierten Analytik von Isotopen-Effekten Chlor und Kohlenstoff wurde eine mechanistische Gegenüberstellung von Bioabbau-Experimenten zu deren chemischen Modellsystemen durchgeführt. Die Ergebnisse der Studie weisen darauf hin, dass der gleiche Abbaumechanismus bei zwei unterschiedlichen Mikroorganismen und bei dem isolierten Dehalogenase-Kofaktor Cobalamin (Vitamin B12) stattfindet. Im Gegensatz dazu wurde ein unterschiedlicher Mechanismus bei dem Modell-Reaktant Cobaloxime ermittelt. Aus dieser Studie lässt sich das vielseitige Potential der dualen Isotopenanalytik erschließen um chemische Modellreaktionen und deren natürliche Vorbildreaktionen auf mechanistischer Ebene abzugleichen.

Darüber hinaus wurde die duale Isotopenanalytik in Bezug auf deren Anwendung für permeable reaktiven Barrieren (PRB) untersucht, welche als Sanierungsmaßnahme für kontaminierte Standorte weit verbreitet sind. Ein dafür typisches nullvalentes Eisen-Material (Zero Valent Iron, ZVI) wurde im Laborversuch für den Schadstoffabbau verwendet. Hierbei wurden einerseits mit der dualen Isotopenanalytik und andererseits mit produktbezogener Isotopenanalytik von Kohlenstoff zwei eigenständige Ansätze verfolgt, um die Effektivität der PRB-Anwendungen einzuschätzen.

Die vorliegende Arbeit ergründet das beachtliche Potential der Isotopenanalytik von Chlor und Kohlenstoff zur Identifizierung eines nachhaltigen Schadstoffabbaus und deren Abbauege in der Umwelt. Darüber hinaus wurde die Perspektive für deren zukünftige Anwendung an Modell-Reaktionen eröffnet, um umweltrelevante Reaktionsmechanismen auf einer fundierten wissenschaftlichen Ebene zu untersuchen.

Summary

Chloroethenes are large-scale industrial products, and detected as toxic contaminants in the environment. Their reductive dechlorination is a clear remediation approach, which has been the focus of several studies, using biotic and abiotic model systems. Despite the progress toward understanding the underlying process the formation of toxic and harmless products remains incompletely understood, and some of the proposed mechanistic hypotheses have led to inconsistencies. A recently developed analytical method of continuous flow compound specific chlorine isotope analysis was used in this study to further uncover the underlying mechanisms of reductive dechlorination.

In the first instance, the newly created chlorine isotope data was analyzed towards the basic question how isotope effects of chlorine are manifested in the respective products during biodegradation. The developed mathematical framework gave first insights into position specific chlorine isotope effects during biodegradation of chloroethenes. From their interpretation, the structural selectivity in the biotic reductive dechlorination of TCE could be allocated to two chlorine substituents. This information allowed a systematic discussion with respect to the hypothesized mechanisms.

Further degradation experiments with two different microbial strains were investigated by combined analysis of carbon and chlorine isotope effects in dual isotope plots in comparison to model reactions that are commonly used to mimic microbial dechlorination. Similar mechanisms were indicated for biodegradation and reactions with cobalamin (Vitamin B12), the enzymatic cofactor of dehalogenase enzymes. In contrast a different mechanism was indicated for reactions with cobaloxime, a commonly used mimicking reagent for cobalamin. The results demonstrate the strength of dual isotope plots as an indicator of the authenticity of a model reaction for the actual system with respect to the underlying mechanisms.

The method of two dimensional isotope analysis was further investigated for its application towards the environmental clean-up technology of permeable reactive barriers (PRB) with zero-valent iron (ZVI). Dual isotope plots and product related carbon isotope fractionation were explored here as two discrete approaches to distinguish the effectiveness of transformation by ZVI as opposed to natural biodegradation.

The results of this work exemplify the potential of chlorine and carbon isotope analysis to assess the sustainable removal of contaminants and their degradation pathways directly in real-world transformations. Moreover, it opens the perspective for future work to pinpoint mechanisms of the important environmental dehalogenation reactions by applying the approach on further model reactions with distinct mechanisms.

1

GENERAL INTRODUCTION

1.1 Importance of chloroethenes and dechlorination reactions

The supply of drinking water is considered as a major challenge for upcoming generations. Rising prosperity and population lead to an increasing demand for clean water, but at the same time its availability runs short due to dissipative handling and discharge of contaminants.¹ A major type of such environmental pollutants are chlorinated hydrocarbons. They are commonly used in industrial applications, for instance as solvents, refrigerants, softeners for plastics and dry cleaning agents for electronic parts, engines and clothes. Most prominent representatives of this compound class are chloroethenes, which have been produced at million ton scales over decades since the 1950's.^{2,3} Initially they were considered as inert, and therefore unproblematic. This misconception led to improper handling and industrial disposal, leaving a legacy of thousands of hazardous waste sites today. Of the recorded sites by the U.S. Environmental Protection Agency's National Priority List alone, 771 of them contain tetrachloroethene (PCE), 861 trichloroethene (TCE) and 563 dichloroethene (DCE).^{4,5}

Their acute toxicity is generally conferred through the chlorine-substituents, which make them reactive to metabolic bioactivation and mutagenic modes of action.⁶ Therefore complete dechlorination to hydrocarbons is a clear approach of detoxification to give benign products. Intriguingly, this process was observed in the biogeochemical response from groundwater ecosystems. Contaminant-degrading microorganisms have been identified that derive energy by stepwise reductive dechlorination. This process has literally been designated as "dehalorespiration", since the bacteria use the chlorinated solvent as electron acceptor.⁷ Such biological dehalogenation commonly occurs by sequential replacement of chlorine by hydrogen (hydrogenolysis), as illustrated in Figure 1. Only few of these organisms are capable of complete transformation to non-toxic end products at appreciable rates, so that

biodegradation often stalls at the stage of DCE and vinyl chloride (VC).⁸ Rather than leading to effective decontamination, such accumulation of problematic intermediates often causes more severe pollution.

This problem has been addressed in a number of remediation technologies. Enhanced biodegradation may either occur through biostimulation (= addition of organic substrate to stimulate intrinsic dehalogenation activity) or through bioaugmentation (= inoculation of dehalogenating bacteria).⁹ An abiotic alternative is to catalyze reactions with zero valent iron (ZVI), which is applied by injecting nanoparticles or the installation of permeable reactive barriers.¹⁰ Reactions with ZVI additionally involve vicinal dichloroelimination, where two chlorine substituents are removed in one step, which offers a more direct pathway to non-problematic end products.¹¹ However, the accumulation of toxic intermediates and incomplete removal of contaminants can also be observed with these engineered approaches of remediation. Therefore there is great interest in the mechanisms leading to this diverse product formation. Furthermore, advanced techniques to assess these processes in the environment are desired.

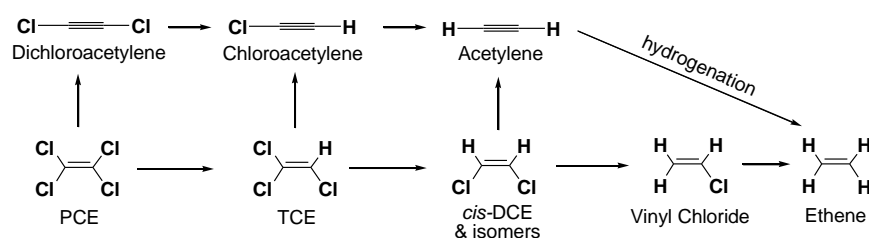


Figure 1: Reductive dechlorination of chloroethenes by stepwise hydrogenolysis (horizontal arrows), and by vicinal dichloroelimination (vertical arrows).

1.2 Assessment of dechlorination reactions and compound specific isotope analysis (CSIA)

1.2.1 Studies of reductive dehalogenation: State of the art

In order to explore the potential of the applied remediation strategies and to steer them towards more sustainable elimination of contaminants, great interest is directed at the underlying chemistry of the desired degradation reactions. An understanding of basic aspects of reductive dehalogenation in nature was approached in several studies using enrichment cultures, pure microorganisms, purified dehalogenase enzymes and chemical model systems mimicking selected types of dehalogenation mechanisms.¹² An essential role in

biodegradation was attributed to cobalamin, commonly known as vitamin B12, which serves as a cofactor for almost all known dehalogenase enzymes.

Nonetheless, reaction mechanisms and product formation via concurring transformation pathways remain incompletely understood. For instance, while a chlorovinyl-cobalamine intermediate has been proposed for reactions mediated by purified dehalogenase,¹³ there are indications that a single electron transfer occurs from cobalamin to form radical intermediates.^{12, 14} This example points out the current knowledge gap regarding the chemical mechanisms of dechlorination and the need for a diagnostic tool to compare the reactions on a mechanistic level.

1.2.2 Concept and application of CSIA

The desired link towards mechanistic information of a chemical reaction can be approached by measurements of kinetic isotope effects (KIEs). The KIE derives from the unequal reaction behavior of isotopologues. Primary isotope effects refer to the different reaction kinetics of heavy isotopes (e.g. ^{13}C) compared to light isotopes (e.g. ^{12}C) in reacting chemical bonds. The mass difference of the nuclides affects the vibrational energies and leads to different zero point energies between isotopologues, and therefore to different activation energies to reach a certain transition state. In a similar way, secondary isotope effects arise when an isotopic substitution occurs in a position adjacent to the reacting bond. Although the adjacent atoms do not directly participate in the chemical reaction, their mass still have an impact on the vibrational energies and thereby again on the zero point energy. With these attributes, the measurement of KIEs is one of the only handles to directly reflect properties of a transition state, and is therefore used to pinpoint transformation mechanisms.

In this context, either isotope labelling of reactants or analysis of non-labelled compounds with NMR techniques are routinely applied for *in vitro* reactions with suitable conditions to reveal the isotope-sensitive information. For chlorinated ethenes, however, these traditional approaches have remained elusive particularly in biotic systems or environmental samples. On the one hand, this is because of the difficulty of synthesizing labeled molecules, and on the other hand because of the interference of NMR signals in complex reaction mixtures and the large amounts of the target compound needed in a sample for NMR analysis.

An analytical solution was brought forward with gas chromatography-isotope ratio mass spectrometry (GC-IRMS), which is recognized as a powerful tool to decipher transformation pathways at contaminated sites and low concentrations of contaminants. Degradation

processes are typically associated with a normal KIE, which means that light isotopes (e.g., ^{12}C) react slightly faster with ^lk than heavy isotopes (e.g., ^{13}C) with ^hk , when present in the reacting chemical bonds.

$$\left(\frac{^l\text{k}}{^h\text{k}}\right) = \text{KIE} \quad (1)$$

As a consequence the remaining reactant becomes enriched with heavy isotopes and the KIE can be observed by measurements of isotopic changes of the reactant during the progress of reaction. When the isotope ratios are measured with gas chromatography-isotope ratio mass spectrometry (GC-IRMS) they are generally obtained as average over all positions in the target molecules, so that the kinetic isotope effect is obtained as a compound average, $\text{KIE}_{\text{compound-average}}$, which is in direct relationship to the fractionation factor α or the enrichment factor ε .

$$\left(1 / \text{KIE}_{\text{compound-average}}\right) - 1 = \alpha - 1 = \varepsilon \quad (2)$$

The isotope ratios of the heavy (^hE) and light (^lE) element in a compound are typically referred to international standard materials, for instance to Vienna Pee Dee Belemnite (VPDB) for carbon or to Standard Mean Ocean Chloride (SMOC) for chlorine. This treatment has the advantage that measurements from different laboratories become comparable on an absolute scale. The isotope values are therefore typically expressed with respect to the international reference material by the delta notation:

$$\delta^h E = \left(\frac{R_{\text{Compound-Average}} - R_{\text{Standard}}}{R_{\text{Standard}}}\right) = \left(\frac{R_{\text{Compound-Average}}}{R_{\text{Standard}}}\right) - 1 \quad (3)$$

$$\text{with } R_{\text{Standard}} = \left(\frac{^h E}{^l E}\right)_{\text{Standard}} \quad \text{and} \quad R_{\text{Compound-Average}} = \left(\frac{^h E}{^l E}\right)_{\text{Compound-Average}} \quad (4)$$

The relationship of an isotope ratio after a certain progress of reaction $\delta^h E$ towards the isotope ratio of the starting material $\delta^h E_0$ is well-established to depend on the remaining fraction f of the starting material and the kinetic isotope effect according to the Rayleigh equation

$$\delta^h E = \delta^h E_0 + \varepsilon \cdot \ln f \quad (5)$$

In a typical application of the Rayleigh equation, the enrichment factor ε is obtained by analysis of compound-specific isotope ratios during a (bio)chemical reaction degradation, which provides characteristic information on the mechanism of a given degradation pathway.

1.2.3 *Masking effects and the need for dual isotope plots*

An even more robust interpretation towards a respective chemical mechanism is possible when isotope fractionation is analysed for two or more elements. Specifically, the mechanistic interpretation of isotopic information of only one element can be biased when a reaction cascade involves rate limiting steps aside from the chemical reaction, such as diffusion through cell membranes or the binding of a substrate to the enzyme. As a consequence, the observable enrichment factor may no longer reflect the intrinsic isotope effect of a certain reaction mechanism. This commitment to catalysis can lead to a dramatic decrease for the apparent kinetic isotope effect (AKIE) of one element. However, the link towards the mechanism can be retained when information of a second element is analysed. The reason is that the additional steps often do not show element-specific isotope effects themselves, so that AKIEs of both elements decrease to the same extent. Therefore, isotope data of two or more elements is particularly insightful for their evaluation in dual isotope plots, which still reflect the characteristics of the justified mechanism.

In order to apply this approach for chloroethenes, a method is required which determines isotopes of a second element besides carbon. This has not been available until recently, since both other elements in these compounds, hydrogen and chlorine, have been considered impractical for isotope analysis. Continuous flow chlorine isotope analysis has been prevented by the necessity of converting compounds into analytes such as methyl chloride or cesium chloride which cannot be generated online in a carrier gas flow. However, innovative approaches were brought forward recently for compound specific isotope analysis of chlorinated ethylenes with the convenient operation in continuous flow of the analytes.

1.2.4 *Recent developments in compound-specific chlorine isotope analysis of chloroethenes*

In the new instrumental method for online compound specific isotope analysis of chlorine a direct transfer of the chlorinated compound to the IRMS is provided in a continuous flow, after separation by gas chromatography. For this application, the configuration of the mass sensitive detectors (Faraday cups) is adapted specifically to the mass fragments of interest, such as $C_2H_2Cl_2^+$ (molecular ion of DCE), $C_2HCl_2^+$ (dechlorinated fragment ion of TCE) or $C_2Cl_2^+$ (double dechlorinated fragment ion of PCE).¹⁵ While this assembly is capable of measurements in high precision, the only two instruments in the world with such a dedicated

configuration are presently located at the University of Waterloo and the Helmholtz Zentrum München.

For chlorine isotope ratio measurements at lower precision, an alternative approach for chlorine isotope analysis was recently established with gas chromatography coupled to conventional quadrupole mass spectrometry (GC-qMS). Here, the detection of analytes is also conducted on non-combusted molecules, but isotope ratios are obtained from ion multiplet intensities of molecular and fragment ions. These two new analytical concepts are promising and each has its specific advantages. Whereas the GC-IRMS provides high precision for a narrow range of compounds, GC-qMS instruments are shown to be not as precise, yet universal in respect to target analytes.

With the emerging application of both approaches for scientific and commercial assessments, a systematic comparison between the performances of the two techniques was required. This was carried out in an interlaboratory comparison by addressing aspects of precision, amount dependency, standardisation and accuracy for the different methods. A detailed discussion is provided in the Appendix A1. The encouraging results of this study lend confidence to compound-specific chlorine isotope analysis, and demonstrate the advantage of precision with GC-IRMS instruments.

1.3 Challenges to assess reactions of chloroethenes in reductive dechlorination

The convenience and high performance of GC-IRMS techniques made CSIA a proven tool in contaminant hydrology, so that also the new chlorine isotope analysis has been taken up quickly as an advanced site diagnostic tool. The evaluation of chlorine isotope effects according to the Rayleigh equation from isotopologue or fragment ratios of the chloroethenes builds on a theoretical basis provided by Elsner and Hunkeler in 2008. The study shows that the conventional Rayleigh equation can be used to obtain fractionation factors of a chlorinated substrate despite the high natural abundance of both stable isotopes of chlorine, ^{35}Cl and ^{37}Cl . However, there is little knowledge about how isotope effects of chlorine are manifested in the respective products after reductive dechlorination. The chlorine substituents of the parent chloroethene are divided in the cleaved chloride and a less chlorinated ethene, so they are subjected to different isotope effects (primary in the reacting bond; secondary in non-reacting positions).

In [chapter 2](#) of this thesis the mathematical framework was developed to model product related chlorine isotope fractionation. The approach was applied as a first benchmark to approach position specific isotope effects of chlorine from experimental data of

biotransformations of PCE to TCE by *Desulfitobacterium* strain VIET-1, and of TCE to cis-DCE by *Geobacter lovleyi* strain SZ. The results are discussed in terms of hypothesized reaction mechanisms and give insights in structural selectivity for the microbial reductive dechlorination of TCE.

Such information on the underlying mechanisms of reductive dechlorination has been of great interest in previous studies as a key to understand the formation of toxic and benign products. Investigations used a broad set of tools and include work with microbial strains and with chemical models such as cobalamine (vitamin B12), the cofactor of dehalogenases, and its simplified analogue cobaloxime in order to mimic *in vivo* reductive dechlorination.^{12, 16} However, in order to understand the authenticity of a model for the actual system, a more robust indicator is needed to compare underlying mechanisms of the systems.

The work presented in [chapter 3](#) aims to compare the mechanisms of the representative systems through measurements of dual element ($^{13}\text{C}/^{12}\text{C}$, $^{37}\text{Cl}/^{35}\text{Cl}$) kinetic isotope effects. These results suggest a similar mechanism in biodegradation of different microbial strains and with isolated cobalamin. In contrast, a different mechanism was indicated for transformations with cobaloxime, so this model should be used with caution. Our results demonstrate the strength of two dimensional isotope analyses to compare *in vitro* model reactions and natural transformations.

With this demonstration of dual element isotope measurements to link chemical transformations on a mechanistic level, there is great potential to assess degradation pathways and the sustainable removal of contaminants in real-world remediation approaches. In this context it is crucial to have access on comparable reference experiments in order to substantiate the interpretation of field data. The presented results in chapters 2 & 3 represent such references for instance when the respective microbial strains are used in bioaugmentation strategies. Another broadly implemented clean-up technology is the installation of permeable reactive barriers (PRB) with zero-valent iron (ZVI).¹⁷ Transformations by ZVI tend to be more efficient than biodegradation and operate with vicinal β -dichloroelimination as an additional pathway to reductive dechlorination.^{11, 18} In [chapter 4](#) an investigation of reference experiments with a typical ZVI material for PRBs is presented. Dual isotope plots and product related carbon isotope fractionation were explored here as two discrete approaches to distinguish the effectiveness of transformation by ZVI as opposed to natural biodegradation.

1.4 References

1. Oki, T.; Kanae, S., Global hydrological cycles and world water resources. *Science* **2006**, *313*, (5790), 1068-1072.
2. Gossett, J. M., Fishing for microbes. *Science* **2002**, *298*, (5595), 974-975.
3. Fetzner, S., Bacterial dehalogenation. *Applied Microbiology and Biotechnology* **1998**, *50*, (6), 633-657.
4. Moran, M. J.; Zogorski, J. S.; Squillace, P. J., Chlorinated Solvents in Groundwater of the United States. *Environ. Sci. Technol.* **2007**, *41*, (1), 74-81.
5. U.S.EPA, Toxicological Profiles - Contaminants Found at Hazardous Waste Sites. <http://www.atsdr.cdc.gov/toxprofiles/index.asp>, downloaded on 14.08.2013.
6. Henschler, D., Toxicity of Chlorinated Organic Compounds: Effects of the Introduction of Chlorine in Organic Molecules. *Angewandte Chemie International Edition in English* **1994**, *33*, (19), 1920-1935.
7. Holliger, C.; Wohlfarth, G.; Diekert, G., Reductive dechlorination in the energy metabolism of anaerobic bacteria. *FEMS Microbiology Reviews* **1998**, *22*, (5), 383-398.
8. Ellis, D. E.; Lutz, E. J.; Odom, J. M.; Buchanan, R. J.; Bartlett, C. L.; Lee, M. D.; Harkness, M. R.; DeWeerd, K. A., Bioaugmentation for Accelerated In Situ Anaerobic Bioremediation. *Environ. Sci. Technol.* **2000**, *34*, (11), 2254-2260.
9. Morrill, P. L.; Lacrampe-Couloume, G.; Slater, G. F.; Sleep, B. E.; Edwards, E. A.; McMaster, M. L.; Major, D. W.; Lollar, B. S., Quantifying chlorinated ethene degradation during reductive dechlorination at Kelly AFB using stable carbon isotopes. *Journal of Contaminant Hydrology* **2005**, *76*, (3-4), 279-293.
10. Lojkasek-Lima, P.; Aravena, R.; Shouakar-Stash, O.; Frappe, S. K.; Marchesi, M.; Fiorenza, S.; Vogan, J., Evaluating TCE Abiotic and Biotic Degradation Pathways in a Permeable Reactive Barrier Using Compound Specific Isotope Analysis. *Ground Water Monit. Remediat.* **2012**, *32*, (4), 53-62.
11. Arnold, W. A.; Roberts, A. L., Pathways and kinetics of chlorinated ethylene and chlorinated acetylene reaction with Fe(O) particles. *Environmental Science & Technology* **2000**, *34*, (9), 1794-1805.
12. Follett, A. D.; McNeill, K., Reduction of Trichloroethylene by Outer-Sphere Electron-Transfer Agents. *J. Am. Chem. Soc.* **2005**, *127*, (3), 844-845.

13. Neumann, A.; Wohlfarth, G.; Diekert, G., Purification and Characterization of Tetrachloroethene Reductive Dehalogenase from *Dehalospirillum multivorans*. *J. Biol. Chem.* **1996**, *271*, (28), 16515-16519.
14. Glod, G.; Angst, W.; Holliger, C.; Schwarzenbach, R. P., Corrinoid-mediated reduction of tetrachloroethylene, trichloroethylene and trichlorofluoroethane in homogeneous aqueous solution: reaction kinetics and reaction mechanisms. *Environmental Science and Technology* **1997**, *31*, (1), 253-260.
15. Shouakar-Stash, O.; Drimmie, R. J.; Zhang, M.; Frappe, S. K., Compound-specific chlorine isotope ratios of TCE, PCE and DCE isomers by direct injection using CF-IRMS. *Applied Geochemistry* **2006**, *21*, (5), 766-781.
16. Kliegman, S.; McNeill, K., Dechlorination of chloroethylenes by cob(I)alamin and cobalamin model complexes. *Dalton Transactions* **2008**, (32), 4191-4201.
17. Slater, G.; Sherwood Lollar, B.; Allen King, R.; O'Hannesin, S. F., Isotopic fractionation during reductive dechlorination of trichloroethene by zero-valent iron: influence of surface treatment. *Chemosphere* **2002**, *49*, 587-596.
18. Elsner, M.; Chartrand, M.; VanStone, N.; Lacrampe Couloume, G.; Sherwood Lollar, B., Identifying Abiotic Chlorinated Ethene Degradation: Characteristic Isotope Patterns in Reaction Products with Nanoscale Zero-Valent Iron. *Environ. Sci. Technol.* **2008**, *42*, (16), 5963-5970.

2

Chlorine Isotope Effects from Isotope Ratio Mass Spectrometry Suggest Intramolecular C-Cl Bond Competition in Trichloroethene (TCE) Reductive Dehalogenation

*Stefan Cretnik*¹, *Anat Bernstein*¹, *Orfan Shouakar-Stash*², *Frank Löffler*^{3,4,5}, *Martin Elsner*^{1,*}

¹ Institute of Groundwater Ecology, Helmholtz Zentrum München, Ingolstädter Landstr. 1, 85764 Neuherberg, Germany; E-Mails: one_fiftyone@hotmail.com (S.C.); anatbern@bgu.ac.il (A.B.)

² Department of Earth and Environmental Sciences, University of Waterloo, Waterloo, ON N2L 3G1, Canada; E-Mail: orfan@uwaterloo.ca

³ Department of Microbiology & Center for Environmental Biotechnology, University of Tennessee, Knoxville, TN 37996-2000, USA; E-Mail: frank.loeffler@utk.edu

⁴ Department of Civil and Environmental Engineering, University of Tennessee, Knoxville, TN 37996-2000, USA

⁵ Oak Ridge National Laboratory (UT-ORNL) Joint Institute for Biological Sciences (JIBS) and Bioscience Division, Oak Ridge National Laboratory, Oak Ridge, TN 37831, USA

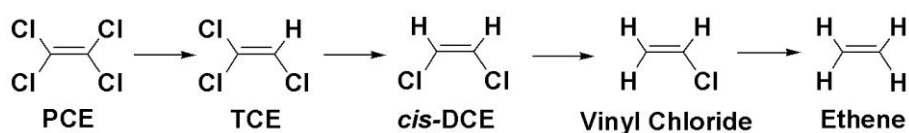
2.1 ABSTRACT

Chlorinated ethenes are prevalent groundwater contaminants. To better constrain (bio)chemical reaction mechanisms of reductive dechlorination, the position-specificity of reductive trichloroethene (TCE) dehalogenation was investigated. Selective biotransformation reactions (i) of tetrachloroethene (PCE) to TCE in cultures of *Desulfotobacterium* sp. strain Viet1; and (ii) of TCE to *cis*-1,2-dichloroethene (*cis*-DCE) in cultures of *Geobacter lovleyi* strain SZ were investigated. Compound-average carbon isotope effects were $-19.0\text{‰} \pm 0.9\text{‰}$ (PCE) and $-12.2\text{‰} \pm 1.0\text{‰}$ (TCE) (95% confidence intervals). Using instrumental advances in chlorine isotope analysis by continuous flow isotope ratio mass spectrometry, compound-average chlorine isotope effects were measured for PCE ($-5.0\text{‰} \pm 0.1\text{‰}$) and TCE ($-3.6\text{‰} \pm 0.2\text{‰}$). In addition, position-specific kinetic chlorine isotope effects were determined from fits of reactant and product isotope ratios. In PCE biodegradation, primary chlorine isotope effects were substantially larger (by $-16.3\text{‰} \pm 1.4\text{‰}$ (standard error)) than secondary. In TCE biodegradation, in contrast, the product *cis*-DCE reflected an average isotope effect of $-2.4\text{‰} \pm 0.3\text{‰}$ and the product chloride an isotope effect of $-6.5\text{‰} \pm 2.5\text{‰}$, in the original positions of TCE from which the products were formed (95% confidence intervals). A greater difference would be expected for a position-specific reaction (chloride would exclusively reflect a primary isotope effect). These results therefore suggest that both vicinal chlorine substituents of TCE were reactive (intramolecular competition). This finding puts new constraints on mechanistic scenarios and favours either nucleophilic addition by Co(I) or single electron transfer as reductive dehalogenation mechanisms.

2.2 INTRODUCTION

Chlorinated organic compounds have natural and anthropogenic sources and are represented in nearly every organic chemical class¹. Much fundamental interest is directed at the underlying reaction chemistry of the C-Cl bond²⁻⁴. The widespread industrial application of chlorinated hydrocarbons as solvents, chemical intermediates and pesticides resulted in environmental contamination, with adverse effects on drinking water quality and ecosystem and human health⁵⁻⁷. A specific focus has therefore been on their reductive dehalogenation to non-halogenated hydrocarbons, where detoxification is achieved by reductive cleavage of the carbon-chlorine bonds. Evolution has brought forward specialized microorganisms that perform organohalide respiration, using chlorinated hydrocarbons for energy conservation.⁸

Considering the importance of biotic reactions involved in the degradation of chlorinated hydrocarbons, surprisingly little is known about the underlying reaction mechanisms. Even the detailed reductive dehalogenation mechanisms of tetrachloroethene (PCE) and trichloroethene (TCE)—the two most abundant dry cleaning and degreasing agents and notorious groundwater pollutants—remain imperfectly understood. Some bacteria produce *trans*-DCE or 1,1-DCE in this reaction⁹, but the typical case is the selective formation of *cis*-DCE as the bottleneck of microbial dehalogenation, which is a major problem in remediation strategies (Scheme 1)¹⁰.

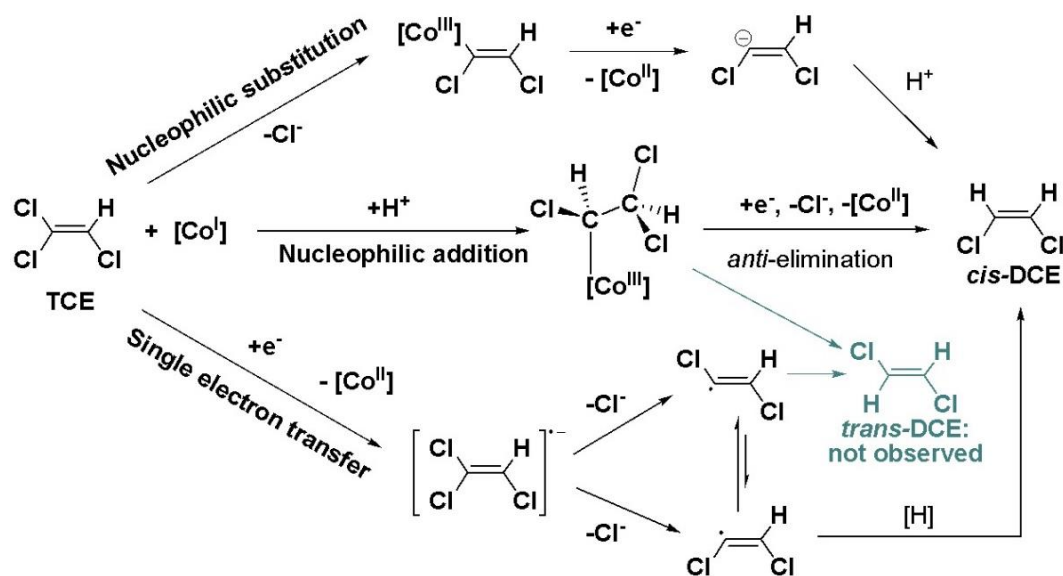


Scheme 1: Typical stepwise reaction sequence in microbial dechlorination of PCE leading to less chlorinated ethenes and to non-toxic ethene.

On the most fundamental level, this product formation depends on the initial reaction step of cob(I)alamin (coenzyme B₁₂), the transition-metal cofactor present in reductive dehalogenases¹¹. It is unclear whether the underlying dehalogenation reaction involves nucleophilic addition by Co(I), nucleophilic substitution by Co(I) or a radical mechanism involving a single electron transfer (SET) from Co(I) to the organohalide (Scheme 2).¹²⁻¹⁸

Specifically, it remains unclear whether the transformation of TCE to *cis*-DCE is stereoselective at the geminal chlorine substituent in *E*-position—as one would presume for a nucleophilic substitution mechanism¹⁹—or whether both geminal *E*- and *Z*-positions are

involved—as brought forward for SET by computational results from Nonnenberg *et al.* resulting in the formation of radical intermediates²⁰. Involvement of both geminal chlorine substituents would also be expected for the pathway of nucleophilic addition, as suggested by a computational study by Pratt and van der Donk²¹. In the light of the selective formation of *cis*-DCE, a direct, complementary line of evidence is therefore warranted, which indicates whether one or two carbon-chlorine bonds are reactive in TCE.



Scheme 2. Proposed degradation pathways of TCE catalyzed by cobalamin.

A potential solution are measurements of kinetic isotope effects (KIEs), either on reacting bonds (primary isotope effects) or on adjacent bonds (secondary isotope effects). If only one C-Cl bond in TCE is reactive, a primary isotope effect would occur specifically in this position leading to a pronounced difference to the other positions where only secondary isotope effects would be expected. In contrast, if two positions are reactive, they would take turns in the reaction so that both would reflect a combination of primary and secondary effects. If isotope effects in both positions are compared, a smaller difference would therefore be expected. On the most fundamental level, however, general knowledge about typical primary and secondary isotope effects of chlorine would first be warranted, since so far only very limited knowledge exists on isotope effects in reductive dechlorination of chlorinated ethenes.

To close this research gap, KIEs on specific positions in a target molecule must be determined. Typical techniques are isotope labelling, or determination of position-specific KIEs by NMR measurements²². However, these approaches do not work well for measurement of chlorine

isotope effects in chlorinated ethenes. Even though the stable isotopes of chlorine (^{35}Cl and ^{37}Cl) are NMR active, they show broad chemical shifts and poor precision in signal integrations so that position-specific $^{37}\text{Cl}/^{35}\text{Cl}$ isotope analysis with NMR is challenging.²³ In addition, the method is not suitable to investigate biodegradation because samples contain diluted compound mixtures and NMR analysis requires large amounts of pure target compounds. Finally, position-specific isotopic labeling is impossible for PCE, where all chlorine substituents are chemically equivalent²⁴.

A potential solution to the problem is offered by recent instrumental developments in gas chromatography-isotope ratio mass spectrometry (GC-IRMS). Compounds are separated by gas chromatography and isotopologue ion multiplets of individual chlorinated ethene molecules are recorded simultaneously in dedicated Faraday cups of isotope ratio mass spectrometers^{25,26}. Measurements of changes in chlorine isotope ratios have therefore become accessible even in complicated reaction mixtures observed in environmental systems. However, the measured isotope effects from such GC-IRMS methods typically reflect the compound average of the target compound.

Even though the recent introduction of chlorine isotope GC-IRMS—combined with routine carbon isotope GC-IRMS—has brought about first dual (carbon and chlorine) isotope effect investigations, these studies have, therefore, only targeted *compound-average* isotope effects of the *reactant*²⁷⁻³⁰. While they could delineate similarities and differences between experimental systems (different microorganisms, chemical reactants)²⁹ direct insight into underlying mechanisms remained elusive.

In this study, we take advantage of the fact that Cl^- is released during reductive dechlorination. Since the chlorine substituents of the parent chlorinated ethene end up in different products (*i.e.*, Cl^- and the less chlorinated ethene), they are subject to different isotope effects (primary effects in the cleaved bond, secondary effects in non-reacting positions). Information on the magnitude of either *position-specific* isotope effect may therefore be retrieved from analysis of isotope ratios in the *products* (Cl^- and the less chlorinated ethene). This approach was discussed in previous work³⁰ and was pursued in a recent experimental study by Kuder *et al.*³⁰. There, it was *a priori* excluded that more than one C-Cl bond is reactive in TCE—in contradiction to the scenarios of Scheme 1. Since this directly affected all further conclusions of this previous study — including estimates of secondary chlorine isotope effects³⁰—resultant mechanistic conclusions were, unfortunately, biased and reliable insight based on Cl-isotope effect interpretations was not possible.

In this study, a more rigorous evaluation was enabled by (i) investigations of one-step dehalogenation reactions only and (ii) application of an appropriate mathematical framework. Cultures of *Desulfotobacterium* sp. strain Viet1, a PCE-to-TCE dechlorinator³², were used to determine the typical magnitude of primary and secondary chlorine isotope effects. Further, cultures of *Geobacter lovleyi* strain SZ, a PCE/TCE-to-cis-DCE dechlorinator³³, were used to specifically investigate whether one or two C-Cl bonds are reactive in TCE as non-symmetric molecule. Mathematical equations were derived for reactant and product isotope ratios to model chlorine isotope trends and to extract primary and secondary chlorine isotope effects. This approach provided a first benchmark how chlorine isotope data can be interpreted in typical scenarios of reductive dechlorination of chlorinated ethenes. Another aim was to explore if information on one *versus* two reactive positions may be obtained and could be useful to constrain the number of possible reaction mechanisms for reductive TCE dehalogenation.

2.3 EXPERIMENTAL SECTION

Biodegradation Experiments and Carbon and Chlorine Isotope Analysis

Selective reductive dechlorination of PCE to TCE was accomplished in anaerobic biodegradation of PCE with the Firmicute *Desulfitobacterium* sp. strain Viet1, and selective transformation of TCE to *cis*-DCE was facilitated by the Deltaproteobacterium *Geobacter lovleyi* strain SZ. The cultures were grown following established procedures inside an anoxic glove box in glass bottles (250 mL) equipped with Mininert valves (Supelco, Bellefonte, PA, USA). The bottles were amended with 10 μ L of neat PCE. After four days of shaking, inoculation was carried out by adding 20 mL of the active culture, which was previously grown in a similar medium. Liquid samples of 7 mL were collected at given time points within 48 h after inoculation until the initial amount of PCE or TCE (45 mg/L and 90 mg/L, respectively) had been dechlorinated. The samples were taken for (i) compound-specific isotope analysis (CSIA) of carbon and chlorine in chlorinated ethenes by GC-IRMS and (ii) concentration analysis using a gas chromatograph equipped with flame ionization detector (GC-FID). Limit of detection in these concentration measurements for the chlorinated ethenes were below 0.05 μ g/L corresponding to less than 0.1% of the initial concentrations. This includes 1,1-DCE and *trans*-DCE as potential dechlorination products, which were not observed in any of the reactions. Abiotic controls were treated with an identical procedure but without inoculation of an active microbial culture. Concentrations in these controls did not decrease in significant amounts. The analytical uncertainty 2σ was $\pm 0.5\%$ for carbon isotope analysis and $\pm 0.2\%$ for chlorine isotope analysis. Detailed descriptions of experimental and analytical methods are provided in the Supporting Information (S.I.).

2.4 MATHEMATICAL APPROACH (I): COMPOUND AVERAGE ISOTOPE EFFECTS

2.4.1 *Fitting Substrate and Product Isotope Ratios: Compound-Average Isotope Effects*

Mass spectrometry can measure the proportion of different stable isotopes of element E in a given molecule. When looking at a given molecular position, this ratio of heavy isotopes ^hE to light isotopes ^lE , denoted with R_0 for the starting material, typically changes during the progress of a reaction to a different ratio R_t at time t :

$$R_0 = \left(\frac{{}^h E}{{}^l E} \right)_0 \quad R_t = \left(\frac{{}^h E}{{}^l E} \right)_t$$

Owing to the kinetic isotope effect (KIE), slower reacting isotopes become enriched during the reaction compared to the original starting material. This KIE_E is given by the ratio of rate constants of the light isotope ${}^l k$ and heavy isotope ${}^h k$:

$$\left(\frac{{}^l k}{{}^h k} \right) = KIE_E \quad (1)$$

For the sake of simplicity, we stick to this this definition even though, strictly speaking, bacterial transformation gives isotope effects on (V/K) — V : maximum enzyme velocity, K : Michaelis-Menten constant—rather than on elementary rate constants k .³⁴

2.4.2 Compound-Average Isotope Effects from Reactant Values

The proportion of R_t/R_0 is well established to depend on the remaining fraction f of the starting material and the KIE according to³⁴:

$$\frac{R_t}{R_0} = f^{(1/KIE)-1} \quad (2)$$

In the case of compound-specific isotope analysis, R represents the isotope ratio as a compound average $R_{Compound-Average}$. This means that also the kinetic isotope effect is obtained as a compound average $KIE_{Compound-Average}$ ³⁵:

$$\frac{R_{Compound-Average}}{R_{0,Compound-Average}} = f^{(1/KIE_{Compound-Average})-1} \quad (3)$$

The exponent of Equation (3) can alternatively be called enrichment factor ϵ and $1/KIE$ be named fractionation factor α with the relationship³⁶:

$$\left(1 / KIE_{Compound-Average} \right) - 1 = \alpha - 1 = \epsilon \quad (4)$$

A $KIE_{Compound-Average}$ of 1.005, for example, corresponds to $\epsilon = -0.005 = -5\text{‰}$, expressing a situation, in which molecules with an additional heavy isotope react on average by 5‰ slower than the respective lighter isotopologue. Combination of Equations (4) and (3) results in:

$$\frac{R_{Compound-Average}}{R_{0,Compound-Average}} = f^\epsilon \quad (5)$$

The isotope ratios of the heavy (${}^h E$) and light (${}^l E$) element in a compound are typically stated relative to reference materials, (Vienna Pee Dee Belemnite (VPDB) for carbon,

Standard Mean Ocean Chloride (SMOC) for chlorine) and the isotope ratio of a substance is typically expressed in the delta notation:

$$\delta^h E = \left(\frac{R_{\text{Compound-Average}} - R_{\text{Standard}}}{R_{\text{Standard}}} \right) = \left(\frac{R_{\text{Compound-Average}}}{R_{\text{Standard}}} \right) - 1 \quad (6)$$

Equation (6) can be rearranged to:

$$R_{\text{Compound-Average}} = (\delta^h E + 1) \cdot R_{\text{Standard}} \quad (7)$$

This can be introduced into Equation (5) according to:

$$\frac{(\delta^h E + 1) \cdot R_{\text{Standard}}}{(\delta^h E_0 + 1) \cdot R_{\text{Standard}}} = f^\varepsilon \Rightarrow \frac{(\delta^h E + 1)}{(\delta^h E_0 + 1)} = f^\varepsilon \quad (8)$$

Equation (8) is typically used in its logarithmic form as the common Rayleigh equation:

$$\begin{aligned} \ln(\delta^h E + 1) - \ln(\delta^h E_0 + 1) &\approx \delta^h E - \delta^h E_0 = \varepsilon \cdot \ln f \\ \Rightarrow \delta^h E &= \delta^h E_0 + \varepsilon \cdot \ln f \end{aligned} \quad (9)$$

The obtained epsilon (ε) represents the isotope fractionation as a compound average and therefore expresses the average positions p of the element in the target compound, including primary as well as secondary positions:

$$\varepsilon = \frac{1}{p} \left(\sum_{i=1}^p \varepsilon_i \right) \quad (10)$$

2.4.3 Expressions for Product Isotope Values

For the products formed during the reaction, an isotopic mass balance must be fulfilled in a closed system:

$$\sum_{i=1}^n m_i \cdot \delta^h E_{P,i} = \frac{m_S \cdot \delta^h E_0 - m_S \cdot f \cdot \delta^h E}{(1-f)} \quad (11)$$

Here, the reactant contains m_S atoms of element E in its structure. $\delta^h E_0$ is the original reactant isotope ratio, whereas $\delta^h E$ is the ratio when reaction has occurred so that only a fraction f of reactant remains. A fraction of $(1-f)$ has then been converted to one or more (up to n) products; m_i is the number of atoms of E inside the structure of product i , $\delta^h E_{P,i}$ is the respective product's isotope value.

2.4.4 Carbon Isotope Effects from Product Values

In the conversion from PCE to TCE or from TCE to *cis*-DCE, the two carbon atoms present in the reactant are passed on to the product. Therefore, in the case of carbon, Equation (11) simplifies to:

$$\begin{aligned} 2 \cdot \delta^{13}C_p &= \frac{2 \cdot \delta^{13}C_0 - 2 \cdot f \cdot \delta^{13}C}{(1-f)} \\ \Rightarrow \delta^{13}C_p &= \frac{\delta^{13}C_0 - f \cdot \delta^{13}C}{(1-f)} \end{aligned} \quad (12)$$

An equation that allows fitting product isotope trends is obtained by combination of Equation (12) with Equation (9) to yield

$$\delta^{13}C_p = \delta^{13}C_0 + \left(\varepsilon_{carbon} \cdot \frac{f \cdot \ln f}{1-f} \right) \quad (13)$$

The parameter ε_{carbon} from product data is identical to ε in Equation (9) for substrate data, because all carbon isotopes are transferred from reactant to product so that the product isotope curve reflects the enrichment trend of the original atoms in the reactant.

2.4.5 Chlorine Isotope Effects from Product Values

When chlorine isotope values are measured, reductive dechlorination of chlorinated ethenes releases chloride and simultaneously forms the less chlorinated ethene so that two chlorine-containing products are formed at the same time ($n = 2$). This circumstance generates information about primary and secondary chlorine isotope effects, as derived in the following section.

2.5 MATHEMATICAL APPROACH (II): PRIMARY AND SECONDARY ISOTOPE EFFECTS

2.5.1 Case 1—PCE: Indistinguishable Molecular Positions

General Equations

In the case of PCE, the molecular positions of all atoms are chemically equivalent so that the same chlorine atoms may potentially end up in TCE or as Cl^- . Accordingly, isotopes partition according to the kinetic isotope effects associated with the formation of either product P_i with $\alpha_i = 1/\text{KIE}_i$. As a consequence, their isotope ratios relate according to:

$$\frac{R_{P_1}}{R_{P_2}} = \frac{\alpha_1}{\alpha_2} \quad (14)$$

With Equation (7), the fractionation factors α_i can be expressed in the delta notation as:

$$\frac{\delta^{37}Cl_{P_1} + 1}{\delta^{37}Cl_{P_2} + 1} = \frac{\alpha_1}{\alpha_2} = \alpha_{Diff} \quad (15)$$

with α_{Diff} expressing the ratio between the primary isotope effect (in the formation of Cl^-) and the average secondary isotope effects (in the three molecular positions that become TCE). This equation can be rearranged and simplified according to:

$$\begin{aligned} \delta^{37}Cl_{TCE} + 1 &= \alpha_{Diff} (\delta^{37}Cl_{Cl^-} + 1) & (16) \\ \Rightarrow \delta^{37}Cl_{TCE} - \alpha_{Diff} \cdot \delta^{37}Cl_{Cl^-} &= \alpha_{Diff} - 1 \\ &\approx 1 \\ \Rightarrow \delta^{37}Cl_{TCE} - \delta^{37}Cl_{Cl^-} &= \alpha_{Diff} - 1 = \varepsilon_{Diff} & (17) \end{aligned}$$

Accordingly, the difference between primary and secondary isotope effects ε_{Diff} is directly obtained from product isotope values, because chlorine isotope ratios of Cl^- and TCE are always separated by ε_{Diff} .

For the reaction of PCE with four chlorine atoms to TCE with three chlorine atoms and Cl^- the enrichment trends of these products must follow Equation (17), as well as an isotopic mass balance. According to the derivation in the supporting information, the following equations apply:

$$\delta^{37}Cl_{Cl^-} = \underbrace{\delta^{37}Cl_{0,PCE} - \frac{3}{4}\varepsilon_{Diff}}_{\text{constant: } K_{Cl^-}} - \varepsilon_{PCE} \cdot \frac{f \cdot \ln f}{(1-f)} \quad (18)$$

$$\delta^{37}Cl_{TCE} = \underbrace{\delta^{37}Cl_{0,PCE} + \frac{1}{4}\varepsilon_{Diff}}_{\text{constant: } K_{TCE}} - \varepsilon_{PCE} \cdot \frac{f \cdot \ln f}{(1-f)} \quad (19)$$

When f approaches 1 in this expression (*i.e.*, in the beginning of the reaction), the last term approaches $+\varepsilon_{PCE}$ in Equations (18) and (19). As a consequence, the intercept (A) between PCE and the TCE formed, and the intercept (B) between PCE and the chloride released are determined by:

$$(A) = \delta^{37}Cl_{0,PCE} - \delta^{37}Cl_{0,TCE} = \underbrace{-\frac{1}{4}\varepsilon_{Diff} - \varepsilon_{PCE}}_{(A)} \quad (20)$$

$$(B) = \delta^{37}Cl_{0,PCE} - \delta^{37}Cl_{0,Cl^-} = \underbrace{\frac{3}{4}\varepsilon_{Diff} - \varepsilon_{PCE}}_{(B)} \quad (21)$$

For interpretation of the experimental PCE degradation data, the product isotope trends of chloride and TCE were fitted in Sigma Plot according to Equations (18) and (19), respectively, with ϵ_{PCE} and ϵ_{Diff} as fitting parameters.

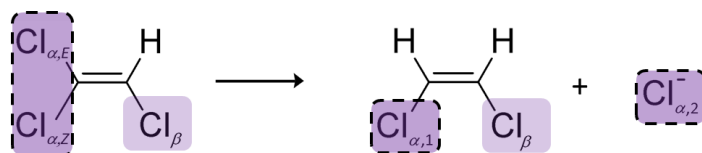
Interpretation of product isotope enrichment trends ($\epsilon_{\text{Chlorine}}$) and intercepts (ϵ_{Diff}) for PCE

In the case of PCE, ϵ_{Diff} —the intercept of the product curves—provides information about primary and secondary isotope effects. The parameter ϵ_{PCE} , in contrast, relates to changes in the four chemically equivalent positions of PCE (average of primary and secondary isotope effects) and is the same in fits of $\delta^{37}\text{Cl}_{PCE}$ [Equation (9)], $\delta^{37}\text{Cl}_{Cl^-}$ [Equation (20)] and $\delta^{37}\text{Cl}_{TCE}$ [Equation (21)], for the same reasons as discussed above for carbon.

2.5.2 Case 2—TCE: Distinguishable Molecular Positions

In contrast to PCE, molecular positions in TCE are not chemically equivalent. In addition, formation of *cis*-DCE is clearly regioselective. No mechanism is known which would convert 1,1-dichloroethene into 1,2-dichloroethene intermediates so that *cis*-DCE can only be formed by cleavage of a C-Cl bond in the geminal α -positions and not in the β -position (see Scheme 3). Otherwise 1,1-dichloroethene would be detected which is not the case for *Geobacter lovleyi* strain SZ [33]. A primary isotope effect is therefore expected in the reacting bond in α -position and a secondary isotope effect in the other geminal bond in α -position that is not cleaved. A secondary isotope effect is also expected in the vicinal bond at Cl_β because it does not experience C-Cl bond cleavage.

Although the two chlorine atoms in *cis*-DCE are chemically equivalent, they have a different history (see Scheme 3). One derives from the β -position of TCE—in which $^{37}\text{Cl}/^{35}\text{Cl}$ ratios change due to a secondary isotope effect—and one from the geminal α -positions of TCE, in which $^{37}\text{Cl}/^{35}\text{Cl}$ ratios may change due to a combination of primary and secondary effects.



Scheme 3. One step reductive dechlorination of TCE with possible locations of primary isotope effects (dotted line) and the location of a secondary isotope effect (Cl_β).

Since no *trans*-DCE is observed, it seems an intuitive interpretation that $\text{Cl}_{\alpha,E}$ should be the only reactive position, in analogy to the considerations for Cl_{β} above. Previous studies, however, considered that selective formation of *cis*-DCE may be caused by cleavage of either C-Cl bond in the α -positions followed by selective interconversion of *cis*-/*trans*-dichloroethene intermediates, as illustrated in Scheme 2^{20,37}. If two reactive positions are considered, one can therefore define

$$\begin{array}{l} x \left\{ \begin{array}{l} \text{- percentage that reacts from } \text{Cl}_{\alpha,E} \text{ to } \text{Cl}^{-}_{\alpha,2} \text{ (chloride)} \\ \text{- percentage that reacts from } \text{Cl}_{\alpha,Z} \text{ to } \text{Cl}_{\alpha,I} \text{ (} \textit{cis}\text{-DCE)} \end{array} \right. \\ 1-x \left\{ \begin{array}{l} \text{- percentage that reacts from } \text{Cl}_{\alpha,E} \text{ to } \text{Cl}_{\alpha,I} \text{ (} \textit{cis}\text{-DCE)} \\ \text{- percentage that reacts from } \text{Cl}_{\alpha,Z} \text{ to } \text{Cl}^{-}_{\alpha,2} \text{ (chloride)} \end{array} \right. \end{array}$$

With $x = 1$ or $x = 0$, the reaction would follow a position-specific cleavage; however with $1 > x > 0$ two positions would be involved. According to the derivation shown in the Supporting Information, the enrichment trends in chlorine isotope values of *cis*-DCE and chloride can be expected to be described by *individual* enrichment factors according to:

$$\varepsilon_{\text{TCE} \rightarrow \text{chloride}} = (x \cdot \varepsilon_{\alpha,E} + (1-x) \cdot \varepsilon_{\alpha,Z}) \quad (22)$$

for the enrichment trend in chloride isotope data, and

$$\varepsilon_{\text{TCE} \rightarrow \textit{cis}\text{-DCE}} = \frac{1}{2} \left[\varepsilon_{\beta} + (x \cdot \varepsilon_{\alpha,Z} + (1-x) \varepsilon_{\alpha,E}) \right] \quad (23)$$

for the enrichment trend in *cis*-DCE isotope data. Here, $\varepsilon_{\alpha,E}$, $\varepsilon_{\alpha,Z}$, and ε_{β} are the position-specific isotope effects in the different bonds according to Scheme 3 (for interpretations see below). The situation is therefore different from the PCE case where both products (TCE and chloride) were formed from indistinguishable molecular positions of PCE so that their isotope enrichment trends reflected, and could be fitted by, the *same* enrichment factor ε_{PCE} . In contrast, distinguishable chlorine atoms are present in TCE so that $\varepsilon_{\text{TCE} \rightarrow \text{chloride}}$ and $\varepsilon_{\text{TCE} \rightarrow \textit{cis}\text{-DCE}}$ are different. They can be obtained by fitting experimental chloride isotope data according to

$$\delta^{37}\text{Cl}_{\text{Cl}^{-}} = K_{\text{Cl}^{-}} - \varepsilon_{\text{TCE} \rightarrow \text{chloride}} \frac{f \ln f}{(1-f)} \quad (24)$$

and

$$\delta^{37}\text{Cl}_{\textit{cis}\text{-DCE}} = K_{\textit{cis}\text{-DCE}} - \varepsilon_{\text{TCE} \rightarrow \textit{cis}\text{-DCE}} \frac{f \ln f}{(1-f)} \quad (25)$$

The introduced constants K in Equations (24) and (25) are fitting constants in Sigma Plot for the respective intercept of each product. For their mathematical definition and interpretation see below, as well as the derivatization in the Supporting Information.

2.5.3 Interpretation of the Product Curve Enrichment Trends $\varepsilon_{TCE \rightarrow \text{chloride}}$ and $\varepsilon_{TCE \rightarrow \text{cis-DCE}}$ for TCE

The parameters $\varepsilon_{TCE \rightarrow \text{chloride}}$ and $\varepsilon_{TCE \rightarrow \text{cis-DCE}}$ describe the enrichment trend (*i.e.*, the steepness) of $\delta^{37}\text{Cl}$ curves of chloride and *cis*-DCE. Intriguingly, these parameters allow a glimpse on $\varepsilon_{\alpha,E}$, $\varepsilon_{\alpha,Z}$ and ε_{β} the position-specific isotope effects, which can tell whether only one, or both positions may react. Specifically, $\varepsilon_{\alpha,E}$ is a weighted average of $\varepsilon_{\alpha,E}$ *primary* and $\varepsilon_{\alpha,E}$ *secondary*. Here, $\varepsilon_{\alpha,E}$ *primary* is defined as the primary isotope effect when position E reacts to release chloride (percentage x), and $\varepsilon_{\alpha,E}$ *secondary* is the secondary isotope effect in E when position Z reacts to release chloride (percentage $(1-x)$):

$$\varepsilon_{\alpha,E} = x \cdot \varepsilon_{\alpha,E,\text{prim}} + (1-x) \cdot \varepsilon_{\alpha,E,\text{sec}} = \varepsilon_{\alpha,E,\text{sec}} + x \cdot \varepsilon_{\text{Diff},\alpha,E} \quad (26)$$

In the same way $\varepsilon_{\alpha,Z}$ is expressed as

$$\begin{aligned} \varepsilon_{\alpha,Z} &= (1-x) \cdot \varepsilon_{\alpha,Z,\text{prim}} + x \cdot \varepsilon_{\alpha,Z,\text{sec}} \\ &= \varepsilon_{\alpha,Z,\text{sec}} + (1-x) \cdot \varepsilon_{\text{Diff},\alpha,Z} \end{aligned} \quad (27)$$

Substitution into Equation (26) gives:

$$\begin{aligned} \varepsilon_{TCE \rightarrow \text{chloride}} &= x \cdot \varepsilon_{\alpha,E} + (1-x) \cdot \varepsilon_{\alpha,Z} \\ &= x \left[x \cdot \varepsilon_{\alpha,E,\text{prim}} + (1-x) \varepsilon_{\alpha,E,\text{sec}} \right] + (1-x) \left[(1-x) \varepsilon_{\alpha,Z,\text{prim}} + x \cdot \varepsilon_{\alpha,Z,\text{sec}} \right] \end{aligned} \quad (28)$$

In the same way, the contribution of $x \cdot \varepsilon_{\alpha,Z} + (1-x) \varepsilon_{\alpha,E}$ in Equation (26)—the one which describes the chlorine atoms of *cis*-DCE stemming from the α -positions of TCE—is given by

$$\begin{aligned} &x \cdot \varepsilon_{\alpha,Z} + (1-x) \varepsilon_{\alpha,E} \\ &= x \left[(1-x) \varepsilon_{\alpha,Z,\text{prim}} + x \cdot \varepsilon_{\alpha,Z,\text{sec}} \right] + (1-x) \left[x \cdot \varepsilon_{\alpha,E,\text{prim}} + (1-x) \varepsilon_{\alpha,E,\text{sec}} \right] \end{aligned} \quad (29)$$

Figure 1 visualizes how both contributions depend on x (*i.e.*, the percentage of $\text{Cl}_{\alpha,E}$ reacting to Cl) assuming exemplary numeric values for chlorine isotope effects ($\varepsilon_{\text{primary}} = -8\text{‰}$ ($\text{KIE}_{\text{Cl}} = 1.008$) and $\varepsilon_{\text{secondary}} = -1\text{‰}$ ($\text{KIE}_{\text{Cl}} = 1.001$)), which are further assumed to be identical in both positions (*Z* and *E*). For qualitatively similar trends with other numerical scenarios see the supporting information.

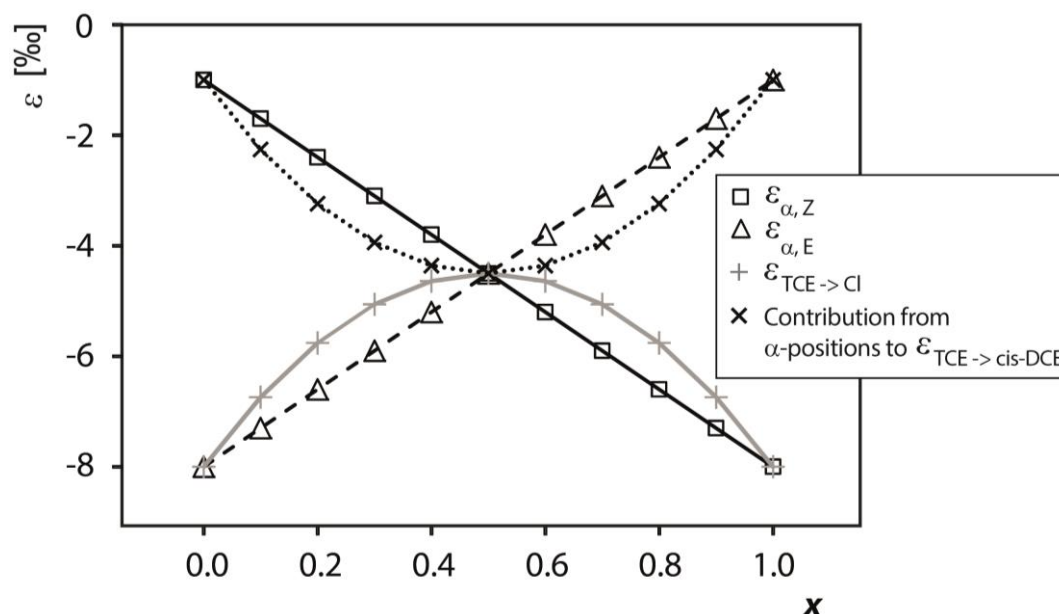


Figure 1: Representation of parameters $\epsilon_{\alpha,E}$, $\epsilon_{\alpha,Z}$, $\epsilon_{TCE \rightarrow \text{chloride}}$ and $\epsilon_{TCE \rightarrow \text{cis-DCE}}$ in dependence of x , the percentage of $\text{Cl}^-_{\alpha,E}$ reacting to Cl^- . Assumed values for primary and secondary isotope effects were $\epsilon_{\text{primary}} = -8\text{‰}$ and $\epsilon_{\text{secondary}} = -1\text{‰}$ in both positions. Similar scenarios are obtained if the values are allowed to vary between the positions (see S.I.).

2.5.4 Contributions from α -Positions to $\epsilon_{TCE \rightarrow \text{chloride}}$ and $\epsilon_{TCE \rightarrow \text{cis-DCE}}$

Figure 1 illustrates that $\epsilon_{\alpha,E}$ and $\epsilon_{\alpha,Z}$ vary linearly with x . In contrast, a non-linear variation with x occurs for $\epsilon_{TCE \rightarrow \text{chloride}}$, as well as for the α -position contribution of $\epsilon_{TCE \rightarrow \text{cis-DCE}}$ for the following reasons. If more chloride is formed from one position (i) ϵ_{α} is stronger in the position from which more chloride is formed with a primary isotope effect; (ii) in addition, more atoms in these positions are released as chloride so that the product curve of chloride more strongly reflects this higher enrichment. The opposite trend can be observed in the product curve of *cis*-DCE. The combination of both contributions (i) and (ii) therefore lends the curves of $\epsilon_{TCE \rightarrow \text{chloride}}$ and $\epsilon_{TCE \rightarrow \text{cis-DCE}}$ their non-linear shape. In the case of $x = 0.5$, finally, both contributions are identical because the isotope enrichment trend from either position is passed on in equal parts to both products (true intramolecular competition; this corresponds to the example of PCE, where TCE and chloride also reflect the average isotope enrichment trend of the reactant).

Figure 1, therefore, predicts that $\epsilon_{TCE \rightarrow \text{chloride}}$ and the contribution of $x \cdot \epsilon_{\alpha,Z} + (1 - x) \epsilon_{\alpha,E}$ to $\epsilon_{TCE \rightarrow \text{cis-DCE}}$ are very sensitive indicators whether the reaction of TCE involves two or only one reactive C-Cl bond(s). As illustrated in Figure 1, if both bonds are involved, the

difference between $\epsilon_{TCE \rightarrow \text{chloride}}$ and $\epsilon_{TCE \rightarrow \text{cis-DCE}}$ is smaller than predicted for a typical difference between primary and secondary isotope effects. In contrast, only in the case that one position reacts (*i.e.*, when x approaches 0 or 1) the positions in TCE can be strictly separated into one reactive chlorine substituent (experiencing a primary isotope effect) and two non-reactive chlorine substituents (experiencing secondary isotope effects). It is therefore only in this case that the enrichment trend of the two product curves reflects a typical difference between primary and secondary isotope effects, because only in this case is $\epsilon_{TCE \rightarrow \text{chloride}} = \epsilon_{\text{primary}}$ and $\epsilon_{TCE \rightarrow \text{cis-DCE}} = \epsilon_{\text{secondary}}$.

2.5.5 Interpretation of Intercepts K for the TCE Case

As illustrated in the supporting information, the difference K in chlorine isotope signatures of the initially formed chloride and *cis*-DCE at $f = 1$ is influenced by two factors. (i) The initial chlorine isotope ratio(s) $\delta^{37}\text{Cl}_{0,i}$ of the position(s), from which the respective product is formed (in contrast to PCE, the positions in TCE are not chemically equivalent and may show relevant variations of $^{37}\text{Cl}/^{35}\text{Cl}$ between each other); (ii) the kinetic isotope effect from the reaction (primary for Cl^- , secondary for *cis*-DCE).

Even though this kinetic isotope effect information is desirable, a direct interpretation like in the case of PCE is not possible because TCE internal isotope distributions cannot experimentally be determined. In contrast to interpretations of the PCE data, insight into position-specific chlorine isotope effects of TCE is therefore *not* given by the intercepts of Equations (24) and (25), but by the parameters $\epsilon_{TCE \rightarrow \text{chloride}}$ and $\epsilon_{TCE \rightarrow \text{cis-DCE}}$. Specifically, while in the case of PCE the parameter ϵ_{PCE} is the same for all product species, $\epsilon_{TCE \rightarrow \text{chloride}}$ and $\epsilon_{TCE \rightarrow \text{cis-DCE}}$ reflect isotope effects in the positions of TCE, from which the respective products are formed. These product enrichment trends are, therefore, a sensitive indicator whether the reaction of TCE involves one or two reactive positions (see Figure 1).

2.6 RESULTS AND DISCUSSION

2.6.1 Compound-Specific Carbon Isotope Effects in Reductive Dehalogenation of PCE to TCE by *Desulfitobacterium* sp. Strain Viet1 and of TCE to *cis*-DCE by *Geobacter Lovleyi* Strain SZ

Selective reductive dechlorination of PCE to TCE and chloride was performed with the microorganism *Desulfitobacterium* sp. strain Viet1, whereas *Geobacter lovleyi* strain SZ converted TCE to stoichiometric amounts of *cis*-DCE and inorganic chloride (note that the TCE data of the latter experiment are identical to those reported in Cretnik *et al.* [29]). Evaluation of compound-specific carbon isotope fractionation during reductive dechlorination of chlorinated ethenes gave fairly consistent results by application of the Rayleigh equation in its different forms. The carbon isotopic enrichment factor ϵ of the transformation was either directly obtained from the difference for the very first product fraction at $f = 1$ (from intercepts: $\epsilon_{PCE} \approx -19\text{‰}$, $\epsilon_{TCE} \approx -9\text{‰}$ see Figure 2). Alternatively, since the product contained less ^{13}C than the substrate from which it was formed, $^{13}\text{C}/^{12}\text{C}$ increased in the remaining reactant pool. Evaluation of reactant isotope data according to the Rayleigh equation [Equation (9)] was therefore an alternative way of determining ϵ (from reactant data: $\epsilon_{PCE} = -19.0\text{‰} \pm 0.9\text{‰}$, $\epsilon_{TCE} = -12.2\text{‰} \pm 1.2\text{‰}$). Finally, since this enrichment trend was reflected also in the steepness of the product $\delta^{13}\text{C}$ curves, ϵ could alternatively be determined from product isotope data according to Equation (13): $\epsilon_{PCE} = -21.1\text{‰} \pm 2.2\text{‰}$ (from TCE data); $\epsilon_{TCE} = -10.0\text{‰} \pm 0.8\text{‰}$ (from *cis*-DCE data, see Figure 2). After complete conversion at $f = 0$, the experimental data confirm that the product isotope signature has the same carbon isotope ratio as the starting material when the isotopic mass balance was closed.

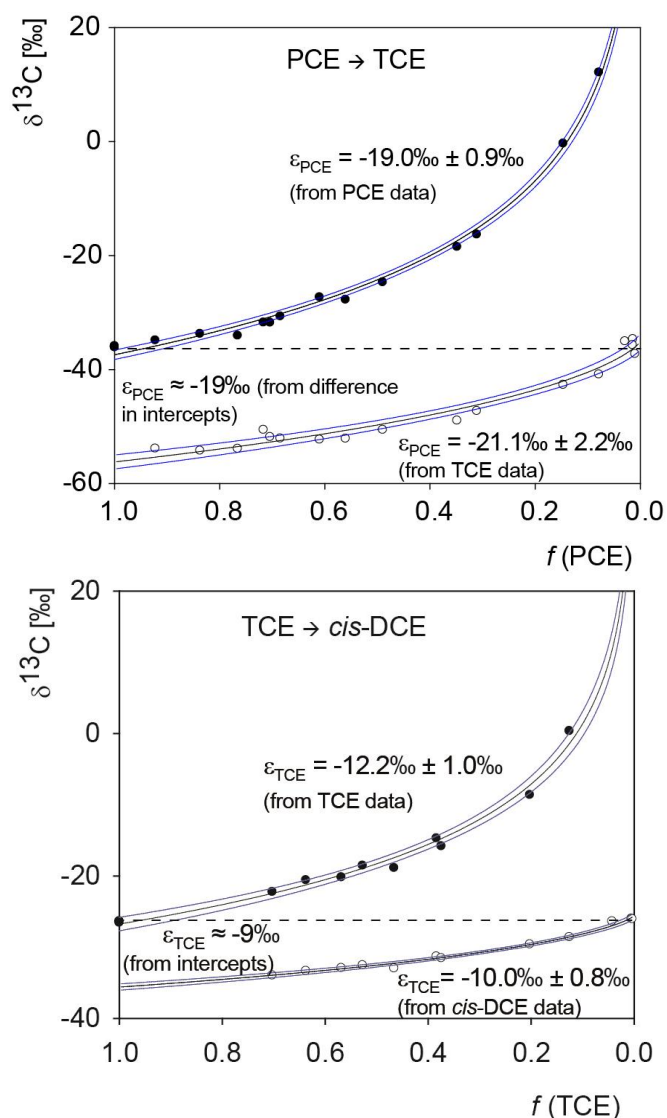


Figure 2. Carbon isotope data from degradation of PCE to TCE by *Desulfitobacterium* sp. strain Viet1, and of TCE to *cis*-DCE by *Geobacter lovleyi* strain SZ.

2.6.2 Compound-Specific and Position-Specific Chlorine Isotope Effects in Reductive Dehalogenation of PCE to TCE by *Desulfitobacterium* sp. Strain Viet1

For the selective reductive dechlorination of PCE to TCE and chloride by *Desulfitobacterium* sp. strain Viet1 chlorine isotope signatures were measured in PCE and TCE, whereas chloride isotope signatures were calculated based on the isotopic mass balance (see S.I.).

Enrichment factors ϵ_{PCE} were obtained from PCE reactant data ($-5.0\text{‰} \pm 0.1\text{‰}$) according to Equation (9), from chloride product data ($-4.1\text{‰} \pm 3.7\text{‰}$) according to equation (18), and from TCE product data ($-5.3\text{‰} \pm 0.3\text{‰}$) according to Equation (19) (uncertainties are 95%

confidence intervals). This confirms that the products TCE and chloride reflect the chlorine isotope enrichment trend of the four chemically equivalent positions of PCE from which they are formed. After full conversion at $f = 0$, the isotope signature of the released chloride must show an offset of $-3/4\varepsilon_{Diff}$ compared to the initial isotope signature of PCE, and the isotope signature of the formed TCE must show an offset of $1/4\varepsilon_{Diff}$, which the data confirm (Figure 3).

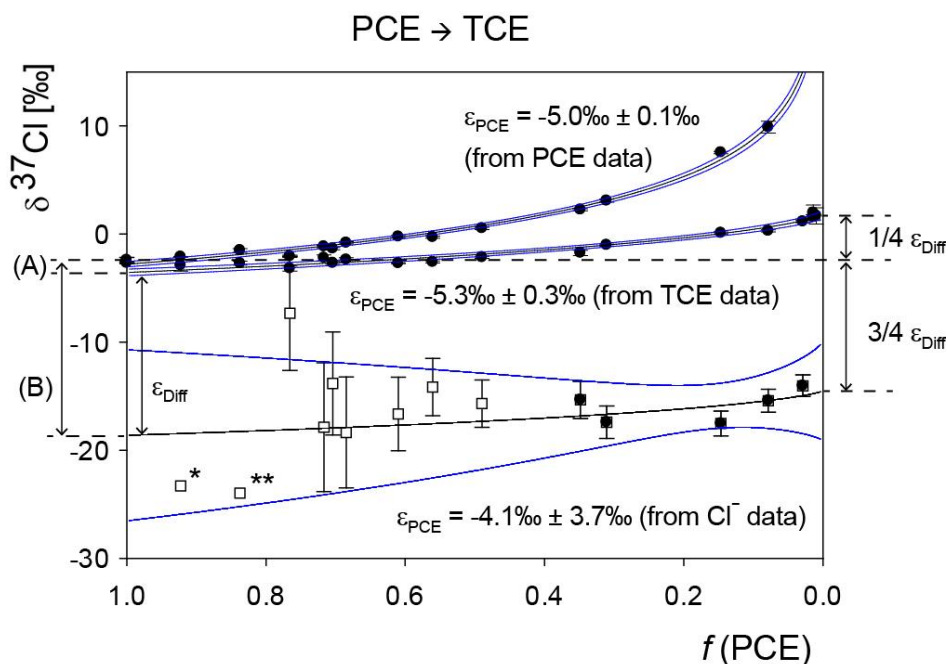


Figure 3: Chlorine isotope data of PCE degradation to TCE and chloride by *Desulfitobacterium* sp. strain Viet1 including fits in Sigma Plot according to the presented mathematical approach and 95% confidence intervals of the nonlinear regressions (for regression data see S.I.). Uncertainties for $\delta^{37}\text{Cl}_{\text{Cl}^-}$ were calculated by error propagation including uncertainties in $\delta^{37}\text{Cl}_{\text{PCE}}$, $\delta^{37}\text{Cl}_{\text{TCE}}$ and $f(\text{PCE})$ (see S.I.). Resultant uncertainties of the first two data points (error bars not shown) were 108% (*) and 24% (**). For regressions only data points with standard errors smaller than 2‰ were considered (black symbols).

In contrast to the isotope pattern of carbon, these intercepts between PCE as starting material and the instantaneously formed products reveal additional information. In the case of a one-step scenario, the secondary and primary isotope effects are accessible from the intercepts according to Figure 4. The secondary chlorine isotope effect with ε_{sec} of $-1.0\text{‰} \pm 0.5\text{‰}$ (standard error) is obtained in the intercept (A) as average of the three non-reacted chlorine substituents that remain in TCE. The primary chlorine isotope effect of

$-16.0\% \pm 4.9\%$ (standard error) is extracted from the isotope signature of the instantaneously formed chloride at the beginning of the reaction in the intercept (B).

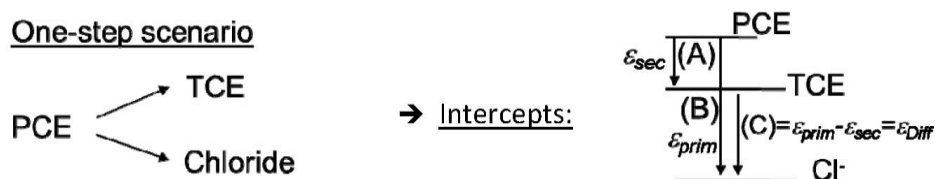


Figure 4: Interpretation of chlorine isotope data in a one-step scenario with respect to intercepts between PCE, TCE and chloride of the applied mathematical fits.

In an alternative approach the primary isotope effect may be extracted in higher precision when considering that the enrichment factor of PCE is a weighted average of primary and secondary effects:

$$\varepsilon = \frac{\varepsilon_{\text{prim}} + \varepsilon_{\text{sec},1} + \varepsilon_{\text{sec},2} + \varepsilon_{\text{sec},3}}{4} \quad (30)$$

The average secondary isotope effect is further given by

$$(A) = \varepsilon_{\text{sec,avg}} = \left(\frac{\varepsilon_{\text{sec},1} + \varepsilon_{\text{sec},2} + \varepsilon_{\text{sec},3}}{3} \right) = -1.0\% \pm 0.5\% \text{ (standard error)} \quad (31)$$

so that the primary isotope effect in PCE can be calculated:

$$\varepsilon_{\text{PCE}} = \frac{\varepsilon_{\text{prim}}}{4} + \left(\frac{\varepsilon_{\text{sec},1} + \varepsilon_{\text{sec},2} + \varepsilon_{\text{sec},3}}{3} \right) \frac{3}{4} \quad (32)$$

$$\Rightarrow \varepsilon_{\text{prim}} = \left(\varepsilon_{\text{PCE}} - (A) \frac{3}{4} \right) \cdot 4 = -17.0\% \pm 1.6\% \text{ (standard error)}$$

In contrast, if a two-step scenario prevails, no *absolute* values are obtained, but instead only the *difference* between primary and secondary isotope effects is accessible from the intercepts of the two products TCE and chloride as illustrated in Figure 5.

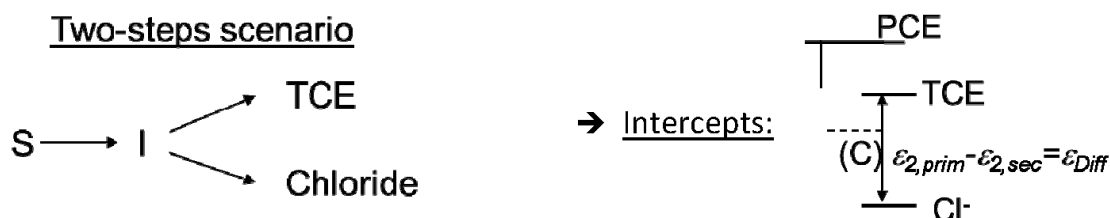


Figure 5: Interpretation of chlorine isotope data in a two-step scenario with respect to intercepts between PCE, TCE and chloride of the applied mathematical fits.

In this case, the observed isotope effect of PCE with $-5.0‰ \pm 0.1‰$ reflects the first step to the intermediate (I). A second rate-limiting step forms TCE and Cl^- . The difference between primary and secondary chlorine isotope effects for the second step is obtained from the difference of the intercepts (ϵ_{Diff}) with $-16.3‰ \pm 1.4‰$ (standard error).

Independent of the prevailing scenario, the difference between primary and secondary isotope effects in reductive dehalogenation of PCE by *Desulfitobacterium* sp. strain Viet1 can therefore be determined as $-16.3‰ \pm 1.4‰$. This indicates that primary chlorine isotope effects are of significantly larger magnitude than secondary isotope effects. In the case of the first scenario (one-step reaction), the exact value of the primary isotope effect ($-17.0‰ \pm 1.6‰$) would even be directly accessible, as well as the average of all secondary isotope effects ($-1.0‰ \pm 0.5‰$), which would be smaller by an order of magnitude.

2.6.3 Compound-Specific and Position-Specific Chlorine Isotope Effects in Reductive Dehalogenation of TCE to *cis*-DCE by *Geobacter lovleyi* Strain SZ

Geobacter lovleyi strain SZ converted TCE to stoichiometric amounts of *cis*-DCE and inorganic chloride. Compound-average chlorine isotope values were measured for TCE and *cis*-DCE, and calculated for chloride based on the closed isotopic mass balance (see S.I.).

In the case of TCE, the intercepts do not provide useful information about primary and secondary isotope effects because the three positions are distinguishable and TCE may have an unequal isotope distribution, which cannot be directly measured. For instance, if the reactive position in TCE contains more $^{37}\text{Cl}/^{35}\text{Cl}$ than the average molecule, a respective “lighter” signature would be found in the formed *cis*-DCE because the produced chloride pool would contain more $^{37}\text{Cl}/^{35}\text{Cl}$. Such a scenario would bias the interpretation of intercepts. The following discussion is therefore only based on the fitted parameters of ϵ , which are independent of the intercepts in the isotope patterns. Since these parameters reflect enrichment trends in molecular positions of the reactant (even if extracted from product data), they reflect precisely those reaction steps that lead up to and include the first irreversible step. Consequently, they incorporate the initial reaction steps and their interpretation does not require consideration of the one vs. two-step case distinction as for PCE above. Figure 6 shows the fit to the obtained enrichment factor of TCE, which is the average of enrichment factors from each of its three chlorinated positions according to:

$$\epsilon_{\text{TCE}} = \frac{1}{3} (\epsilon_{\alpha,\text{E}} + \epsilon_{\alpha,\text{Z}} + \epsilon_{\beta}) = -3.6‰ \pm 0.2‰ \text{ (95\% confidence interval)} \quad (33)$$

Since no 1,1-DCE is formed in *Geobacter lovleyi* cultures, the position Cl_β in TCE does not react and will strictly represent a β -secondary isotope effect that is directly passed on to the formed *cis*-DCE with the enrichment factor ε_β . In contrast, as discussed above, we considered the possibility that both α -chlorines may undergo C-Cl cleavage. The resultant product isotope enrichment for the formed *cis*-DCE was fitted in Sigma Plot according to Equation (25) derived previously to give

$$\varepsilon_{\text{TCE} \rightarrow \text{cis-DCE}} = -2.4\text{‰} \pm 0.3\text{‰} \text{ (95\% confidence interval)}$$

Likewise, data on chloride were fitted according to Equation (24) to yield

$$\varepsilon_{\text{TCE} \rightarrow \text{Chloride}} = -6.5\text{‰} \pm 2.5\text{‰} \text{ (95\% confidence interval)}$$

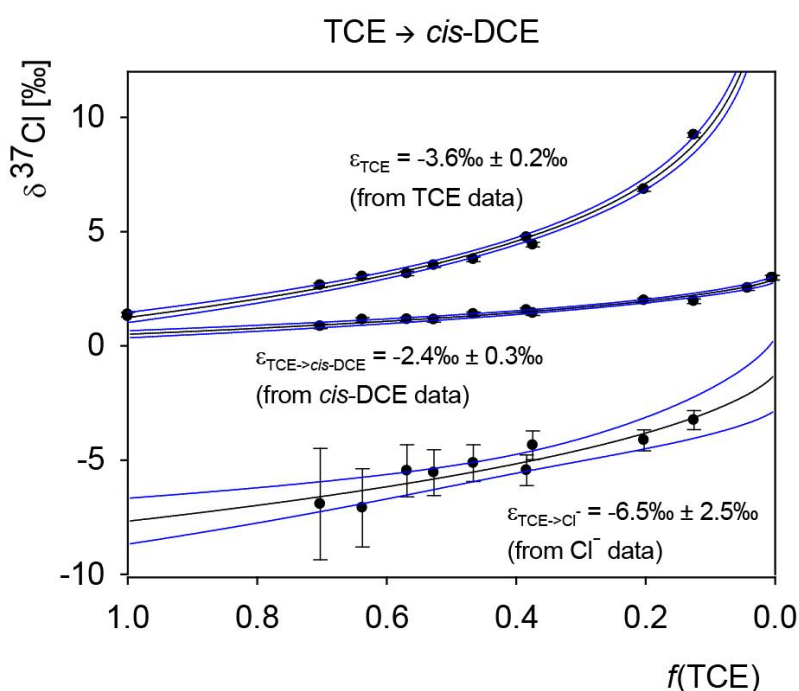


Figure 6: Chlorine isotope data of TCE degradation to *cis*-DCE and chloride by *Geobacter lovleyi* strain SZ including mathematical fits in Sigma Plot according to the presented mathematical approach. Error bars of individual data points indicate standard deviations; uncertainties of the regressions are 95% confidence intervals.

As derived above, our considerations show that these parameters reflect enrichment trends in the molecular positions of TCE according to

$$\varepsilon_{\text{TCE} \rightarrow \text{cDCE}} = \frac{1}{2} \left[\varepsilon_\beta + \left(x \cdot \varepsilon_{\alpha,Z} + (1-x) \varepsilon_{\alpha,E} \right) \right] \quad (23)$$

$$\varepsilon_{\text{TCE} \rightarrow \text{chloride}} = \left(x \cdot \varepsilon_{\alpha,E} + (1-x) \cdot \varepsilon_{\alpha,Z} \right) \quad (22)$$

Assuming that only $\text{Cl}_{\alpha,E}$ is reacting ($x = 1$), the obtained enrichment trend of the formed chloride would strictly reflect a primary isotope effect with $-6.5\% \pm 2.5\%$. It follows that the formed *cis*-DCE would reflect only the average of secondary isotope effects, resulting in a remarkably large magnitude of secondary isotope effects with $-2.4\% \pm 0.3\%$. Therefore, this scenario of strictly one reactive position contrasts strongly with insight from PCE data, both regarding the absolute magnitude of primary isotope effects (too small) and secondary effects (too large) as well as the difference ϵ_{Diff} between them (too small). It may be argued that small values (and small differences) could be attributable to commitment in enzyme catalysis, since our data relates to isotope effects on (V_{max}/K_m) rather than to elementary rate constants³⁴. This would affect the interpretation of the TCE data, because the products *cis*-DCE and chloride reflect position-specific effects in the reactant TCE, and such reactant data are subject to masking³⁵. The interpretation of the PCE data, in contrast, would not be affected, because product-curve intercepts reflect the differences in isotope effects in a situation of intramolecular competition, which is not subject to masking. While this could explain the small primary isotope effect of $-6.5\% \pm 2.5\%$ for TCE, it would be unable to rationalize the surprisingly large secondary isotope effect of $-2.5\% \pm 0.3\%$. Invoking commitment to catalysis would have to make this value even larger. Therefore, the assumption of only one reactive position appears to be questionable because it opposes the observation in PCE where a substantial difference in the magnitude of primary and secondary isotope effects was observed.

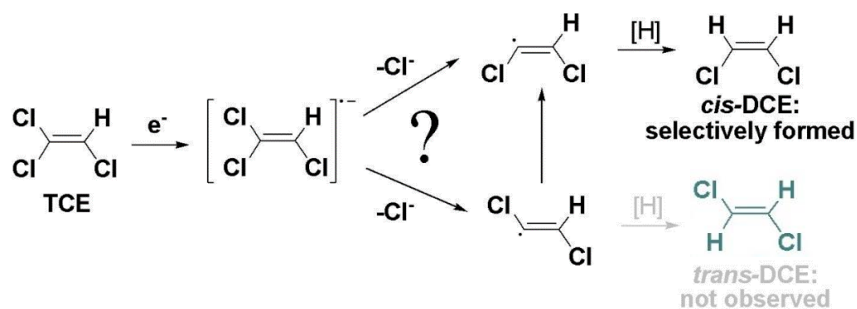
A more consistent picture arises when the possibility of two reactive positions is considered, as encountered for any $1 > x > 0$ in Figure 1. As illustrated in Figure 1, this scenario explains the relatively large isotope fractionation in the formed *cis*-DCE from a different angle, where a decrease in the difference between the isotope effects in cleaved chloride goes along with an increasingly even participation of both positions in the reaction. Therefore, the observation of the pronounced isotope effect of $-2.5\% \pm 0.3\%$ in the formation of *cis*-DCE with the relatively small difference to the isotope effect in the cleaved chloride of $-6.5\% \pm 2.5\%$ suggests that both positions react and primary and secondary chlorine isotope effects are reflected in both products.

Our results therefore indicate that the two chlorine substituents in the α -positions are accessible for reductive dechlorination of TCE. In this context, the selective formation of *cis*-DCE as the only dichloroethene-isomer is an intriguing observation, because it requires that:

(i) that two different positions react; (ii) different chlorovinyl-intermediates are formed, and (iii) these intermediates selectively react to *cis*-DCE despite their different stereochemistry.

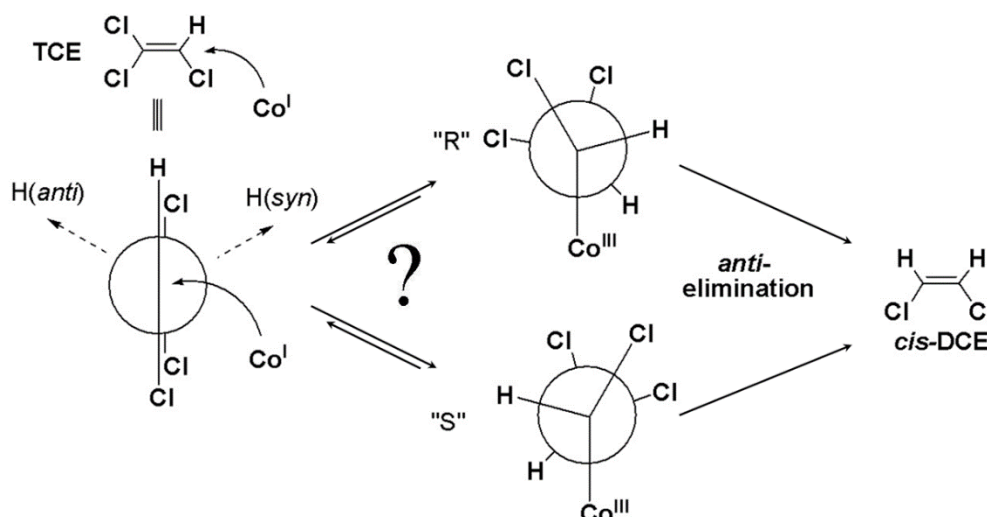
In previous mechanistic studies, the nucleophilic substitution of a chlorine substituent by the cobalt centre has been discussed as a potential pathway, leading to the formation of a dichlorovinyl-anion in the subsequent step of reduction^{38,39}. Respective anionic intermediates have been investigated in a computational study by Nonnenberg *et al.*, which suggest that these intermediates are not susceptible to interconversion²⁰, which would be necessary to explain the observed selectivity to form the *cis*-conformation. Based on our results, the scenario of a direct nucleophilic substitution can, therefore, be ruled out for reduction of TCE by *Geobacter lovleyi*.

Recent studies pointed out that radical intermediates are involved in reductive dechlorination with cobalamin as model system^{15,17}. The behaviour of chlorovinyl-radical species was investigated in the computational study by Nonnenberg *et al.*²⁰. From their calculations, the dichlorovinyl-radicals may indeed be susceptible to a selective interconversion from the *trans*- into the energetically preferred *cis*-conformation of DCE (Scheme 4). If this preference was further enforced by steric constraints at the catalytic site, this could explain an exclusive formation of *cis*-DCE observed in biodegradation experiments, which would otherwise even exceed thermodynamic predictions. According to the chlorine isotope effects from the presented biodegradation experiments of TCE, the involvement of radical intermediates therefore appears to be a possible pathway.



Scheme 4: Mechanistic proposal for dechlorination of TCE via a single electron transfer with selective formation of *cis*-DCE. Adapted from Nonnenberg *et al.* [20].

Based on theoretical considerations, such a conformational change could also occur in a pathway of nucleophilic addition, where the addition of the cobalt centre of the corrinoid would lead to a change of hybridisation from sp^2 to sp^3 and create a freely rotating bond (Scheme 5).



Scheme 5: Mechanistic proposal for dechlorination of TCE via nucleophilic addition followed by *anti*-elimination with selective formation of *cis*-DCE. Adapted from Pratt and van der Donk [21].

This intermediate was computed by Pratt and van der Donk ²¹, where they suggested that its minimum energy conformation may lead to a preferential formation of *cis*-DCE in the following step of *anti*-elimination. It is noteworthy that this scenario requires an extraordinary selectivity to engage this hypothesized conformation prior to the elimination reaction in order to produce exclusively *cis*-DCE. Furthermore, the pronounced chlorine isotope effects in TCE would indicate another exceptional feature of this scenario. In order to relate the obtained isotope effects to primary chlorine isotope effects, the elimination-step must be the rate-limiting step, while the first addition step would have to be reversible. The reversibility of the formation of the chlorinated alkylcobalt complex appears to be unlikely; however, since its formation is computed to have a notable driving force of -30.3 kcal/mol ¹⁴, and this reverse reaction would demand for the elimination of the hydrogen substituent. Therefore, the first step of the nucleophilic addition would not be predicted to be reversible.

With these considerations, the scenario of nucleophilic addition would combine several unusual attributes, including a strict conformational selectivity at an sp^3 hybridized carbon centre and an unexpectedly large magnitude of secondary chlorine isotope effects. Nonetheless, this pathway cannot be strictly ruled out as a possible transformation pathway.

2.7 CONCLUSIONS

With chlorine isotope effects from GC-IRMS measurements, our study brings forward a new perspective for investigating initial mechanisms of reductive chlorinated ethene dehalogenation. Mathematical equations accurately describe reactant and product isotope data, allow extracting position-specific chlorine isotope effect information and may serve as a benchmark for similar evaluations in the future. In reductive biotransformation of PCE, this evaluation allowed us to constrain the difference between primary and average secondary chlorine isotope effects to an unexpectedly large value of $-16.3\text{‰} \pm 1.4\text{‰}$ (standard error). This novel insight on primary and secondary chlorine isotope effects in chlorinated ethenes falls outside the range of typical chlorine isotope effects⁴⁰.

Our evaluation further allowed us to test whether one or two C-Cl bonds in TCE were reactive. In the first case (only one C-Cl position reacts), isotope values of chloride would be expected to exclusively reflect the primary isotope effect of the C-Cl bond cleavage, whereas isotope values of *cis*-DCE would reflect the secondary isotope effects in the remaining bonds. In contrast, in the second case both positions would take turns in reacting, they would end up in both products and the products would show a mixture of primary and secondary isotope effects. Their isotopic enrichment trends would, therefore, be more similar. Our data showed indeed only a relatively small difference between an average chlorine isotope effect of $-6.5\text{‰} \pm 2.5\text{‰}$ (95% confidence interval) in the C-Cl bond(s) from which chloride was formed, compared to an average effect of $-2.5\text{‰} \pm 0.3\text{‰}$ (95% confidence interval) in the C-Cl bonds that are precursors of *cis*-DCE. This small difference contrasts with the large difference between primary and secondary chlorine isotope effects observed in the PCE data. These findings suggest that two C-Cl bonds in TCE were reactive (case 2).

This insight, in turn, significantly constrained the mechanistic scenarios for the initial step in TCE reductive dehalogenation. Direct nucleophilic substitution via dichlorovinyl-anion intermediates could be ruled out for reduction of TCE by *Geobacter lovleyi*, whereas single electron transfer followed by radical formation, as well as nucleophilic addition followed by *anti*-elimination remain possible scenarios.

Finally, this insight can support current interpretations of dual element (C and Cl) isotope fractionation during TCE and PCE dehalogenation. Figure 7 shows the dual element isotope plots that are obtained when combining the carbon and chlorine data of the present study.

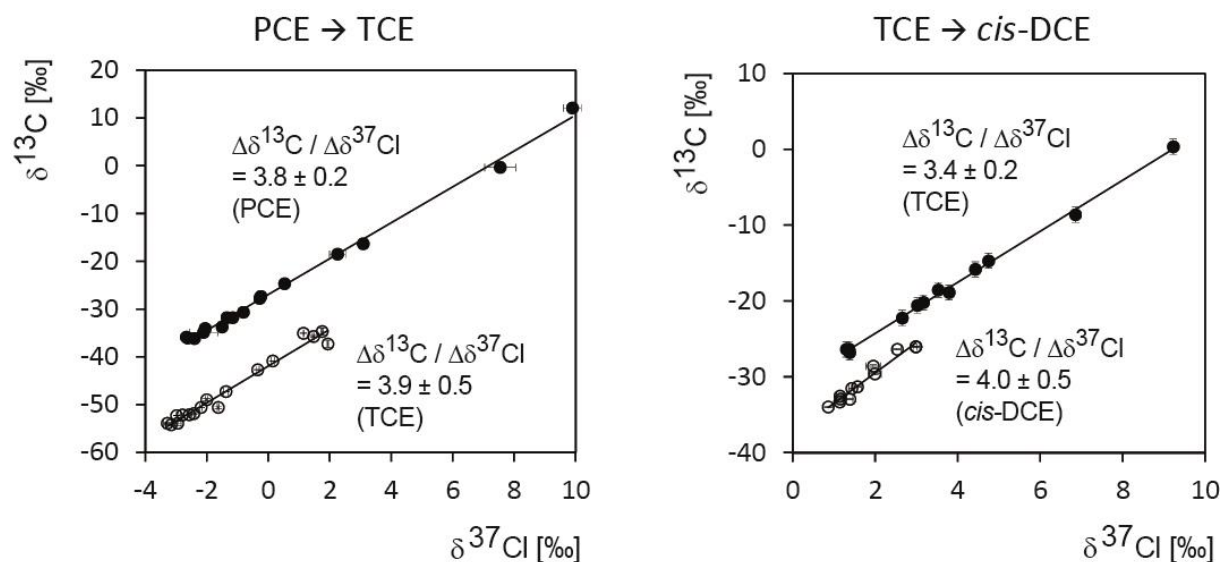


Figure 7: Dual element (carbon and chlorine) isotope plots for degradation of PCE to TCE by *Desulfitobacterium* sp. strain Viet1, and of TCE to *cis*-DCE by *Geobacter lovleyi* strain SZ. Error bars are standard deviations, uncertainties are 95% confidence intervals).

The value of $\Delta\delta^{13}\text{C}_{\text{TCE}}/\Delta\delta^{37}\text{Cl}_{\text{TCE}} = 3.4 \pm 0.2$ (95% confidence interval) during dehalogenation of TCE by *Geobacter lovleyi* is based on the same data reported in Cretnik *et al.* [29]. There, a remarkable similarity was observed compared to experiments with *Desulfitobacterium hafniense* and with vitamin B₁₂. The present study complements this finding with underlying mechanistic insight. Taken together, our results suggest that this insight may also be of relevance for reductive dehalogenation by vitamin B₁₂. In addition, our calculations can explain the different numerical values in the TCE degradation experiment when $\Delta\delta^{13}\text{C}/\Delta\delta^{37}\text{Cl}$ of TCE is compared to $\Delta\delta^{13}\text{C}/\Delta\delta^{37}\text{Cl}$ of *cis*-DCE. While the slope for TCE is equal to $\epsilon_{\text{TCE,carbon}}/\epsilon_{\text{TCE,chlorine}}$ ³¹, the slope for *cis*-DCE corresponds to $\epsilon_{\text{TCE,carbon}}/\epsilon_{\text{TCE} \rightarrow \text{cis-DCE,chlorine}}$. The observation that $\epsilon_{\text{TCE} \rightarrow \text{cis-DCE,chlorine}} < \epsilon_{\text{TCE,chlorine}}$ (see above) therefore explains the steeper slope for the *cis*-DCE data.

In the case of PCE, the dual element isotope slope of $\Delta\delta^{13}\text{C}_{\text{PCE}}/\Delta\delta^{37}\text{Cl}_{\text{PCE}} = 3.8 \pm 0.2$ (confidence interval) is, to our knowledge, the first value reported under defined conditions with a pure bacterial strain. The treatment of our study can explain in part why the value is greater compared to $\Delta\delta^{13}\text{C}_{\text{TCE}}/\Delta\delta^{37}\text{Cl}_{\text{TCE}}$ in the TCE experiment. In the compound-average chlorine ϵ_{PCE} of the PCE experiment, the primary isotope effect in the reacting C-Cl bond is “diluted” with three secondary isotope effects according to Equation (32). In the TCE experiment, only two secondary isotope effects contribute so that the primary isotope effect is more strongly represented in $\epsilon_{\text{TCE,chlorine}}$. This, in turn, leads to a greater proportion of $\epsilon_{\text{chlorine}}/\epsilon_{\text{carbon}}$ and a smaller

value of the dual element isotope slope, since $\varepsilon_{TCE,carbon}/\varepsilon_{TCE,chlorine} = \Delta\delta^{13}C_{TCE}/\Delta\delta^{37}Cl_{TCE}$. Finally, the value of $\Delta\delta^{13}C_{PCE}/\Delta\delta^{37}Cl_{PCE} = 3.8 \pm 0.2$ coincides with the range of 2.2 to 4.2 observed by Wigert *et al.*²⁸ in an enrichment culture from a contaminated site (calculated from their value $\varepsilon_{chlorine}/\varepsilon_{carbon} = 0.35 \pm 0.11$). The combined results give a first indication of the range of $\Delta\delta^{13}C_{PCE}/\Delta\delta^{37}Cl_{PCE}$ that is expected for reductive dechlorination of PCE and TCE at contaminated sites.

2.8 ACKNOWLEDGEMENTS

We thank Kris McNeill from the ETH Zürich and Stefan Haderlein from University of Tübingen for helpful discussions and critical comments. We further thank Wolfgang zu Castell-Rüdenhausen and Michael Hagen from the Institute of Bioinformatics, Helmholtz Zentrum Munich, for helpful initial discussions on alternative approaches to mathematical fitting. This work was supported by the German Research Foundation (DFG), EL 266/3-1, as well as by the Initiative and Networking Fund of the Helmholtz Association. A.B. was supported by a fellowship of the Minerva Foundation, Max-Planck-Gesellschaft.

2.9 REFERENCES

1. Gribble, G.W. Naturally occurring organohalogen compounds. *Acc. Chem. Res.* **1998**, *31*, 141–152.
2. Patai, S. *The Chemistry of the Carbon-Halogen Bond: Part 1*; John Wiley & Sons: London, UK; New York, NY, USA; Sidney, Australia; Toronto, ON, Canada, 1973.
3. Wang, C.B.; Zhang, W.X. Synthesizing nanoscale iron particles for rapid and complete dechlorination of TCE and PCBs. *Environ. Sci. Technol.* **1997**, *31*, 2154–2156.
4. Gillham, R.W.; O'Hannesin, S.F. Enhanced Degradation of Halogenated Aliphatics by Zero-Valent Iron. *Ground Water* **1994**, *32*, 958–967.
5. Holliger, C.; Wohlfarth, G.; Diekert, G. Reductive dechlorination in the energy metabolism of anaerobic bacteria. *FEMS Microbiol. Rev.* **1998**, *22*, 383–398.
6. Adrian, L.; Szewzyk, U.; Wecke, J.; Gorisch, H. Bacterial dehalorespiration with chlorinated benzenes. *Nature* **2000**, *408*, 580–583.
7. Grostern, A.; Duhamel, M.; Dworatzek, S.; Edwards, E.A. Chloroform respiration to dichloromethane by a Dehalobacter population. *Environ. Microbiol.* **2010**, *12*, 1053–1060.
8. He, J.Z.; Ritalahti, K.M.; Yang, K.L.; Koenigsberg, S.S.; Löffler, F.E. Detoxification of vinyl chloride to ethene coupled to growth of an anaerobic bacterium. *Nature* **2003**, *424*, 62–65.
9. Griffin, B.M.; Tiedje, J.M.; Löffler, F.E. Anaerobic microbial reductive dechlorination of tetrachloroethene to predominately trans-1,2-dichloroethene. *Environ. Sci. Technol.* **2004**, *38*, 4300–4303.
10. Duhamel, M.; Wehr, S.D.; Yu, L.; Rizvi, H.; Seepersad, D.; Dworatzek, S.; Cox, E.E.; Edwards, E.A. Comparison of anaerobic dechlorinating enrichment cultures maintained on tetrachloroethene, trichloroethene, *cis*-dichloroethene and vinyl chloride. *Water Res.* **2002**, *36*, 4193–4202.
11. Smidt, H.; de Vos, W.M. Anaerobic microbial dehalogenation. *Annu. Rev. Microbiol.* **2004**, *58*, 43–73.
12. Jensen, F.; Buchanan, D. Preparation of 1-Methyl-2,2-diphenylcyclopropylcobaloxime and Theoretical Considerations for Its Mode of Formation. *J. Am. Chem. Soc.* **1973**, 153–154.
13. Semadeni, M.; Chiu, P.C.; Reinhard, M. Reductive transformation of trichloroethene by cobalamin: Reactivities of the intermediates acetylene, chloroacetylene, and the DCE isomers. *Environ. Sci. Technol.* **1998**, *32*, 1207–1213.
14. Buhl, M.; Golubnychiy, V. On the intermediacy of chlorinated alkylcobalt complexes in the reductive dehalogenation of chloroalkenes. A first-principles molecular dynamics study. *Organometallics* **2007**, *26*, 6213–6218.
15. Glod, G.; Angst, W.; Holliger, C.; Schwarzenbach, R.P. Corrinoid-mediated reduction of tetrachloroethylene, trichloroethylene and trichlorofluoroethane in homogeneous

- aqueous solution: Reaction kinetics and reaction mechanisms. *Environ. Sci. Technol.* **1997**, *31*, 253–260.
16. Kliegman, S.; McNeill, K. Dechlorination of chloroethylenes by cob(i)alamin and cobalamin model complexes. *Dalton Trans.* **2008**, 4191–4201.
 17. Kliegman, S.; McNeill, K. Reconciling Disparate Models of the Involvement of Vinyl Radicals in Cobalamin-Mediated Dechlorination Reactions. *Environ. Sci. Technol.* **2009**, *43*, 8961–8967.
 18. Schumacher, W.; Holliger, C.; Zehnder, A.J.B.; Hagen, W.R. Redox chemistry of cobalamin and iron-sulfur cofactors in the tetrachloroethene reductase of *Dehalobacter restrictus*. *FEBS Lett.* **1997**, *409*, 421–425.
 19. Follett, A.D.; McNabb, K.A.; Peterson, A.A.; Scanlon, J.D.; Cramer, C.J.; McNeill, K. Characterization of Co-C bonding in dichlorovinylcobaloxime complexes. *Inorg. Chem.* **2007**, *46*, 1645–1654.
 20. Nonnenberg, C.; van der Donk, W.A.; Zipse, H. Reductive Dechlorination of Trichloroethylene: A Computational Study. *J. Phys. Chem. A* **2002**, *106*, 8708–8715.
 21. Pratt, D.A.; van der Donk, W.A. On the role of alkylcobalamins in the vitamin B₁₂-catalyzed reductive dehalogenation of perchloroethylene and trichloroethylene. *Chem. Commun.* **2006**, 558–560.
 22. Singleton, D.A.; Thomas, A.A. High-Precision Simultaneous Determination of Multiple Small Kinetic Isotope Effects at Natural-Abundance. *J. Am. Chem. Soc.* **1995**, *117*, 9357–9358.
 23. Perras, F.A.; Bryce, D.L. Direct Investigation of Covalently Bound Chlorine in Organic Compounds by Solid-State ³⁵Cl NMR Spectroscopy and Exact Spectral Line-Shape Simulations. *Angew. Chem. Int. Ed.* **2012**, *51*, 4227–4230.
 24. Thoreson, K.A. Probing Reduced Metal Center-Mediated Dechlorination Mechanisms through the Use of Model Complexes and Isotope Ratio Mass Spectrometry. Ph.D. Thesis, University of Minnesota, Minneapolis, MN, USA, June 2010.
 25. Shouakar-Stash, O.; Drimmie, R.J.; Zhang, M.; Frape, S.K. Compound-specific chlorine isotope ratios of TCE, PCE and DCE isomers by direct injection using CF-IRMS. *Appl. Geochem.* **2006**, *21*, 766–781.
 26. Elsner, M.; Hunkeler, D. Evaluating Chlorine Isotope Effects from Isotope Ratios and Mass Spectra of Polychlorinated Molecules. *Anal. Chem.* **2008**, *80*, 4731–4740.
 27. Abe, Y.; Aravena, R.; Zopfi, J.; Shouakar-Stash, O.; Cox, E.; Roberts, J.D.; Hunkeler, D. Carbon and Chlorine Isotope Fractionation during Aerobic Oxidation and Reductive Dechlorination of Vinyl Chloride and cis-1,2-Dichloroethene. *Environ. Sci. Technol.* **2009**, *43*, 101–107.
 28. Wiegert, C.; Mandalakis, M.; Knowles, T.; Polymenakou, P.N.; Aeppli, C.; Macháčková, J.; Holmstrand, H.; Evershed, R.P.; Pancost, R.D.; Gustafsson, Ö. Carbon and Chlorine Isotope Fractionation During Microbial Degradation of Tetra- and Trichloroethene. *Environ. Sci. Technol.* **2013**, *47*, 6449–6456.

29. Cretnik, S.; Thoreson, K.A.; Bernstein, A.; Ebert, K.; Buchner, D.; Laskov, C.; Haderlein, S.; Shouakar-Stash, O.; Kliegman, S.; McNeill, K.; *et al.* Reductive Dechlorination of TCE by Chemical Model Systems in Comparison to Dehalogenating Bacteria: Insights from Dual Element Isotope Analysis ($^{13}\text{C}/^{12}\text{C}$, $^{37}\text{Cl}/^{35}\text{Cl}$). *Environ. Sci. Technol.* **2013**, *47*, 6855–6863.
30. Kuder, T.; van Breukelen, B.M.; Vanderford, M.; Philp, P. 3D-CSIA: Carbon, Chlorine, and Hydrogen Isotope Fractionation in Transformation of TCE to Ethene by a Dehalococcoides Culture. *Environ. Sci. Technol.* **2013**, *47*, 9668–9677.
31. Hunkeler, D.; van Breukelen, B.M.; Elsner, M. Modeling Chlorine Isotope Trends during Sequential Transformation of Chlorinated Ethenes. *Environ. Sci. Technol.* **2009**, *43*, 6750–6756.
32. Amos, B.K.; Christ, J.A.; Abriola, L.M.; Pennell, K.D.; Löffler, F.E. Experimental Evaluation and Mathematical Modeling of Microbially Enhanced Tetrachloroethene (PCE) Dissolution. *Environ. Sci. Technol.* **2007**, *41*, 963–970.
33. Sung, Y.; Fletcher, K.F.; Ritalaliti, K.M.; Apkarian, R.P.; Ramos-Hernandez, N.; Sanford, R.A.; Mesbah, N.M.; Löffler, F.E. *Geobacter lovleyi* sp nov strain SZ, a novel metal-reducing and tetrachloroethene-dechlorinating bacterium. *Appl. Environ. Microbiol.* **2006**, *72*, 2775–2782.
34. Melander, L.; Saunders, W.H. *Reaction Rates of Isotopic Molecules*; John Wiley: New York, NY, USA, 1980.
35. Elsner, M.; Zwank, L.; Hunkeler, D.; Schwarzenbach, R.P. A new concept linking observable stable isotope fractionation to transformation pathways of organic pollutants. *Environ. Sci. Technol.* **2005**, *39*, 6896–6916.
36. Elsner, M. Stable isotope fractionation to investigate natural transformation mechanisms of organic contaminants: Principles, prospects and limitations. *J. Environ. Monit.* **2010**, *12*, 2005–2031.
37. Follett, A.D.; McNeill, K. Reduction of Trichloroethylene by Outer-Sphere Electron-Transfer Agents. *J. Am. Chem. Soc.* **2005**, *127*, 844–845.
38. McCauley, K.M.; Wilson, S.R.; van der Donk, W.A. Synthesis and characterization of chlorinated alkenylcobaloximes to probe the mechanism of vitamin B-12-catalyzed dechlorination of priority pollutants. *Inorg. Chem.* **2002**, *41*, 393–404.
39. Follett, A.D.; McNeill, K. Evidence for the Formation of a *cis*-Dichlorovinyl Anion upon Reduction of *cis*-1,2-Dichlorovinyl(pyridine)cobaloxime. *Inorg. Chem.* **2006**, *45*, 2727–2732.
40. Paneth, P. Chlorine kinetic isotope effects on enzymatic dehalogenations. *Acc. Chem. Res.* **2003**, *36*, 120–126.

3

Reductive dechlorination of TCE by chemical model systems in comparison to dehalogenating bacteria: Insights from dual element isotope analysis (^{13}C & ^{37}Cl)

Stefan Cretnik^a, Kristen A. Thoreson^a, Anat Bernstein^a, Karin Ebert^b, Daniel Buchner^b, Christine Laskov^b, Stefan Haderlein^b, Orfan Shouakar-Stash^c, Sarah Kliegman^d, Kristopher McNeill^d, Martin Elsner^{a,}*

^aInstitute of Groundwater Ecology, Helmholtz Zentrum München, Ingolstädter Landstr. 1, 85764 Neuherberg, Germany

^bUniversität Tübingen, Umweltmineralogie, Hölderlinstr. 12, 72076 Tübingen, Germany

^cDepartment of Earth Sciences, University of Waterloo, Waterloo, Ontario, Canada N2L 3G1

^dInstitute of Biogeochemistry and Pollutant Dynamics (IBP), ETH Zurich, CH-8092 Zurich, Switzerland

Published in: *Environmental Science & Technology*, **2013**, 47, 13, 6855-63.

3.1 ABSTRACT

Chloroethenes like trichloroethylene (TCE) are prevalent environmental contaminants, which may be degraded through reductive dechlorination. Chemical models such as cobalamine (vitamin B₁₂) and its simplified analogue cobaloxime have served to mimic microbial reductive dechlorination. To test whether *in vitro* and *in vivo* mechanisms agree, we combined for the first time carbon and chlorine isotope effect measurements of TCE. Degradation-associated enrichment factors ϵ_{carbon} and $\epsilon_{\text{chlorine}}$ were $-12.2\text{‰} \pm 0.5\text{‰}$ and $-3.6\text{‰} \pm 0.1\text{‰}$ with *Geobacter lovleyi* strain SZ; $-9.1\text{‰} \pm 0.6\text{‰}$ and $-2.7\text{‰} \pm 0.6\text{‰}$ with *Desulfitobacterium hafniense* Y51; $-16.1\text{‰} \pm 0.9\text{‰}$ and $-4.0\text{‰} \pm 0.2\text{‰}$ with the enzymatic cofactor cobalamin; $-21.3\text{‰} \pm 0.5\text{‰}$ and $-3.5\text{‰} \pm 0.1\text{‰}$ with cobaloxime. Dual element isotope slopes $m = \Delta\delta^{13}\text{C} / \Delta\delta^{37}\text{Cl}$ of TCE showed strong agreement between biotransformations (3.4 to 3.8) and cobalamin (3.9), but differed markedly for cobaloxime (6.1). These results (i) suggest a similar biodegradation mechanism despite different microbial strains, (ii) indicate that transformation with isolated cobalamin resembles *in vivo* transformation and (iii) suggest a different mechanism with cobaloxime. This model should therefore be used with caution. Our results demonstrate the strength of two dimensional isotope analyses to compare *in vitro* model reactions and natural transformations.

3.2 INTRODUCTION

Chloroethenes such as trichloroethylene (TCE) are commonly used industrial solvents, and are among the most ubiquitous groundwater contaminants.¹ In order to reduce the risk of exposure through groundwater, remediation techniques aim to remove these compounds under anoxic conditions through reductive dechlorination. However, such efforts do not always lead to the desired detoxification. Biotransformation sequentially replaces the chlorine substituents by hydrogen (hydrogenolysis), but only few organisms are capable of complete dechlorination.^{2,3} This leads to accumulation of toxic degradation products such as *cis*-dichloroethylene (*cis*-DCE) at contaminated sites.⁴

Ultimately, product formation is determined by the underlying reaction chemistry. For chlorinated ethylenes, cobalamin (vitamin B₁₂), which is the active cofactor of dehalogenase enzymes (Figure 1), has been investigated in detail.^{5,6} Nucleophilic substitution by Co(I), nucleophilic addition of Co(I),⁷ and single electron transfer have been brought forward as possible initial mechanisms.^{8,9} Investigations used a broad set of tools and include work with enrichment cultures,¹⁰ pure microorganisms,¹¹ studies with purified dehalogenases,^{12,13} and on the most fundamental level, with chemical model reactants to mimic putative dehalogenation mechanisms.^{8,14,15} Among the most prominent model systems for dehalogenase enzymes are cobaloxime and isolated cobalamin. Cobaloxime, a cobalt complex with a similar but simplified ligand structure compared to vitamin B₁₂ (Figure 1), has been successfully applied to synthesize putative intermediates with TCE and to study their subsequent reactions.⁸ However, in order to understand the authenticity of a model for the actual system, a more robust indicator is needed to compare underlying mechanisms of the systems.

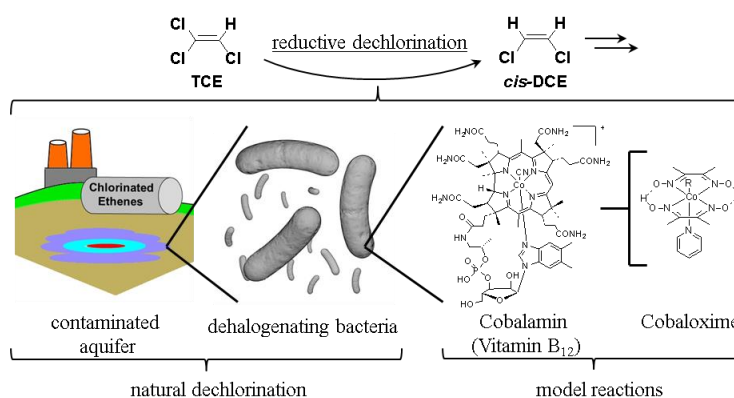


Figure 1: Reductive dechlorination of TCE to *cis*-DCE in different experimental systems, reaching from environmental scenarios (left) to chemical model reactants (right).

The work presented in this study aims to compare the mechanisms of the representative systems through measurements of dual element ($^{13}\text{C}/^{12}\text{C}$, $^{37}\text{Cl}/^{35}\text{Cl}$) kinetic isotope effects. Isotope effects serve as a direct indicator for different initial reaction mechanisms, since the magnitude of isotope effects depends on the order and manner (i.e., transition state structure) of chemical bond breakage or bond formation. Position-specific isotope effect studies with labeled substrate have a long tradition in chemistry, but require dedicated synthesis.¹⁶ In comparison, recent developments in gas chromatography coupled to isotope ratio mass spectrometry (GC-IRMS) have made it possible to measure compound-specific isotope effects of environmental contaminants with much greater ease. Measurements can be conducted at natural isotopic abundance meaning that no label is required and the analysis can be conducted on environmental samples. In exchange, isotope effects are not position-specific, but reflect the compound average. On the other hand, compound-specific isotope effects can be measured for multiple elements. When changes in compound-specific isotope values (e.g., $^{13}\text{C}/^{12}\text{C}$ versus $^2\text{H}/^1\text{H}$) are visualized in dual element isotope plots, the given slopes correspond to characteristic combinations of compound-specific isotope effects, which relate to the respective mechanisms.

Such dual element isotope representations have the additional advantage that their slopes are remarkably insensitive towards masking. Masking occurs when observable (apparent) kinetic isotope effects (A)KIE decrease because other steps become rate-determining (e.g., mass transfer, substrate binding to enzymes (“commitment to catalysis”)).^{17,18} While the effect can be dramatic for isotope effects of one element, slopes in dual element isotope plots often remain constant. The reason is that the additional steps often do not show element-specific isotope effects themselves so that KIE of both elements decrease in the same proportion.¹⁹ If these steps do show isotope effects, (A)KIE is the weighted average of them and depends on respective relative rates.²⁰ Therefore, dual isotope plots have the potential to bridge the gap between model and real life systems, since (i) identical transition states result in the same slope, whereas (ii) different slopes are indicative of different mechanisms, or may reflect a change in kinetics towards other rate-determining steps.²⁰ Such information has the potential to demonstrate similarities, and to uncover differences, in the (bio)chemical reaction mechanisms in different experimental systems.

Contrasting with the insight obtained for other environmental contaminants,²¹⁻²³ such an approach has not been possible for chloroethenes until recently. While routine compound-specific isotope analysis of chlorinated ethylenes has been well established for carbon,²⁴ it had

yet to be achieved for chlorine and hydrogen. An analytical breakthrough has been brought about by the latest developments in compound-specific chlorine isotope analysis.^{25,26,27} By now, online measurements of compound-specific chlorine isotope signatures²⁷, chlorine isotope fractionation^{28,29} and dual isotope plots of carbon and chlorine are within reach.^{30,31}

The objective of this study was, therefore, to measure dual element ($^{13}\text{C}/^{12}\text{C}$, $^{37}\text{Cl}/^{35}\text{Cl}$) isotope measurements of TCE for the first time in some of the most relevant experimental systems for reductive dehalogenation. We investigated biodegradation with different dehalogenating strains (i) *Geobacter lovleyi* strain SZ and (ii) *Desulfitobacterium hafniense* Y51, (iii), transformation by the enzymatic cofactor cobalamin and (iv) by the simplified chemical model system cobaloxime.^{32,15} Differences in dual element isotope slopes are discussed with respect to the questions (a) if microbial strains with substantial biological differences employ similar reaction mechanisms for degradation of TCE, and (b) how authentic *in vivo* transformations are reflected by their corresponding *in vitro* model systems.

3.3 MATERIALS AND METHODS

Chemicals

Cobalamin (Acros), dimethylglyoxime (Alfa Aesar), pyridine (Alfa Aesar), zinc (20-30 mesh; Sigma Aldrich), TiCl_3 (15% in 10% HCl; Merck), $\text{Co}(\text{OAc})_2 \cdot 4\text{H}_2\text{O}$ (Alfa Aesar), dimethoxyethane (Alfa Aesar), sodium citrate (Sigma Aldrich) and tris(hydroxymethyl)-aminomethane (Sigma) were used as received. Trichloroethene was purchased from Dow, PPG California and Merck.

Biodegradation with *Geobacter lovleyi* Strain SZ

Biodegradation experiments were carried out using the microbial strain *Geobacter lovleyi* strain SZ, purchased from the German Collection of Microorganisms and Cell Cultures (DSMZ, Germany). This strain reductively dechlorinates TCE to the final product *cis*-DCE. A growth medium was prepared according to DSMZ instructions, medium 732, with the exception that neither hexadecane nor perchloroethylene was added to the medium. The growth medium for the experiment was prepared in glass bottles (250 ml), equipped with Mininert valves (Supelco, Bellefonte, Pennsylvania, USA), and filled with 150 ml of medium, leaving a headspace of 40%. The bottles were amended with 10 μl of neat TCE and constantly shaken on a horizontal shaker at 120 rpm for four days. Inoculation was carried out by adding

14 ml of active culture, which was previously grown in a similar medium. To eliminate carry-over of the degradation product (*cis*-DCE) to the fresh medium, the media with the culture that was used for inoculation was flushed with N₂/CO₂ gas stream (80/20%) for 5 hours prior transferring to the fresh medium. A complete removal of chloroethenes after degassing was controlled by GC-FID measurements. This procedure was followed for three biological replicates in the main degradation experiment (“experiment 2”). Abiotic control batches were prepared similarly, but without inoculation of the active culture. In preliminary experiments, a similar procedure was followed with the exception that they were conducted in serum bottles closed with Viton stoppers (“experiment 1”). Sampling was carried out 20 min after inoculation for the initial sample, and at given time points along the degradation. A total sample volume of 7 ml was taken with a glass syringe (Hamilton), which was distributed in portions of 1 ml each into 7 amber vials with an active volume of 1.6 ml. In order to stop biological activity, the vials were spiked with 50 µl of NaOH (1M) and closed with PTFE-lined screw caps. All vials were frozen upside down for subsequent isotope analysis, except one vial, which was used immediately for concentration analysis.

Biodegradation with *Desulfitobacterium hafniense* Strain Y51

Biodegradation experiments at University of Tuebingen were carried out using the microbial strain *Desulfitobacterium hafniense* Y51, which degrades TCE to the final product *cis*-DCE. A growth medium was prepared according to modified DSMZ instructions medium 720. The growth medium for the experiment was prepared in glass serum bottles (560 ml) filled with 500 ml of medium, leaving a headspace of 11%. The bottles were closed with butyl stoppers. The bottles were amended with 25 µl of neat TCE and constantly shaken on a horizontal shaker at 120 rpm for 12 hours. Inoculation was carried out by adding 10 ml of active culture, which was previously grown on a similar medium with pyruvate as electron donor and TCE as electron acceptor. To eliminate carry-over of the degradation products (TCE and *cis*-DCE) to the fresh medium, the media with the culture that was used for inoculation was flushed with N₂/CO₂ gas stream (80/20%) for 1 hour prior transferring to the fresh medium. Complete removal of chloroethenes after degassing was controlled by GC-MS measurements. This procedure was followed for three biological replicates in the degradation experiments. One abiotic control batch was prepared similarly, but without inoculation of the active culture. Sampling was carried out before inoculation for the initial concentration and at given time points along the degradation. For concentration analysis, 500 µl of aqueous sample

were taken with a gastight glass syringe (Hamilton), distributed into 10 ml crimp vials (amended with 5 ml milipore water and 100 μ l H₃PO₄) and crimped with aluminium crimp caps with PTFE septum. For isotope analysis a total sample volume of 10 ml was taken with a gastight glass syringe (Hamilton), which was distributed in portions of 1 ml each into ten amber vials with an active volume of 1.9 ml. In order to stop biological activity, the vials were spiked with 50 μ l of NaOH (10M) and closed with PTFE-lined screw caps. All vials were frozen upside down for subsequent carbon isotope analysis. Two vials were shipped to Munich on dry ice for chlorine isotope analysis.

Cobalamin

Aqueous stock solution of Ti(III)citrate solutions was prepared from tris(hydroxymethyl)-aminomethane (8 g), sodium citrate (16 g) and TiCl₃ (25 ml; 10% in HCl) under anoxic conditions in 50 ml of degassed ultrapure H₂O.³³ Addition of Na₂CO₃ followed to adjust to pH 9. Cobalamin (100 μ M, 0.027 g, 19.9 μ mol) and tris(hydroxymethyl)aminomethane (90 mM, 2.18 g, 18.0 mmol) were weighed into a glass bottle of 250 ml, and transferred into an anoxic chamber. Here aqueous TCE stock solution (190 ml, 0.58 mM) was added. The bottle was closed with a mininert valve (Supelco, Bellefonte, Pennsylvania, USA) and constantly shaken on a horizontal shaker at 120 rpm for 4 h. To initiate the reaction, 10 ml of the Ti(III)citrate stock solution were added. Sampling volumes of 1 ml were taken at given time points and diluted 1:10 in H₂O. From these solutions, headspace vials were prepared directly for concentration analysis; the remaining volume was frozen for isotope analyses. Two experimental replicates were performed and measured according to this preparation. A similar procedure, but without the addition of cobalamin, was followed as a negative control to exclude any other processes of TCE reduction.

Cobaloxime

A stock solution of dimethylglyoxime (dmgH; 4.7 g, 81 mM) and pyridine (py, 4.85 ml, 120 mM) was prepared in 500 ml of dimethoxyethane (glyme). In total, ten 100 ml sealed reaction vessels were evacuated, back-filled with N₂ and charged with 25 ml of the dmG/py stock solution under N₂ flow. Co(OAc)₂·4H₂O (0.25 g; 1.0 mmol) and granular Zn (2.0 g; 30.6 mmol) were added using a glass funnel. The vessels were then sealed under N₂ flow, and placed in an oil bath for 60 min at 40 °C to complete the reduction. After reduction, the vessels were cooled in an ice-water bath prior to the addition of neat TCE in varying molar

ratios relative to cobalt of 10; 6.7; 5.0; 3.0; 2.0; 1.8; 1.5; 1.3; 1.2 and 1.1 respectively to each vessel. Subsequently, the reaction was heated in a closed vessel at 40 °C in an oil bath for 16 hours with constant stirring. A colour change into a red-orange indicated the formation of the chlorovinylcobalt complex as reported in Follett et al. 2007. After cooling, the vessel was transferred into an anoxic glove box. Samples were taken with a glass syringe by filling two amber glass vials with 1.6 ml of liquid without headspace.

From these samples 20 µl were dissolved in 2 ml of aqueous Ti(III)citrate (40 mM) solution present in headspace vials with a total volume of 10 ml. The vials were quickly closed after addition and shaken for 1h. In total, nine vials were prepared in this way. Two of them served for concentration measurements, the others were frozen for isotope analysis. A similar procedure was followed in the absence of cobalt, as a negative control to exclude any other processes of TCE reduction.

Concentration measurements

TCE and *cis*-DCE concentrations in the biodegradation experiments were measured by a gas chromatograph equipped with flame ionization detector (GC-FID, Hewlett Packard 5890 Series II) equipped with a 30 m VOCOL column (Supelco, Bellefonte, Pennsylvania, USA) 0.25 mm inner diameter, with a film thickness of 1.5 µm and operated with nitrogen as carrier gas at 1.6 ml/min. Automated headspace injections of 1 ml from 10 ml headspace vials were carried out using a CombiPal Autosampler (CTC Analytics), and an injector temperature on the GC of 200 °C. For cobaloxime experiments, the temperature program started at 40 °C (14 min) and increased at 60 °C/min to 200 °C (2 min). For cobalamin experiments the temperature program started at 45 °C, increasing at 25 °C/min to 90 °C (5 min) and increasing at 60 °C/min to 180 °C (1 min). For the biodegradation experiments, the temperature program started at 85 °C (0.3 min), increasing at 40 °C/min to 140 °C (2.70 min), and at 40 °C/min to 180 °C (1 min). One-point calibrations were performed along each measurement using TCE solutions with defined concentrations. The resulting total relative error in concentrations was estimated as ±10%.

TCE and *cis*-DCE concentrations in experiments with *D. hafniense* were measured by a GC-MS system in SIM mode. An Agilent 7890A GC coupled to an Agilent 5975C quadrupole mass selective detector (Santa Clara, CA) equipped with a 60 m RTX-VMS column (Restek, Bellefonte, Pennsylvania, USA) 0.25 mm inner diameter, with a film thickness of 1.4 µm and operated with helium as carrier gas at 1 ml/min was used for measurements of TCE and *cis*-

DCE. Automated headspace injections of 500 µl from 10 ml headspace vials were performed using an automatic multipurpose sampler (Gerstel, Muelheim an der Ruhr, Germany), and an injector temperature on the GC of 200 °C. The temperature program started at 40 °C (2 min), increased at 25 °C/min to 110 °C (0 min) and further increased at 15 °C/min to 200 °C (5 min). Calibration curves were obtained using TCE solutions with defined concentrations between 0 and 1000 µg/l.

Stable Carbon Isotope Analysis

Compound Specific Isotope Analysis (CSIA) for carbon was conducted by injection of headspace samples on a GC-IRMS system (Thermo Fisher Scientific, Waltham, Massachusetts, USA) consisting of a Trace GC with a Pal autosampler (CTC Analytics), coupled to a MAT 253 IRMS through a GC/C III combustion interface. For biodegradation and samples of the cobaloxime experiment, the gas chromatograph was equipped with a 30 m VOCOL column (Supelco, Bellefonte, Pennsylvania, USA), 0.25 mm inner diameter, with a film thickness of 1.5 µm and operated with He carrier gas at 1.4 ml/min. The GC program started at 85 °C (8 min) and increased at 60 °C/min to 205 °C (1 min).

For cobalamin samples a 60 m DB624 column was used, 0.32 mm inner diameter (Agilent, Santa Clara, California). The GC program started at 70 °C (2 min), increasing at 30 °C/min to 120 °C (9 min), and increasing at 30 °C/min to 220 °C (0 min). The analytical uncertainty 2σ of carbon isotope measurements was $\pm 0.5\text{‰}$. An internal standard of TCE was used along the measurements with a carbon isotope signature ($\delta^{13}\text{C}$) of $-27.1\text{‰} \pm 0.2\text{‰}$. The given delta notation refers to the Vienna Pee Dee Belemnite international standard (VPDB) according to the equation:

$$\delta^{13}\text{C} = \frac{(^{13}\text{C}/^{12}\text{C}_{\text{Sample}} - ^{13}\text{C}/^{12}\text{C}_{\text{Standard}})}{^{13}\text{C}/^{12}\text{C}_{\text{Standard}}} \quad (1)$$

Compound-specific carbon isotope analyses in experiments with *D. hafniense* were performed using GC/IRMS. The GC/IRMS system consists of a Trace GC Ultra (Thermo Finnigan, Milan, Italy) coupled to a DeltaPLUS XP (Thermo FinniganMAT, Bremen, Germany) via a combustion interface (GC Combustion III, Thermo Finnigan MAT) operated at 940 °C. Headspace samples were enriched with SPME using a StableFlex-Fibre, covered with 85 µm Carboxen/Polydimethylsiloxan (Supelco, Bellefonte, USA). After a sorption time of 20 min at 35 °C the compounds were desorbed for 30 s. A 60 m x 0.32 mm RTX-VMX capillary column with a film thickness of 1.8 µm was used. Following temperature program was applied: 4 min

at 40 °C, 7 °C/min to 180 °C, held for 3 min, total time 27 min. An internal standard of TCE was used along the measurements with a carbon isotope signature ($\delta^{13}\text{C}$) of $-26.7\text{‰} \pm 0.1\text{‰}$

Stable Chlorine Isotope Analysis

Chlorine isotope analysis of TCE was performed according to a method adapted from Shouakar-Stash et al. (2006). In this new approach for GC/IRMS the TCE is directly transferred in the gas phase to the IRMS through the He carrier stream, where TCE is ionized and fragmented for isotope ratio measurements. The measurements were conducted at masses $m/z = 95, 97$ on a GC-IRMS system (Thermo Scientific, Waltham, Massachusetts, USA) consisting of a Trace GC that was connected to a MAT 253 IRMS with dual inlet system via a heated transfer line. The gas chromatograph was equipped with a 30 m VOCOL column (Supelco, Bellefonte, Pennsylvania, USA) with 0.25 mm inner diameter, a film thickness of 1.5 μm and operated with a He carrier gas at 1.4 ml/min. The GC program used started at 50 °C (7 min), increasing at 60 °C/min to 70 °C (2.70 min) and at 80 °C/min to 140 °C (0.10 min). External standards were measured daily for calibration of $\delta^{37}\text{Cl}$ values according to Bernstein *et al.*²⁷

Briefly, a reference gas of TCE is introduced via a dual inlet system at the end of each measurement. The conversion to delta values relative to the international reference Standard Mean Ocean Chloride (SMOC) was performed by an external two-point calibration analysing TCE-standards “Eil-1” and “Eil-2” with a chlorine isotope signature ($\delta^{37}\text{Cl}$) of +3.05‰ and -2.7‰ respectively,²⁷ as previously characterized in the Department of Earth Sciences, University of Waterloo.²⁶ Each of these standards was added in triplicates before, during and at the end of each sequence, in order to calibrate the obtained values of the samples with respect to SMOC. The analytical uncertainty 2σ of chlorine isotope analysis was $\pm 0.2\text{‰}$.

Evaluation of carbon and chlorine isotope fractionation

Isotope enrichment factors of carbon (ϵ_{C}) in TCE were evaluated using Sigma-Plot[®] with curve fittings ($r^2 > 0.96$) according to the Rayleigh equation:

$$\delta^{13}\text{C} = \delta^{13}\text{C}_0 + [\epsilon_{\text{C}} \cdot \ln f] \quad (2)$$

where $\delta^{13}\text{C}_0$ and $\delta^{13}\text{C}$ are carbon isotope values in the beginning and at a given time (t) respectively, and f is the fraction of substrate remaining at time t. Elsner and Hunkeler demonstrated that chlorine isotope fractionation also follows in good approximation to a

Rayleigh trend despite a high abundance of ^{37}Cl compared to ^{13}C .³⁴ Thus chlorine isotope data was treated similarly using the Rayleigh equation:

$$\delta^{37}\text{Cl} = \delta^{37}\text{Cl}_0 + [\varepsilon_{\text{Cl}} \cdot \ln f] \quad (3)$$

where $\delta^{37}\text{Cl}_0$ and $\delta^{37}\text{Cl}$ are chlorine isotope ratios in the beginning and at a given time (t) respectively. An apparent kinetic chlorine isotope effect (AKIE) may be estimated under the assumption of negligible secondary isotope effects from the following equation:

$$AKIE_{\text{Cl}} = \frac{1}{1 + (n \cdot \varepsilon_{\text{Cl}} / 1000)} \quad (4)^{34}$$

where n is the number of three chlorine atoms for TCE. Dual element isotope fractionation can be compared by (a) either considering the ratio of $\varepsilon_{\text{C}}/\varepsilon_{\text{Cl}}$ or (b) by plotting isotope values of $\delta^{13}\text{C}$ vs $\delta^{37}\text{Cl}$ (as shown in Figure 3). Uncertainties were obtained from 95% confidence intervals (CI).

3.4 RESULTS AND DISCUSSION

Isotope fractionation according to the Rayleigh equation

An overview of the obtained data is presented in Figure 2. It reflects the results of all experimental replicates, which were highly consistent. Pronounced carbon isotope effects of TCE were observed in all experiments. Biodegradation experiments with *Geobacter lovleyi* strain SZ and *Desulfitobacterium hafniense* Y51 showed enrichment factors of $\varepsilon_{\text{carbon}} = -12.2\text{‰} \pm 0.5\text{‰}$ and $-9.1\text{‰} \pm 0.6\text{‰}$, respectively. Although the value for *Geobacter lovleyi* is higher than reported by Cichoka *et al.* ($\varepsilon_{\text{carbon}} = -8.5\text{‰} \pm 0.6\text{‰}$), both values fall in the range of previously reported values for reductive biodegradation of TCE.^{35,36,37,38} The obtained value for cobalamin reactions of $-16.1\text{‰} \pm 0.9\text{‰}$ agrees with previously reported data of Slater *et al.* ($-16.5\text{‰} \pm 0.6\text{‰}$).³⁹ These data compare to an enrichment factor of the cob(D)aloxime reaction of $-21.3\text{‰} \pm 0.5\text{‰}$, to our knowledge the first reported for this reaction.

As expected, the significant carbon isotope enrichment factors indicate that the rate-limiting step of all investigated reactions involves the carbon atoms in TCE to some extent. However, a statement on the individual pathways remains elusive because masking effects potentially may decrease enrichment trends to an unknown degree. Consequently, the individual enrichment factors of one element may not be representative for the intrinsic isotope effects of the transformation, particularly with biotic systems. With these constraints, underlying mechanisms cannot be compared between experimental systems using isotope effects of only

one element. However, that obstacle can be overcome by including isotope information from a second element: chlorine.

For the first time, we report not only carbon but also chlorine isotope fractionation associated with biotransformation of TCE (Figure 2). All reactions feature pronounced chlorine isotope fractionation of TCE in a range of $\epsilon_{\text{chlorine}} = -2.7\text{‰}$ to -4.0‰ . When converting these bulk isotope effects into apparent kinetic isotope effects under the assumption of negligible secondary isotope effects (Equation 4) they would result in AKIE values between 1.008 and 1.012 reaching to the upper end of Streitwieser limits in C-Cl bonds.⁴⁰ This indicates that primary isotope effects are active in the investigated systems and that C-Cl bond cleavage is at least partially rate-limiting.

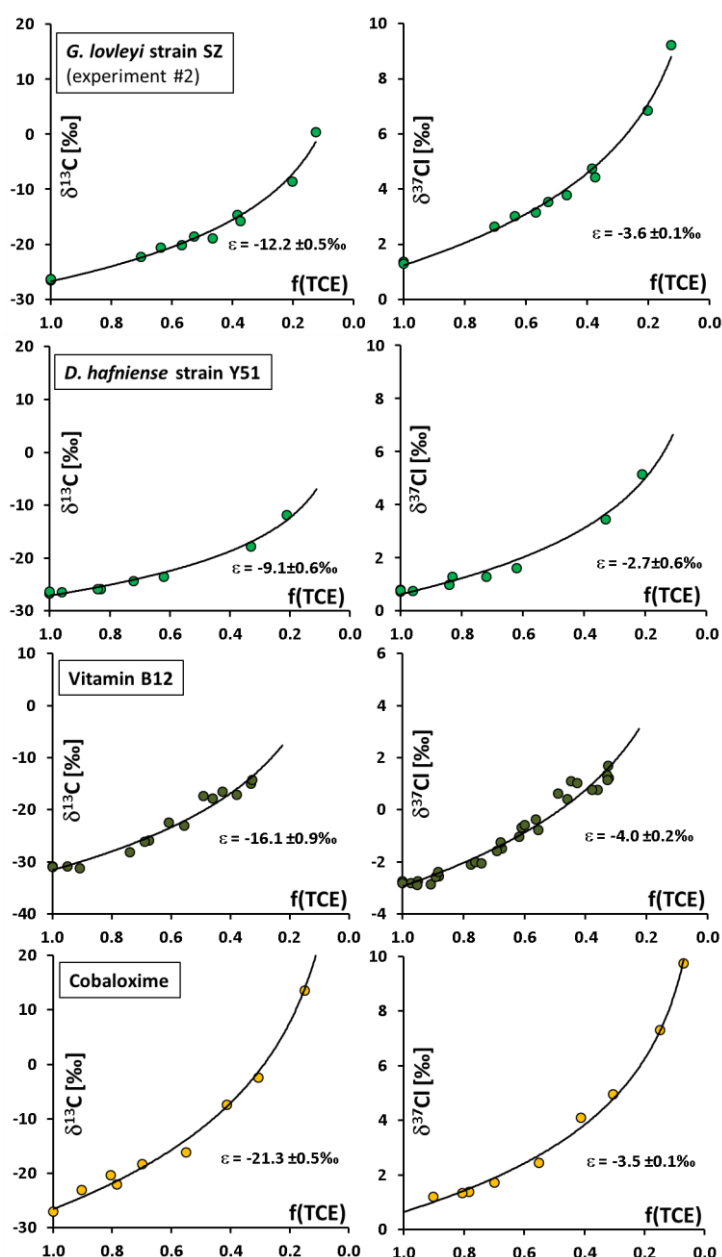


Figure 2:

Isotope fractionation patterns in TCE of $\delta^{13}\text{C}$ (left) and $\delta^{37}\text{Cl}$ (right) measured during degradation in the different experimental systems. The fraction of remaining TCE is presented as $f(\text{TCE})$ on the x-axis. Enrichment factors were extracted from curve fittings according to the Rayleigh equation (Eq. 1 and Eq 2.). Uncertainties for ϵ are 95% CI.

Dual Isotope approach

While the individual C and Cl isotope data alone do not allow a conclusive comparison of the given reactions of TCE, a different picture is given in the dual isotope plot in Figure 3. Slopes of biodegradation experiments (3.4 ± 0.2 , 3.4 ± 0.2 and 3.8 ± 0.2) and reaction with cobalamin (3.9 ± 0.2) are essentially indistinguishable, within the given 95% CI. In contrast, these results differ significantly from the trend observed with cobaloxime (6.1 ± 0.5). In the following, the implications of this result are discussed for the different experimental systems.

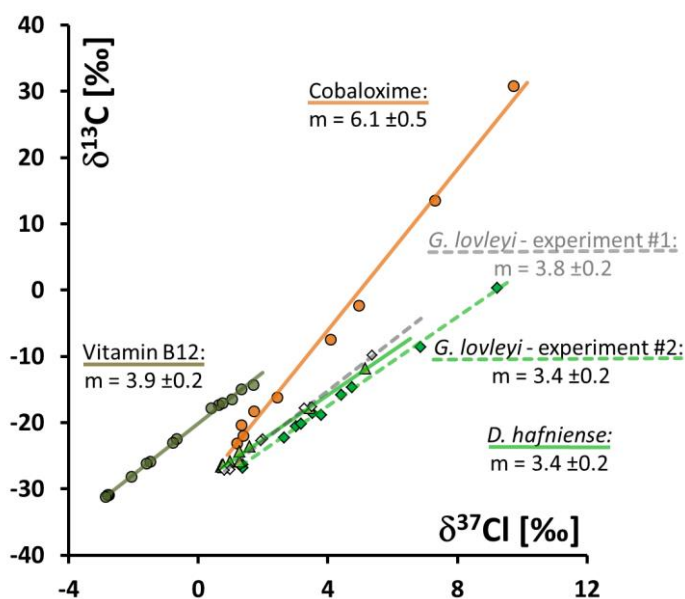


Figure 3:
Dual isotope plots of $\delta^{13}\text{C}$ versus $\delta^{37}\text{Cl}$ during degradation of TCE in the investigated experimental systems.

Biodegradation experiments

The study involves biodegradation experiments with two different strains of dehalorespiring bacteria, *Geobacter lovleyi* strain SZ and *Desulfitobacterium hafniense* strain Y51. Both microorganisms feature a metabolic pathway of degrading TCE strictly to *cis*-DCE as the final product. When comparing isotope fractionation during this reaction, a difference in ϵ_{C} of 3.1‰ and in ϵ_{Cl} of 0.9‰ was obtained between the two strains (Figure 2). Previous studies have addressed differences in carbon isotopic enrichment factors of TCE biodegradation in the context of possible variations in enzyme structures or kinetic processes such as transport and enzyme-substrate binding prior to the cleavage of the carbon-chlorine bond.^{36,18,35} Since such parameters may mask the kinetic isotope effect (KIEs) of a reaction, the observed variations are plausible but an interpretation from enrichment factors of only one element can be problematic.^{36,18,35}

In contrast, the good agreement of the slopes in their dual element isotope plots suggests that the δ -proteobacterium *Geobacter lovleyi* strain SZ and *Desulfitobacterium hafniense* Y51 share the same TCE degradation mechanism, despite their biological differences: The two strains belong to different branches of the phylogenetic tree, and have low similarities in their BlastP matches of dehalogenase enzymes.⁴¹ However, an important common feature is their dependency on cobalamin. The identical dual element isotope plots suggest that the rate limiting step in the C-Cl cleavage is likely to be similar in the two strains, which emphasizes once more the role of this cofactor in microbial dehalogenation.^{7,41} In this context, the value strength of the presented dual isotope approach becomes evident: While the observable KIEs of one element may decrease dramatically with the influence of masking effects, the ratio of KIEs from two elements remained constant, most likely because KIEs of both elements decreased in the same proportion.

Cobalamin

The individual carbon and chlorine isotope effects of TCE in the dechlorination mediated by cobalamin are larger than during biodegradation. Again, this observation may potentially indicate different mechanisms. Alternatively, it may indicate that the same mechanism prevailed but that masking simply decreases - and isotope effects increase - with diminishing cell-integrity so that effects became greater in the chemical reaction with cobalamin.^{18,42} Again, a comparison of dual isotope plots of cobalamin *in vitro* to the biotic reactions gave evidence for the second hypothesis. In this case the respective slopes match within their range of errors, suggesting that the transformation with isolated cobalamin occurs in a similar fashion as it does *in vivo* when it is incorporated in the dehalogenase enzyme.^{7,43} This may serve as an important reference in the use of this model system, since it is the first experimental confirmation that directly refers to the rate limiting step of the dechlorination.

A remarkable difference between the two systems, however, lies in the product formation: Whereas in biodegradation *cis*-DCE is selectively formed as final and only product, a more diverse set of products is found with cobalamin. Besides the major product *cis*-DCE, also 1,1-DCE; *trans*-DCE and others were observed here and in previous studies under identical conditions.^{44,7} Despite these differences, the rate limiting step in the reaction between TCE and the cobalt center appears to be the same in both experimental systems. This indicates that the formation of toxic versus harmless products is not yet determined in the initial rate-determining step, but rather in subsequent reactions of short-lived intermediates. Here,

another strength of the dual element isotope approach becomes evident compared to product studies: Isotope effects are diagnostic of the initial rate limiting step, allowing it to disentangle this step from subsequent steps of product formation. Based on these findings we propose that a putative initial intermediate formed from cobalamin and TCE has similar properties *in vitro* compared to the species formed at the active site of the enzyme. However, direct structural insights of this specific intermediate are missing.⁸

Cobaloxime

In previous studies cobaloxime has been employed as a simplified model of cobalamin.⁸ Key findings have included the ability to isolate a stable vinyl-cobalt complex upon reaction with TCE. Further, reduction of this species with Ti(III)citrate in protic solvents leads to selective formation of cis-DCE, similar to the biodegradation experiments.^{32,45} As a result a vinyl-cobalt species has been suggested as a putative reaction intermediate in the case of cobalamin. However, a verification of the reaction chemistry on a more fundamental level is still missing.

From the individual isotope effects in Figure 2 a notably high carbon isotope enrichment factor of $-21.3\text{‰} \pm 0.5\text{‰}$ was observed, while the fractionation in chlorine stayed in the range of the previously discussed systems with $-3.5\text{‰} \pm 0.2\text{‰}$. As mentioned before, a comparison of the reactions based on the individual isotope effects from Figure 2 can be problematic. A different picture arises if isotope effects of both elements are considered together in the dual element isotope plot (Figure 3). Contrasting with the slopes between 3.4 and 3.9 observed with cobalamin and the two bacterial strains, a significantly higher slope of 6.1 was obtained for the degradation of TCE with cobaloxime. The difference can be ascribed to the high enrichment factor of carbon, which indicates that the reaction pathway with cobaloxime involves a stronger participation of carbon in the rate-limiting step. The fact that stable complexes of TCE with cobaloxime can be synthesized may indicate a stronger affinity to form Co-C bonds, compared to cobalamin, where similar complexes are not known.⁸

With these considerations, our results point out differences in the rate-determining step of reductive dehalogenation of TCE when comparing the model system cobaloxime with cobalamin or biodegradation. Previous studies discuss single electron transfer or nucleophilic attack as potential mechanisms.^{7,9,8,33} With our new approach of dual element isotope analysis, more conclusive evidence may now be within reach when chemical model systems are investigated with known initial reaction mechanisms.

3.5 ENVIRONMENTAL SIGNIFICANCE

An exciting feature of the presented dual isotope approach is the possibility to directly compare transformation mechanisms of environmental scenarios, biotic transformations, and their putative chemical lab scale systems. Our results suggest that different microbial strains, as well as *in vitro* reactions with cobalamin, all share a common initial reaction step of TCE degradation. For cobalamin, previous studies have brought forward evidence for single electron transfer as the initial mechanism.^{7,33} This suggests that the same mechanism may be active in biodegradation. Since these strains are only two among a large variety of dehalogenating micro-organisms, however, different mechanisms in strains with other dehalogenase enzymes cannot be excluded. Neumann et al. hypothesized that the degradation with a purified dehalogenase enzyme involved nucleophilic attack.⁶ With dual element isotope analysis there is now a tool available to test such hypotheses and investigate if different microbial strains involve different dechlorination mechanisms, despite using the same cofactor cobalamin. In addition, our approach even allows comparing *in vitro* model reagents with natural transformations. Such information is not only important for process understanding from a fundamental scientific point of view, it is also essential when using the dual isotope approach to assess the fate of chlorinated compounds in the environment.^{3,28}

3.6 ACKNOWLEDGMENTS

This work was supported by the German Research Foundation (DFG), EL 266/3-1, as well as by the Initiative and Networking Fund of the Helmholtz Association. A.B. was supported by a fellowship of the Minerva Foundation, Max-Planck-Gesellschaft. K.E and D.B. were supported by the Landesgraduiertenförderungsgesetz LGFG of the state Baden-Württemberg. K.A.T, S.K. and K.M. gratefully acknowledge support from the US National Science Foundation (Grant no. CHE-0809575), as well as by funds from ETH Zurich.

3.7 REFERENCES

1. Fetzner, S., Bacterial dehalogenation. *Applied Microbiology and Biotechnology* **1998**, *50* (6), 633-657.
2. Dugat-Bony, E.; Biderre-Petit, C.; Jaziri, F.; David, M. M.; Denonfoux, J.; Lyon, D. Y.; Richard, J. Y.; Curvers, C.; Boucher, D.; Vogel, T. M.; Peyretailade, E.; Peyret, P., In situ TCE degradation mediated by complex dehalorespiring communities during biostimulation processes. *Microb. Biotechnol.* **2012**, *5* (5), 642-653.
3. Wiegert, C.; Aepli, C.; Knowles, T.; Holmstrand, H.; Evershed, R.; Pancost, R. D.; Macháčková, J.; Gustafsson, Ö., Dual Carbon-Chlorine Stable Isotope Investigation of Sources and Fate of Chlorinated Ethenes in Contaminated Groundwater. *Environmental Science & Technology* **2012**, *46* (20), 10918-10925.
4. Ellis, D. E.; Lutz, E. J.; Odom, J. M.; Buchanan, R. J.; Bartlett, C. L.; Lee, M. D.; Harkness, M. R.; DeWeerd, K. A., Bioaugmentation for Accelerated In Situ Anaerobic Bioremediation. *Environ. Sci. Technol.* **2000**, *34* (11), 2254-2260.
5. Lesage, S.; Brown, S.; Millar, K., A different mechanism for the reductive dechlorination of chlorinated ethenes: Kinetic and spectroscopic evidence. *Environmental Science & Technology* **1998**, *32* (15), 2264-2272.
6. Neumann, A.; Wohlfarth, G.; Diekert, G., Purification and Characterization of Tetrachloroethene Reductive Dehalogenase from *Dehalospirillum multivorans*. *J. Biol. Chem.* **1996**, *271* (28), 16515-16519.
7. Glod, G.; Brodmann, U.; Werner, A.; Holliger, C.; Schwarzenbach, R. P., Cobalamin-mediated reduction of *cis*- and *trans*-dichloroethene, and vinylchloride in homogeneous aqueous solution: reaction kinetics and mechanistic considerations. *Environmental Science and Technology* **1997**, *31* (11), 3154-3160.
8. Kliegman, S.; McNeill, K., Dechlorination of chloroethylenes by cob(i)alamin and cobalamin model complexes. *Dalton Transactions* **2008**, (32), 4191-4201.
9. Shey, J.; van der Donk, W. A., Mechanistic studies on the vitamin B-12-catalyzed dechlorination of chlorinated alkenes. *Journal of the American Chemical Society* **2000**, *122* (49), 12403-12404.
10. Duhamel, M.; Wehr, S. D.; Yu, L.; Rizvi, H.; Seepersad, D.; Dworatzek, S.; Cox, E. E.; Edwards, E. A., Comparison of anaerobic dechlorinating enrichment cultures maintained

on tetrachloroethene, trichloroethene, cis-dichloroethene and vinyl chloride. *Water Research* **2002**, *36* (17), 4193-4202.

11. Seshadri, R.; Adrian, L.; Fouts, D. E.; Eisen, J. A.; Phillippy, A. M.; Methe, B. A.; Ward, N. L.; Nelson, W. C.; Deboy, R. T.; Khouri, H. M.; Kolonay, J. F.; Dodson, R. J.; Daugherty, S. C.; Brinkac, L. M.; Sullivan, S. A.; Madupu, R.; Nelson, K. T.; Kang, K. H.; Impraim, M.; Tran, K.; Robinson, J. M.; Forberger, H. A.; Fraser, C. M.; Zinder, S. H.; Heidelberg, J. F., Genome sequence of the PCE-dechlorinating bacterium *Dehalococcoides ethenogenes*. *Science* **2005**, *307* (5706), 105-108.

12. Maillard, J.; Schumacher, W.; Vazquez, F.; Regeard, C.; Hagen, W. R.; Holliger, C., Characterization of the Corrinoid Iron-Sulfur Protein Tetrachloroethene Reductive Dehalogenase of *Dehalobacter restrictus*. *Appl. Environ. Microbiol.* **2003**, *69* (8), 4628-4638.

13. Neumann, A.; Siebert, A.; Trescher, T.; Reinhardt, S.; Wohlfarth, G.; Diekert, G., Tetrachloroethene reductive dehalogenase of *Dehalospirillum multivorans*: substrate specificity of the native enzyme and its corrinoid cofactor. *Archives of Microbiology* **2002**, *177* (5), 420-426.

14. Follett, A. D.; McNeill, K., Reduction of Trichloroethylene by Outer-Sphere Electron-Transfer Agents. *J. Am. Chem. Soc.* **2005**, *127* (3), 844-845.

15. McCauley, K. M.; Wilson, S. R.; van der Donk, W. A., Synthesis and characterization of chlorinated alkenylcobaloximes to probe the mechanism of vitamin B-12-catalyzed dechlorination of priority pollutants. *Inorg. Chem.* **2002**, *41* (2), 393-404.

16. Simon, H.; Palm, D., Isotopeneffekte in der organischen Chemie und Biochemie. *Angewandte Chemie* **1966**, *78* (22), 993-1007.

17. Northrop, D. B., The expression of isotope effects on enzyme-catalyzed reactions. *Annual Review of Biochemistry* **1981**, *50*, 103-131.

18. Nijenhuis, I.; Andert, J.; Beck, K.; Kastner, M.; Diekert, G.; Richnow, H. H., Stable isotope fractionation of tetrachloroethene during reductive dechlorination by *Sulfurospirillum multivorans* and *Desulfitobacterium* sp. Strain PCE-S and abiotic reactions with cyanocobalamin. *Appl. Environ. Microbiol.* **2005**, *71* (7), 3413-3419.

19. Elsner, M., Stable isotope fractionation to investigate natural transformation mechanisms of organic contaminants: principles, prospects and limitations. *J. Environ. Monit.* **2010**, *12* (11), 2005-2031.

20. Penning, H.; Cramer, C. J.; Elsner, M., Rate-Dependent Carbon and Nitrogen Kinetic Isotope Fractionation in Hydrolysis of Isoproturon. *Environ. Sci. Technol.* **2008**, *42* (21), 7764-7771.
21. Rosell, M.; Gonzalez-Olmos, R.; Rohwerder, T.; Rusevova, K.; Georgi, A.; Kopinke, F.-D.; Richnow, H. H., Critical Evaluation of the 2D-CSIA Scheme for Distinguishing Fuel Oxygenate Degradation Reaction Mechanisms. *Environmental Science & Technology* **2012**, *46* (9), 4757-4766.
22. Meyer, A. H.; Penning, H.; Elsner, M., C and N isotope fractionation suggests similar mechanisms of microbial atrazine transformation despite involvement of different Enzymes (AtzA and TrzN). *Environ. Sci. Technol.* **2009**, *43* (21), 8079-8085.
23. Hofstetter, T. B.; Bernasconi, S. M.; Schwarzenbach, R. P.; Kretzschmar, R., New methods for the environmental chemist's toolbox. *Environ. Sci. Technol.* **2008**, *42* (21), 7727-7727.
24. Elsner, M.; Jochmann, M. A.; Hofstetter, T. B.; Hunkeler, D.; Bernstein, A.; Schmidt, T. C.; Schimmelmann, A., Current challenges in compound-specific stable isotope analysis of environmental organic contaminants. *Analytical and Bioanalytical Chemistry* **2012**, *403* (9), 2471-2491.
25. Sakaguchi-Soder, K.; Jager, J.; Grund, H.; Matthaus, F.; Schuth, C., Monitoring and evaluation of dechlorination processes using compound-specific chlorine isotope analysis. *Rapid Communications in Mass Spectrometry* **2007**, *21* (18), 3077-3084.
26. Shouakar-Stash, O.; Drimmie, R. J.; Zhang, M.; Frape, S. K., Compound-specific chlorine isotope ratios of TCE, PCE and DCE isomers by direct injection using CF-IRMS. *Applied Geochemistry* **2006**, *21* (5), 766-781.
27. Bernstein, A.; Shouakar-Stash, O.; Ebert, K.; Laskov, C.; Hunkeler, D.; Jeannotat, S.; Sakaguchi-Söder, K.; Laaks, J.; Jochmann, M. A.; Cretnik, S.; Jager, J.; Haderlein, S. B.; Schmidt, T. C.; Aravena, R.; Elsner, M., Compound-Specific Chlorine Isotope Analysis: A Comparison of Gas Chromatography/Isotope Ratio Mass Spectrometry and Gas Chromatography/Quadrupole Mass Spectrometry Methods in an Interlaboratory Study. *Analytical Chemistry* **2011**, *83* (20), 7624-7634.
28. Hunkeler, D.; Abe, Y.; Broholm, M. M.; Jeannotat, S.; Westergaard, C.; Jacobsen, C. S.; Aravena, R.; Bjerg, P. L., Assessing chlorinated ethene degradation in a large scale contaminant plume by dual carbon-chlorine isotope analysis and quantitative PCR. *Journal of Contaminant Hydrology* **2011**, *119* (1-4), 69-79.

29. Lojkasek-Lima, P.; Aravena, R.; Shouakar-Stash, O.; Frappe, S. K.; Marchesi, M.; Fiorenza, S.; Vogán, J., Evaluating TCE Abiotic and Biotic Degradation Pathways in a Permeable Reactive Barrier Using Compound Specific Isotope Analysis. *Ground Water Monit. Remediat.* **2012**, *32* (4), 53-62.
30. Abe, Y.; Aravena, R.; Zopfi, J.; Shouakar-Stash, O.; Cox, E.; Roberts, J. D.; Hunkeler, D., Carbon and Chlorine Isotope Fractionation during Aerobic Oxidation and Reductive Dechlorination of Vinyl Chloride and cis-1,2-Dichloroethene. *Environmental Science & Technology* **2009**, *43* (1), 101-107.
31. Audí-Miró, C.; Cretnik, S.; Otero, N.; Palau, J.; Shouakar-Stash, O.; Soler, A.; Elsner, M., Cl and C isotope analysis to assess the effectiveness of chlorinated ethene degradation by zero-valent iron: Evidence from dual element and product isotope values. *Applied Geochemistry* (0).
32. Rich, A. E.; DeGreeff, A. D.; McNeill, K., Synthesis of (chlorovinyl) cobaloxime complexes, model complexes of proposed intermediates in the B-12-catalyzed dehalogenation of chlorinated ethylenes. *Chem. Commun.* **2002**, (3), 234-235.
33. Kliegman, S.; McNeill, K., Reconciling Disparate Models of the Involvement of Vinyl Radicals in Cobalamin-Mediated Dechlorination Reactions. *Environmental Science & Technology* **2009**, *43* (23), 8961-8967.
34. Elsner, M.; Hunkeler, D., Evaluating Chlorine Isotope Effects from Isotope Ratios and Mass Spectra of Polychlorinated Molecules. *Analytical Chemistry* **2008**, *80* (12), 4731-4740.
35. Cichocka, D.; Imfeld, G.; Richnow, H.-H.; Nijenhuis, I., Variability in microbial carbon isotope fractionation of tetra- and trichloroethene upon reductive dechlorination. *Chemosphere* **2008**, *71* (4), 639-648.
36. Lee, P. K. H.; Conrad, M. E.; Alvarez-Cohen, L., Stable Carbon Isotope Fractionation of Chloroethenes by Dehalorespiring Isolates. *Environ. Sci. Technol.* **2007**, *41* (12), 4277-4285.
37. Slater, G. F.; Sherwood Lollar, B.; Sleep, B. E.; Edwards, E. A., Variability in carbon isotopic fractionation during biodegradation of chlorinated ethenes: Implications for field applications. *Environmental Science and Technology* **2001**, *35* (5), 901-907.
38. Aeppli, C.; Berg, M.; Cirpka, O. A.; Holliger, C.; Schwarzenbach, R. P.; Hofstetter, T. B., Influence of Mass-Transfer Limitations on Carbon Isotope Fractionation during Microbial Dechlorination of Trichloroethene. *Environmental Science & Technology* **2009**, *43* (23), 8813-8820.

39. Slater, G. F.; Sherwood Lollar, B.; Lesage, S.; Brown, S., Carbon isotope fractionation of PCE and TCE during dechlorination by vitamin B12. *Ground Water Monit. Remediat.* **2003**, *23* (4), 59-67.
40. Huskey, W. P., Origin and interpretation of heavy-isotope effects. In *Enzyme mechanism from isotope effects*, Cook, P. F., Ed. CRC Press: Boca Raton, FL, USA, 1991; pp 37-72.
41. Wagner, D. D.; Hug, L. A.; Hatt, J. K.; Spitzmiller, M. R.; Padilla-Crespo, E.; Ritalahti, K. M.; Edwards, E. A.; Konstantinidis, K. T.; Löffler, F. E., Genomic determinants of organohalide-respiration in *Geobacter lovleyi*, an unusual member of the Geobacteraceae. *BMC Genomics* **2012**, *13*.
42. Hunkeler, D.; Elsner, M., Principles and Mechanisms of Isotope Fractionation. In *Environmental Isotopes in Biodegradation and Bioremediation*, Aelion, C. M.; Hohener, P.; Hunkeler, D.; Aravena, R., Eds. CRC Press: Boca Raton, London, New York, 2010.
43. McCauley, K. M.; Wilson, S. R.; van der Donk, W. A., Characterization of Chlorovinylcobalamin, A Putative Intermediate in Reductive Degradation of Chlorinated Ethylenes. *Journal of the American Chemical Society* **2003**, *125* (15), 4410-4411.
44. Burris, D. R.; Delcomyn, C. A.; Smith, M. H.; Roberts, A. L., Reductive dechlorination of tetrachloroethylene and trichloroethylene catalyzed by Vitamin B₁₂ in homogeneous and heterogeneous systems. *Environmental Science and Technology* **1996**, *30* (10), 3047-3052.
45. Follett, A. D.; McNabb, K. A.; Peterson, A. A.; Scanlon, J. D.; Cramer, C. J.; McNeill, K., Characterization of Co-C bonding in dichlorovinylcobaloxime complexes. *Inorg. Chem.* **2007**, *46* (5), 1645-1654.

4

Cl and C isotope analysis to assess the effectiveness of chloroethene degradation by zero-valent iron: Evidence from dual element and product isotope values

*Carme Audí-Miró^{a,◦}, Stefan Cretnik^{b,◦}, Neus Otero^a, Jordi Palau^a, Orfan Shouakar-Stash^c,
Albert Soler^a, Martin Elsner^b*

^aGrup de Mineralogia Aplicada i Medi Ambient. Departament de Cristal·lografia, Mineralogia i Dipòsits Minerals. Facultat de Geologia. Universitat de Barcelona. Martí Franquès s/n, 08028. Barcelona, Spain

^bInstitute of Groundwater Ecology, Helmholtz Zentrum München-National Research Center for Environmental Health, Ingolstädter Landstrasse 1, D-85764 Neuherberg, Germany,

^cDepartment of Earth Sciences, University of Waterloo, Waterloo, Ontario, Canada N2L 3G1

[◦]Audí-Miró, C. and Cretnik, S., contributed equally to this work

4.1 ABSTRACT

This study investigated carbon and, for the first time, chlorine isotope fractionation of trichloroethene (TCE) and *cis*-dichloroethene (*cis*-DCE) during reductive dechlorination by cast zero-valent iron (ZVI). Hydrogenolysis and β -dichloroelimination pathways occurred as parallel reactions, with ethene and ethane deriving from the β -dichloroelimination pathway. Carbon isotope fractionation of TCE and *cis*-DCE was consistent for different batches of iron studied. Transformation of TCE and *cis*-DCE showed chlorine isotopic enrichment factors (ϵ_{Cl}) of $-2.6 \pm 0.1\text{‰}$ (TCE) and $-6.2 \pm 0.8\text{‰}$ (*cis*-DCE), with AKIE_{Cl} values of 1.0079 ± 0.0005 (TCE) and 1.0127 ± 0.0023 (*cis*-DCE). This indicates that a C-Cl bond breakage is the rate-limiting step in TCE and *cis*-DCE transformation by ZVI. Two approaches were investigated to evaluate if isotope fractionation analysis can distinguish the effectiveness of transformation by ZVI as opposed to natural biodegradation. (i) Dual isotope plots. Our study reports the first dual (C, Cl) element isotope plots for TCE and *cis*-DCE degradation by ZVI. The pattern for *cis*-DCE differs remarkably from that reported for biodegradation of the same compound by KB-1. This trend delineates an expedient approach to distinguish abiotic and biotic transformation, but needs to be confirmed in future studies. (ii) Product-related isotope fractionation. Carbon isotope ratios of the hydrogenolysis product *cis*-DCE differed consistently by 10‰ compared to the β -dichloroelimination products ethene and ethane providing a second line of evidence to differentiate abiotic or biotic degradation pathways.

4.2 INTRODUCTION

Chlorinated aliphatic hydrocarbons (CAHs) are used in a wide variety of applications as dry cleaning solvents and degreasers. Historical management of wastes containing CAHs has resulted in subsurface contamination, where the CAHs are often released as a mixture of dense non-aqueous phase liquids (DNAPL). Since DNAPLs have a higher density than water, they migrate vertically through the water table until they reach a confining layer forming pools (U.S. EPA, 2003). Moreover, within an aquifer, DNAPLs can be entrapped in fractures and matrix porosity constituting a long-term source of contamination of groundwater due to their low solubility (Dridi *et al.*, 2009).

Chlorinated solvents can have detrimental effects to both the environment and human health. Of particular relevance is trichloroethene (TCE). Although TCE may undergo natural or stimulated biodegradation, often intermediates such as *cis*-dichloroethene (*cis*-DCE) or vinyl chloride (VC) accumulate (lower pathway of Figure 1), which are more toxic than the parent compound. Different remediation techniques have therefore been explored for clean-up (Clark *et al.*, 2003). In particular, in situ zero-valent iron (ZVI) permeable reactive barriers (PRB) have been implemented as cost effective technology for treatment (Dries *et al.*, 2005; Liu *et al.*, 2006). ZVI is capable of effectively removing CAHs through reductive dechlorination. One of the most commonly used ZVI in field applications of PRBs is cast iron, which contains impurities, in particular graphite (Slater *et al.*, 2002). The virtue of transformation by ZVI is two-fold. On the one hand, in adequately designed barriers hydrogenolysis reactions (i.e., the lower pathway of Figure 1) tend to be more efficient than in biodegradation so that toxic intermediates do not accumulate (Arnold & Roberts, 2000; Elsner *et al.*, 2008; Liu *et al.*, 2006). On the other hand, a second reductive dechlorination pathway is operative with ZVI: vicinal β -dichloroelimination where two Cl substituents are cleaved off leading rapidly to harmless products such as ethene and ethane (upper pathway of Figure 1) (Arnold & Roberts, 2000; Elsner *et al.* 2008).

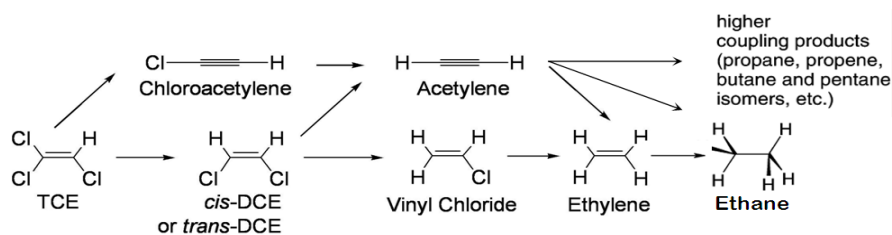


Figure 1: Concurring pathways proposed in chlorinated ethane dehalogenation (Elsner et al. 2008). Biodegradation generally involves sequential hydrogenolysis to ethene (lower pathway), while abiotic dehalogenation includes also β -dichloroelimination (upper pathway).

ZVI barriers are usually installed within existing contaminant plumes and elevated concentrations of contaminants are observed downgradient of PRBs, even long after the system has been installed. The presence of contaminants downgradient of a barrier hinders the monitoring of the PRB based on concentration data alone. In order to evaluate the PRB performance accurately, discrimination between (i) hydraulic bypasses around the barrier, (ii) incomplete abiotic degradation within the PRB, and (iii) biotic degradation stimulated by the resultant lower redox potential is necessary.

Compound Specific Isotope Analysis (CSIA) bears potential to provide precisely such discrimination. When a transformation process takes place -such as biotic or abiotic reductive dechlorination- a significant kinetic isotope effect usually occurs, in contrast to non-degradative processes (dilution, dispersion, and volatilization). As a consequence, reacting compounds become enriched in heavy isotopes, and the products formed are initially lighter than their parent compounds. Previous studies have determined carbon isotopic enrichment factors (ϵ_C) during CAHs reaction with ZVI ranging from -5.7 to -25.3‰ for tetrachloroethene (PCE); -8.6 to -27‰ for TCE; -6.9 to -23.1‰ for *cis*-DCE; and -6.9 to -20.1‰ for VC (Dayan *et al.*, 1999; Elsner *et al.*, 2008; Slater *et al.*, 2002; Vanstone *et al.*, 2004). The wide range of reported ϵ_C values limits the use of carbon isotopic enrichment to assess the extent of degradation and to differentiate from biodegradation, since ranges of ϵ_C values overlap (Liu, *et al.*, 2010). In particular, it is unclear whether such variation is attributable to (i) fundamentally different chemical reaction mechanisms, (ii) the same mechanism, but different rate-limiting steps (i.e., mass transfer limitation) or (iii) mixed isotope fractionation of simultaneously ongoing degradation pathways. Combination with isotope analysis of other elements (chlorine or hydrogen) bears potential to provide additional insight into transformation mechanisms and is, therefore, expected to increase the insight

from isotope data. In particular, dual isotope plots of the reacting contaminant have the potential to distinguish different transformation pathways (Abe *et al.*, 2009; Elsner *et al.*, 2005; Hunkeler *et al.*, 2011). The recent development of continuous flow compound specific chlorine isotope analysis (Shouakar-Stash *et al.*, 2006) has made such determinations of chlorine isotope fractionation and the use of dual carbon – chlorine isotope plots possible. Abe *et al.* (2009) successfully used the dual isotope approach (C/Cl) to distinguish between biotic aerobic oxidation and biotic reductive dechlorination reactions for *cis*-DCE and VC. The slopes (i.e., ϵ_C/ϵ_{Cl}) obtained for the reductive dechlorination biodegradation model for *cis*-DCE and VC were 12.3 and 14, respectively. In contrast, chlorine isotope fractionation values for degradation of chlorinated ethenes by ZVI have not been reported so far.

Another approach to distinguish biotic and abiotic transformation of chlorinated ethenes does not involve chlorine isotope ratios, but relies instead on carbon isotope analysis of daughter compounds (Elsner *et al.*, 2010, 2008). As sketched in Figure 1, the same products that are formed in sequential order during biodegradation are formed in parallel during abiotic degradation by ZVI. If these products show different isotope trends depending on whether they are formed in parallel or in sequence, the type of pathway that produced them and consequently their abiotic or biotic origin may be identified. Elsner *et al.* (2008) obtained that hydrogenolysis and β -dichloroelimination byproducts during transformation by nanoparticulate ZVI differed consistently by 10‰ in carbon isotope values. A follow-up field study used these results to attempt for the first time a discrimination of abiotic versus biotic transformation in the field (Elsner *et al.*, 2010). Therefore, two lines of evidence have recently been brought forward to discriminate between abiotic and biotic pathways: (i) evidence from dual isotope plots, (ii) evidence from product isotope ratios.

In this study TCE and *cis*-DCE batch experiments were carried out in order to investigate a) carbon and chlorine isotope fractionation and b) carbon isotope fractionation of parent compounds and daughter products during their transformation with cast ZVI. Our motivation was to evaluate the potential of both approaches for assessing the effectiveness of ZVI barrier treatment. Our main objectives were i) to evaluate whether the concurring pathways of Figure 1, hydrogenolysis and β -dichloroelimination were operative with this type of iron; ii) to determine not only carbon, but for the first time also chlorine isotope enrichment factors for abiotic transformation of TCE and *cis*-DCE by cast ZVI; (iii) to construct a Dual Element Isotope Plot of both carbon and chlorine isotope data and compare it to reported data on

biodegradation, and iv) to investigate the potential of carbon isotope values of daughter products as an independent line of evidence to delineate their abiotic versus biotic origin.

4.3 MATERIALS AND METHODS

4.3.1 Experimental Procedure

Batch experiments were carried out in duplicates in closed 250 mL bottles equipped with Mininert valves (Supelco, Bellefonte, Pennsylvania, USA). Each bottle contained 20 ± 0.1 g of cast iron and 100 mL of aqueous solutions containing 60 mg/L of either TCE or *cis*-DCE, or 12 mg/L of VC, leaving 150 mL of headspace. To this end, TCE (99%, Merck, Darmstadt, Germany), *cis*-DCE (97%, Sigma-Aldrich, St. Louis, Missouri, USA) and VC (2000 mg/L in Methanol, Supelco, Bellefonte, Pennsylvania, USA) were used. Control bottles were filled with 100 mL of aqueous chloroethene solutions, without addition of cast iron.

The specific surface area of the cast iron determined by nitrogen gas adsorption (BET method) (Brunauer *et al.*, 1938) was 0.7038 ± 0.0045 m²/g. Prior to the experiment the iron was acid-cleaned and dried inside an anaerobic chamber operated with a gas mixture of 90% N₂ and 10% H₂. During acid cleaning, the iron was soaked in 1N degassed HCl for 1 h, then rinsed five times with degassed deionized water, and dried and stored in the anaerobic chamber (Dayan *et al.*, 1999; Matheson *et al.*, 1994; Slater *et al.*, 2002). The iron was weighted before and after the treatment to verify it was dry. Spike solutions of chlorinated ethenes were prepared by dissolving defined aliquots of pure compound in deionized water (Milli-Q Plus UV, Millipore™, Billerica, Massachusetts, USA), under vigorous stirring for 12 hours and in the absence of a headspace. Bottles were filled with the iron and deionized water inside the glovebox, closed, taken out and spiked outside with anoxic stock solutions of the chlorinated ethene by injection through the Mininert Valve.

After preparation, bottles were immediately covered with aluminum foil to avoid light oxidation and were rotated on a horizontal roller table (Wheaton, Millville, New Jersey, USA) at 60 rpm about their longitudinal axes to ensure rapid solid/water and water/air mass transfer. Samples were taken from the headspace of the reaction bottles through the Mininert valve by a Pressure-Lok® Analytical Syringe (VICI, Houston, Texas, USA) with sideport taper needle (1000 µL for compound concentration analysis, 250 to 2000 µL for carbon isotope analysis and 30 to 500 µL for chlorine isotope analysis). In order to keep reaction bottles overpressurized during the experiments, an equal volume of argon gas was injected into the reaction bottles before samples were withdrawn. Headspace sampling from the same bottle for

concentration, carbon and chlorine isotope measurements was performed right after each other, and samples were analyzed immediately to obtain values at the same time point. Duplicate experimental vials were sampled and analyzed right afterwards.

4.3.2 Preliminary Experiments

Prior to the Dual Element isotope study, *cis*-DCE and TCE preliminary experiments were performed in two series of 25 mL vials and analyzed for carbon isotope fractionation. Vials were filled with 2.5 ± 0.1 g of iron and with a previously prepared solution of TCE and *cis*-DCE (one compound each series). Each pair of vials (duplicates) was prepared at different starting points, they were covered with aluminum foil and put in a rotator (Heidolph, Schwabach, Germany) (23 rpm). All vials were sacrificed at the same time, assuring the same storage conditions and that they were analyzed on the same day. Solutions were separated from the iron and split in two aliquots, one was kept at 4 °C without headspace for concentration analysis performed the day after, and the second one was frozen with headspace for isotopic analysis (Elsner *et al.*, 2006) and performed 10 days after. Controls were prepared at three different time points along the experiments to ensure that other degradation mechanisms or losses were not affecting the TCE concentration.

4.4 CONCENTRATION AND ISOTOPE ANALYSIS

4.4.1 Dual Element isotope study

Analysis of compound concentrations were performed on a gas chromatograph with flame ionization detector (GC/FID, Hewlett Packard, Palo Alto, California, USA), equipped with a 60 m GS-Q (Agilent J&W, Santa Clara, California, USA) column, 0.32 mm inner diameter, using nitrogen as the carrier gas at 1.6 mL/min flow rate. The injector temperature was 200°C and the temperature program used was of 34°C (9 min), increasing at 15°C/min to 53°C (2.70 min), at 13°C/min to 134°C (3.30 min) and at 10°C/min to 190°C (23 min). This temperature program allowed separation of the chlorinated ethene byproducts, methane, ethane, ethene, acetylene, propene, n-propane, propyne, n-butane as well as of the chlorinated ethylenes VC, *cis*-DCE and TCE. Before the start of the experiment a four point calibration for TCE, *cis*-DCE and VC was conducted, and one point calibrations were conducted daily during the experiment by injecting standard solutions of the three compounds. For methane, ethane, ethene, acetylene, propene, n-propane, propyne and n-butane an initial one point calibration was done before the start of the experiment and daily one-point calibrations were performed during the experiment by injecting gas mixtures of standards with 15 ppm of each compound in helium (Scotty[®] Analyzed Gases, Sigma-Aldrich, St. Louis, Missouri, USA). The resulting total relative error in concentrations is estimated as $\pm 10\%$.

Carbon isotope analysis of TCE, *cis*-DCE and their byproducts were conducted by Compound Specific Isotope Analysis (CSIA) by injection of headspace samples on a GC-C-IRMS system (Thermo Fisher Scientific, Waltham, Massachusetts, USA) consisting of a Trace GC coupled to a MAT 253 IRMS through a GC/C III combustion interface. The gas chromatograph was equipped with a 60 m GS-Q column (Agilent J&W, Santa Clara, California, USA), 0.32 mm inner diameter, and operated with He carrier gas at 1.4 mL/min. The temperature program was similar to the one used for concentration analysis, 34°C (9 min), increasing at 5°C/min to 53°C, at 13°C/min to 134°C (3.30 min) and at 10°C/min to 190°C (21 min). Carbon isotopic signatures ($\delta^{13}\text{C}$) of TCE and *cis*-DCE internal standards used were -27.07‰ and -25.48‰ respectively, characterized against international reference materials (referred to the Vienna Pee Dee Belemnite international standard (VPDB)). The analytical uncertainty 2σ of carbon isotopic measurements was $\pm 0.5\text{‰}$ (Elsner *et al.*, 2012).

Chlorine isotope analyses of TCE and *cis*-DCE were determined according to a method adapted from Shouakar-Stash *et al.* (2006). This method is a new approach for GC/IRMS

which does not include a combustion step; instead, intact chlorinated ethene molecules are directly transferred to the IRMS source through the He carrier stream, ionized and fragmented for the isotopic ratio measurement. In order to correct for instrument drifts, values are measured in comparison to reference peaks which are introduced via a dual inlet system consisting of the same target analyte and converted to delta values relative to the international SMOC (Standard Mean Ocean Chloride) standard (Bernstein *et al.*, 2011).

In this study measurements were conducted on a GC-IRMS system (Thermo Scientific, Waltham, Massachusetts, USA) consisting of a Trace GC that was connected to a MAT 253 IRMS with dual inlet system *via* a heated transfer line. For the simultaneous determination of TCE and *cis*-DCE (product) a peak jump routine was performed, with *cis*-DCE monitoring gas peaks added at the beginning and TCE monitoring gas peaks added at the end of each analytic run. The gas chromatograph was equipped with a 30 m VOCOL column (Supelco, Bellefonte, Pennsylvania, USA) and 0.25 mm inner diameter, with a film thickness of 1.5 μm and operated with He carrier gas at 1.4 mL/min. The GC program used was 50°C (7 min), increasing at 60°C/min to 70°C (2.70 min) and at 80°C/min to 140°C (0.10 min). External standards were measured daily for calibration of $\delta^{37}\text{Cl}$ values against the SMOC scale (Bernstein *et al.*, 2011). They had been characterized in the Department of Earth Sciences, University of Waterloo. TCE Eil-1 and Eil-2 internal standards (supplied by Orfan Shouakar-Stash, Canada) were +3.05 and -2.7‰ respectively, regarding the international standard SMOC. The chlorine isotopic signature ($\delta^{37}\text{Cl}$) of *cis*-DCE internal standards used, *cis*F and IS-63 (supplied by Orfan Shouakar-Stash, Canada), is -1.52 and +0.07‰ respectively. The analytical uncertainty of chlorine isotopic measurements was $\pm 0.2\%$ (Bernstein *et al.*, 2011).

4.4.2 Preliminary Experiments

Headspace (HS) concentration analysis was performed using a FOCUS gas chromatograph coupled with a DSQ II mass spectrometer (GC-MS) (Thermo Fisher Scientific, Waltham, Massachusetts, USA). The GC was equipped with a split/splitless injector and a 60 m, 0.32 mm inner diameter DB-624 capillary column (Agilent, Santa Clara, California, USA) with a film thickness of 1.8 μm and operated with He carrier gas at 4.0 mL/min. The following temperature program was used: 60 °C (2 min) and then increased at 8 °C/min to 220 °C (5 min). The injector was set at 220 °C. The compounds were identified in comparison to retention times and mass spectrum of calibration standards, and the concentrations were quantified using a set of multi-component external standards at different concentrations. Low

molecular weight byproducts from *cis*-DCE degradation (ethene, ethane, methane) were semi-quantitatively determined by a gas chromatograph with a thermal conductivity detector (GC-TCD) (5890 Hewlet Packard, Palo Alto, California, USA). The following temperature program was used: 35 °C (5 min) and then increased at 25 °C/min to 220 °C (5 min). A headspace volume of 1 mL was manually injected with a gas syringe (Hamilton).

Carbon isotope ratios were determined using headspace solid-phase microextraction (HS-SPME) and a GC-C-IRMS system consisting of a Trace GC Ultra equipped with a splitless injector, coupled to a Delta V Advantage isotope ratio mass spectrometer through a combustion interface. The method and equipment used are described in detail in Palau *et al.* (2007). A 60 m long column and 0.32 mm inner diameter (SPB-624 Supelco, Bellefonte, Pennsylvania, USA) with a film thickness of 1.8 µm was used with He as carrier gas with a flow rate of 2.2 mL/min. The temperature program was: 60 °C (5 min), increase at 8 °C/min to 165 °C and then at 25 °C/min to 220 °C (1 min). The injector was set at 250 °C at a split ratio of 5:1.

Prior to extraction, samples were diluted to 20 µg/L with Milli-Q water to a final volume of 100 mL. Then, the samples were put in agitation and the SPME fiber was introduced through the septum. The SPME fiber remained in the sample headspace during 15 minutes after which it was injected manually into the GC injector. Accuracy of isotope analysis was daily verified by measurements of laboratory standards characterized against international reference materials (referred to the VPDB international standard). The carbon isotopic signature ($\delta^{13}\text{C}$) of the TCE and *cis*-DCE laboratory standard are $-30.8 \pm 0.2\text{‰}$ and $-26.1 \pm 0.2\text{‰}$, respectively (Palau *et al.*, 2007).

4.5 EVALUATION OF C AND CI ISOTOPE FRACTIONATION

Carbon isotopic enrichment factor (ϵ_C) was evaluated according to a Rayleigh regression not forced through the origin (Scott *et al.*, 2004):

$$R/R_0 = (1000 + \delta^{13}\text{C}) / (1000 + \delta^{13}\text{C}_0) = f^{\epsilon_C / 1000} \quad (1)$$

where R_0 and R are carbon isotope ratios at the beginning and at a given time (t) respectively, $\delta^{13}\text{C}_0$ and $\delta^{13}\text{C}$ are the same values in delta notation and f is the fraction of substrate remaining at time t . According to Equation 1, if the ϵ_C has been obtained in laboratory experiments for a specific transformation, if the initial (= “source”) $\delta^{13}\text{C}_0$ is known and if

$\delta^{13}\text{C}$ is determined at a given time point without further knowledge of the extent of transformation, isotope data alone allows estimating the fraction of remaining reactant (f). This approach may be used to quantify the real extent of a specific transformation reaction in the field. The approach is independent of estimations based on concentration ratios of parent and daughter compounds, which are subject to sorption, dilution and further degradation so that these ratios may not show the actual extent of degradation.

The specific isotope fractionation pattern of the byproducts can be expressed by determining the product-specific isotope fractionation ($\epsilon_{\text{substrate} \rightarrow \text{product}}$). According to Elsner *et al.* (2008), it can be calculated through the following abbreviated equation:

$$\epsilon_{\text{substrate} \rightarrow \text{product}} = \delta^{13}\text{C}_{0,\text{product}} - \delta^{13}\text{C}_{0,\text{substrate}} = D(\delta^{13}\text{C}) + \epsilon_{\text{C}} \quad (2)$$

where $D(\delta^{13}\text{C})$ is the deviation that a product can experience from the weighted average of all products, expressed as $D(\delta^{13}\text{C}) = \delta^{13}\text{C}_{\text{product}} - \delta^{13}\text{C}_{\text{product, average}}$. The $D(\delta^{13}\text{C})$ has been obtained from the iteration and graphical representation with “Sigma Plot 12” of the following equation (Elsner *et al.*, 2008):

$$(1000 + \delta^{13}\text{C}_{\text{product}}) / (1000 + \delta^{13}\text{C}_{0,\text{substrate}}) = (1 + (D(\delta^{13}\text{C})/1000)) \times ((1 - f^{\epsilon_{\text{C}}/(1000+1)}) / (1 - f)) \quad (3)$$

Equation 2 allows the determination of product-specific isotope fractionation even without knowledge of absolute reaction rates, product distribution, or molar balances, since they rely solely on isotope measurements of the substrate and a given product (Elsner *et al.*, 2008).

Elsner and Hunkeler (2008) demonstrated that chlorine isotope fractionation also follows in good approximation a Rayleigh trend despite a high abundance of ^{37}Cl compared to ^{35}Cl . Thus the Rayleigh regression was used again to evaluate the chlorine isotope data. An apparent kinetic chlorine isotope effect (AKIE) may be estimated from the following equation (Elsner and Hunkeler, 2008):

$$\text{AKIE}_{\text{Cl}} = 1 / (1 + (n \cdot \epsilon_{\text{Cl}} / 1000)) \quad (4)$$

where “ n ” is the total number of chlorine atoms which are considered to be located in the reactive positions, with negligible secondary isotope effects.

Dual element isotope fractionation can be compared by (a) either considering the ratio of $\epsilon_{\text{C}} / \epsilon_{\text{Cl}}$ or, alternatively, (b) by plotting changes in isotope values $\delta^{13}\text{C} / \delta^{37}\text{Cl}$ (as shown exemplary for MTBE with $\delta^2\text{H} / \delta^{13}\text{C}$ in Elsner *et al.* (2007)).

4.6 RESULTS AND DISCUSSION

4.6.1 Reactivity Trends and product formation

Suspensions of 200 g/L of ZVI achieved 50% transformation of TCE leading to the formation of dehalogenated products in almost 3 days (Figure 2A). Under identical experimental conditions, observed half-lives for *cis*-DCE and VC were more than 50 and 80 days, respectively (Table S1). Figure 2 shows the kinetics for disappearance of TCE and simultaneous product formation in the dual element isotope experiment. Transformation rates decreased in the order TCE > *cis*-DCE > VC (Figure 2, Table S1). It can therefore be expected that isotope ratios of *cis*-DCE are primarily influenced by its formation from TCE, rather than by its further degradation to VC. While the observed trend in transformation rates is consistent with earlier studies by Dayan *et al.* (1999), Elsner *et al.* (2008), Gillham and O'Hannesin (1994) and Hunkeler *et al.* (2011), the opposite trend (TCE < *cis*-DCE) was observed in preliminary experiments (Table S1) and is consistent with previous studies by Arnold and Roberts (2000) and Elsner *et al.* (2008). At present, the reasons for these reactivity trends remain imperfectly understood.

Even though mass balance were typically not closed, the detection of several products allows conclusions about concurring transformation pathways. All experiments yielded ethene, ethane and methane as final products of the degradation sequence, with small amounts of *cis*-DCE, acetylene and VC intermediates produced during TCE degradation (Figure 2 A-B), and acetylene and VC from *cis*-DCE degradation. Complete products are listed in Table 1. According to Arnold and Roberts (2000) and Prommer *et al.* (2008), ethene may be produced either (i) from hydrogenation of acetylene, previously formed through the β -dichloroelimination pathway or (ii) through VC hydrogenolysis. The evolution of VC and acetylene concentration profiles, however, suggests that acetylene is the main responsible intermediate of ethene formation, (i) due to an extremely rapid acetylene concentration decrease while ethene appeared (Figure 2B), and (ii) because VC concentrations, in contrast, accumulated over time. These observations point out that both hydrogenolysis and β -dichloroelimination pathways (Figure 1) are occurring simultaneously as parallel reactions rather than as consecutive reactions and that ethene and ethane are produced primarily through the β -dichloroelimination pathway. As observed by Burris *et al.* (1995) traces of methane were formed. Also, traces of longer chain hydrocarbons were observed, as C3 (propene, propane) and C4 (n-butane), probably coming from a concurrent acetylene

degradation pathway (Arnold and Roberts, 2000; Elsner *et al.*, 2008) (Figure 1). Only the 20% of degraded TCE was transformed to *cis*-DCE, which, in his turn was transformed with much slower rate to VC (see reactivity trends above).

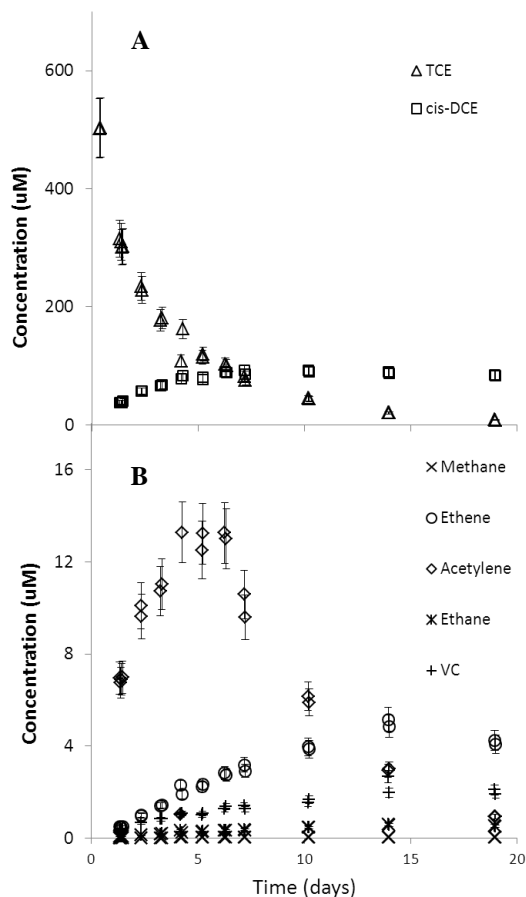


Figure 2:

2A) Changes in concentration of TCE (panel A), from Dual Element TCE experiments, and its byproducts over time (A and B).

2B) Panel B is a zoom of Panel A without TCE and *cis*-DCE to see by-products curve shape clearly. Error bars indicate total instrumental uncertainty of $\pm 10\%$.

4.7 RAYLEIGH FITS OF ISOTOPE FRACTIONATION

The enrichment factors ϵ_c for TCE in both preliminary and Dual Element isotope experiments are within error (Table 1 and Figure 3A), and although ϵ_c for *cis*-DCE are distinguishable, their error ranges are also close (Table 1 and Figure 4A). This indicates that the carbon isotope fractionation that we observed in this study is fairly consistent with this type of iron, even despite different reactivity trends (see above and Table S1). VC was not evaluated, since it was hardly transformed. Literature carbon isotopic enrichment factors for TCE exhibit a wide range of almost 20‰, depending on the type of ZVI-material (-8.6 to -27‰) (Dayan *et al.*, 1999; Slater *et al.*, 2002; Elsner *et al.*, 2008). Therefore, prior to

applying the ϵ_C at field scale to evaluate the extent of the reductive dechlorination, the ϵ_C value produced by a specific ZVI-material should be accurately determined. For conservative estimates of degradation in the field according to a modified version of the Rayleigh equation (Eq. 1), the more negative value of epsilon should be chosen (Hunkeler *et al.*, 2008).

Table 1. Summary of the Rayleigh fractionation for carbon and chlorine, the carbon product-related fractionation, and all the byproducts detected for TCE and *cis*-DCE Dual Element and preliminary experiments, and for VC Dual Element experiment.

Experiment	Substrate	Initial Conc. (μM)	$\delta^{13}\text{C}$					$\delta^{37}\text{Cl}$			Detected products	
			$\epsilon_C(\text{‰}) \pm 95\% \text{ CI}^{\text{a}}$ Individual Experiments	$\epsilon_C(\text{‰}) \pm 95\% \text{ CI}^{\text{a}}$ Combined Data	$\epsilon_{\text{substrate} \rightarrow \text{product}}(\text{‰})$ for each particular product	D($\delta^{13}\text{C}$) ^b	R ²	$\epsilon_{\text{Cl}}(\text{‰})$ Individual Experiments	$\epsilon_{\text{Cl}}(\text{‰})$ Combined Data	AKIE _{Cl}		
Dual Element Experiments	TCE	441	-14.9 \pm 0.9	-14.8 \pm 0.6	cis-DCE: -7.9‰ Ethene: -18.2‰ Acetylene: -17.3‰ Ethane: -19.3‰	6.9 -3.4 -2.5 -4.5	0.55 0.71 0.34 0.69	-2.6 \pm 0.2	-2.6 \pm 0.1	1.008	cis-DCE Acetylene VC Ethene Ethane n-butane Propane Propene Methane	
		503	-14.8 \pm 0.9		cis-DCE: -10.4‰ Ethene: -20.8‰ Acetylene: -14.7‰ Ethane: -22.9‰	4.4 -6.0 0.1 -8.1	0.87 0.72 0.60 0.73					-2.7 \pm 0.1
	cisDCE	787	-21.2 \pm 2.1	-20.5 \pm 1.8	VC: 1.8‰ Ethene: -25.4‰ Acetylene: -19.0‰ Ethane: -25.7‰	22.2 -5.0 1.4 -5.3	0.45 0.93 0.33 0.97	-6.9 \pm 1.1	-6.2 \pm 0.8	1.013	Acetylene VC Ethene Ethane n-butane Propane Propene Methane	
		852	-20.2 \pm 4.2		VC: --- Ethene: -24.1‰ Acetylene: -23.5‰ Ethane: -23.3‰	n.q. -3.7 -3.2 -3.0	n.q. 0.78 0.34 0.95					-6.2 \pm 0.9
	VC	VC	185	n.q.	n.q.	n.q.	n.q.	n.q.	n.q.	n.q.	n.q.	Acetylene Ethene Ethane Methane
			187	n.q.								
Preliminary Experiments	TCE	50	-14.3 \pm 2.9	-12.0 \pm 2.8	-----	-----	-----	-----	-----	-----	cisDCE VC non chlorinated compounds not determined	
		50	-13.9 \pm 4.8									
	cisDCE	cisDCE	186	-15.2 \pm 2.7	-16.8 \pm 1.2	-----	-----	-----	-----	-----	-----	VC ethene ethane methane butene
			186	-12.0 \pm 2.9								

^aNote that duplicates are listed separately so that each entry represents one experimental batch. 95% confidence interval. ^bD($\delta^{13}\text{C}$): is the deviation that each product has experienced from the weighted average of all products. n.q., not quantified

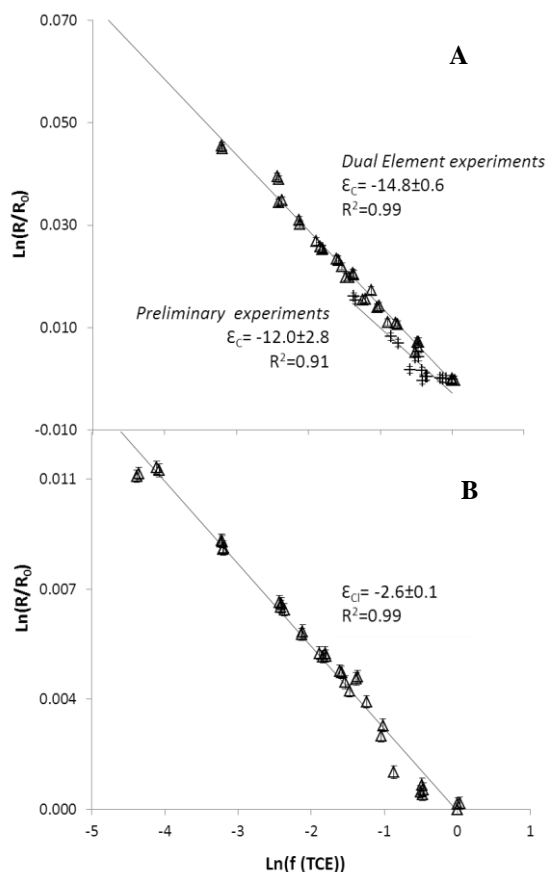


Figure 3:

3A) Carbon isotope values of residual TCE fraction in a double logarithmic plot over the respective concentrations. The isotope enrichment factor ϵ can be calculated from the slope of the regression line according to Equation 1. Triangles represent TCE Dual Element combined experiments and crosses represent TCE preliminary combined experiments.

3B) Chlorine isotope values of residual TCE fraction in a double logarithmic plot over the respective concentrations. The isotope enrichment factor ϵ has been obtained according to Equation 1. In 3A and 3B, error bars represent the calculated error due to a total instrumental uncertainty of 0.5‰ for compound-specific carbon isotope measurements, and of 0.2‰ for compound specific chlorine isotope measurements.

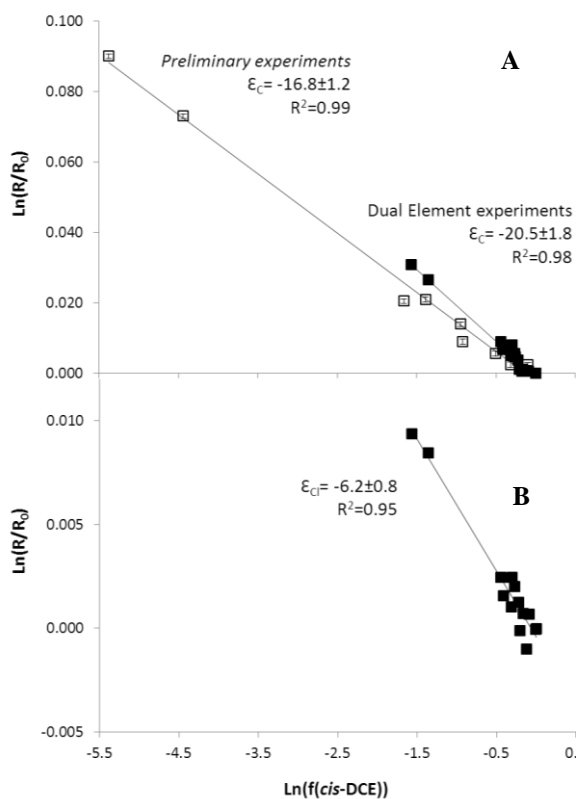


Figure 4:

4A) Carbon isotope values of residual *cis*-DCE fraction in a double logarithmic plot over the respective concentrations. The isotope enrichment factor ϵ can be calculated from the slope of the regression line according to Equation 1. Black squares represent *cis*-DCE Dual Element combined experiments and white squares represent *cis*-DCE preliminary combined experiments.

4B) Chlorine isotope values of residual *cis*-DCE fraction in a double logarithmic plot over the respective concentrations. The isotope enrichment factor ϵ has been obtained according to Equation 1. In 4A and 4B, error bars represent the calculated error due to a total instrumental uncertainty of 0.5‰ for compound-specific carbon isotope measurements, and of 0.2‰ for compound specific chlorine isotope measurements.

Our study also reports the first chlorine isotope fractionation data associated with ZVI transformation. Results show that transformation of TCE and *cis*-DCE was associated with pronounced chlorine isotope fractionation, $-2.6 \pm 0.1\%$ for TCE and $-6.2 \pm 0.8\%$ for *cis*-DCE (see Table 1 and Figures 3B and 4B). This chlorine isotope fractionation may provide an additional line of evidence for degradation in the field.

Following Equation 4, it is also possible to calculate $AKIE_{Cl}$ from TCE and *cis*-DCE dual element isotope experiments resulting in values of 1.0079 ± 0.0005 and 1.0127 ± 0.0023 , respectively. Compared to other studies (Dybala-Defratyka *et al.*, 2008; Dybala-Defratyka *et al.*, 2004; Hofstetter *et al.*, 2007; Wolfsberg *et al.*, 2010) these numbers are typical, or even at the higher end of ranges reported for chlorine isotope effects. This indicates that a C-Cl bond is cleaved in the rate-determining step of the ZVI-catalyzed transformation and that this intrinsic isotope effect is not significantly masked by mass transfer, adsorption, etc.. In particular, our estimated values are much higher than the $AKIE_{Cl} = 1.003$ calculated for biotransformation of *cis*-DCE by the mixed culture KB-1 (Abe *et al.*, 2009) suggesting potential differences in the underlying transformation mechanism.

In contrast to what Hunkeler *et al.* (2009) predicted, *cis*-DCE, as a TCE product, contained slightly more ^{37}Cl compared to TCE from which it was formed (Figure 5) showing an initial enrichment in ^{37}Cl instead of ^{35}Cl of the product *cis*-DCE. The reason of this observation in the $\delta^{37}Cl$ values may be an inverse secondary isotope effect or an unequal distribution of isotope ratios in different positions of TCE so that the position containing more ^{37}Cl is preferably transferred to the product pool. An inverse secondary isotope effect can occur, for instance, if an intermediate of the reaction has a more cramped coordination sphere, e.g. when the carbon changes from sp^2 to sp^3 hybridisation. In this case the positions adjacent to reactive bonds have stiffer vibrations and preferably contain heavy isotopes. These preliminary results give an exciting glimpse on the potential insight that can be obtained from chlorine isotope measurements to investigate the reaction chemistry of TCE and *cis*-DCE in future studies.

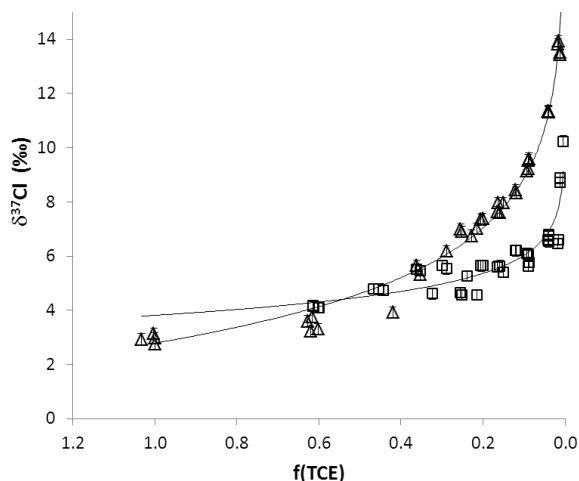
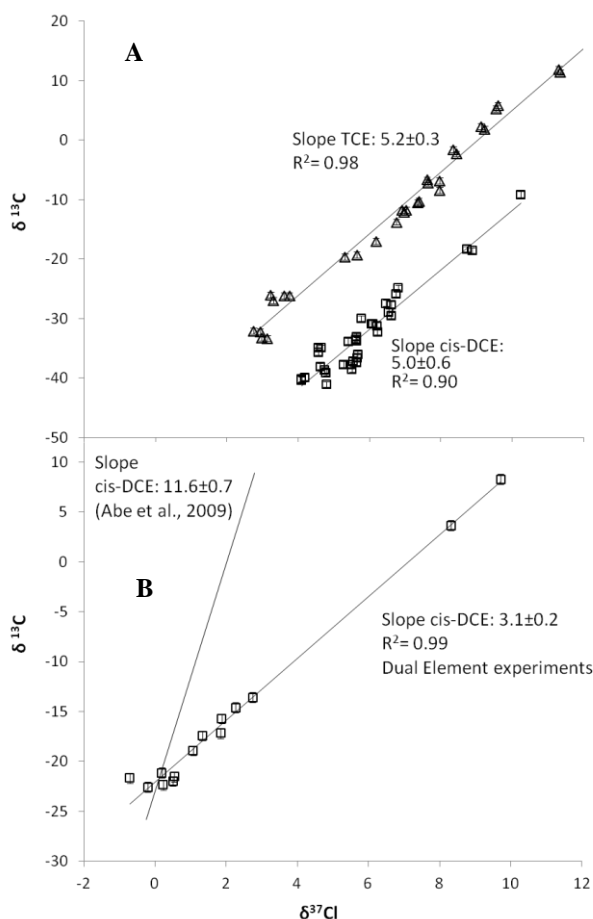


Figure 5:
Changes in chlorine isotope values of TCE (triangles), as substrate, and *cis*-DCE (squares), as product, during TCE combined Dual Element experiments. Error bars represent the total instrumental uncertainty of 0.2‰ for compound-specific chlorine isotope measurements.

4.8 DUAL ISOTOPE APPROACH

Figure 6 shows a dual element isotope plot of (a) the TCE transformation experiment with $\delta^{13}\text{C}$ and $\delta^{37}\text{Cl}$ values of TCE and one of its products, *cis*-DCE (Figure 6A); and (b) the analogous plot for transformation of *cis*-DCE (Figure 6B). To our knowledge, these are the first dual (C, Cl) isotope plots reported for chlorinated ethene transformation by ZVI. Figure 6A shows that the graphs for TCE and *cis*-DCE show a parallel trend, as predicted for cases when further transformation of *cis*-DCE is very slow or even negligible (Hunkeler *et al.*, 2009)

To evaluate whether such a dual element isotope plot can discriminate between abiotic and biotic degradation reactions, a comparison to dual element isotope data on biodegradation was attempted. For TCE (Figure 6A), no such reference data is available yet. In the case of *cis*-DCE, however, the dual element isotope plot can be compared to data of Abe *et al.* (2009) on reductive dechlorination by the mixed culture KB-1. The slope of 3.1 ± 0.2 observed in our experiments is almost 4 times smaller than that observed by Abe *et al.* (2009) (11.4 ± 0.6) (Figure 6B). This observation provides further evidence that the small isotope fractionation observed with KB-1 by Abe *et al.* (2009) is not primarily attributable to masking / commitment to catalysis, but that fundamentally different chemical transformation mechanisms are at work. If this trend can be confirmed, then our results would delineate an expedient new way to discriminate biodegradation and abiotic reductive dechlorination from a PRB in the field. To this end, however, more data is necessary to substantiate these initial patterns.

**Figure 6:**

6A) Dual isotope plot $\delta^{13}\text{C}$ versus $\delta^{37}\text{Cl}$ obtained from TCE Dual Element combined experiments. The slope of TCE (triangles) and *cis*-DCE as a product (squares), are represented.

6B) Dual isotope plot $\delta^{13}\text{C}$ versus $\delta^{37}\text{Cl}$ obtained from *cis*-DCE Dual Element combined experiments. The slope of the *cis*-DCE as a substrate, is represented and compared to the Abe et al. (2009) slope obtained for the same compound and degraded through reductive dechlorination by the mixed culture KB-1.

Error bars in 6A and 6B represent the total instrumental uncertainty of 0.5‰

4.9 PRODUCT RELATED ISOTOPE FRACTIONATION

Carbon isotope ratios of *cis*-DCE, ethene and ethane were evaluated as a second, independent approach to distinguish abiotic from biotic chlorinated ethene degradation. Figure 7 shows that products were initially depleted in ^{13}C compared to their parent compound, but subsequently became enriched in ^{13}C reflecting the enrichment trend of the substance from which they were formed. VC concentrations were too small for precise carbon isotope analysis. The product-specific isotope fractionation ($\epsilon_{\text{substrate} \rightarrow \text{product}}$) revealed a notable difference of about 10‰ between β -dichloroelimination (ethene, ethane) and hydrogenolysis (*cis*-DCE) products. (Figure 7 and Table 1). This 10‰ difference in $\delta^{13}\text{C}$ of products formed with ZVI confirms the pattern observed in previous studies (Elsner *et al.*, 2008). As brought forward in Elsner *et al.*, (2008, 2010) these parallel product curves may be considered characteristic of abiotic degradation, since they contrast with trends during biodegradation, where products are generated in sequence and, therefore, different isotope patterns are obtained that vary in time and space (Elsner *et al.*, 2008). Our study, therefore, confirms the

potential of product isotope values to distinguish biotic from abiotic degradation with ZVI and to serve as an indicator of abiotic degradation processes in the field.

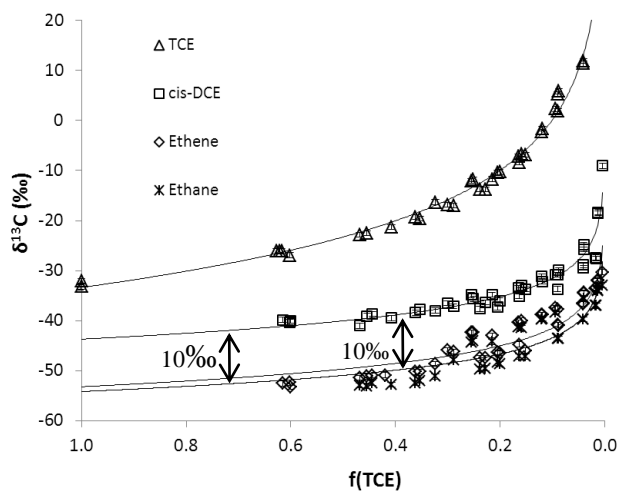


Figure 7:

Isotope values of TCE and its by-products, with a 10‰ isotope difference between hydrogenolysis *cis*-DCE byproduct and β -dichloroelimination ethylene and ethane by-products. Curves are fits of the data according to Equations 1 and 2. Error bars represent the total instrumental uncertainty of 0.5‰ for compound-specific carbon isotope measurements.

4.10 CONCLUSIONS

This study presents the very first results on chlorine isotope fractionation of TCE and *cis*-DCE in transformation with ZVI. Apparent kinetic isotope effects $AKIE_{Cl}$ of 1.0079 ± 0.0005 and 1.0127 ± 0.0023 for TCE and *cis*-DCE, respectively, indicate that (i) a C-Cl bond was broken in the rate-determining step, and (ii) that the intrinsic effect was therefore not significantly masked by other processes. Chlorine isotope analyses therefore bears great potential to investigate reaction mechanisms of CAHs in future studies.

This study also presents the first dual element (C, Cl) isotope plots of TCE and *cis*-DCE isotope ratios during degradation by cast zero-valent iron. Pronounced differences are visible in comparison to a dual element (C, Cl) isotope slope obtained for biodegradation of *cis*-DCE by the dehalogenating mixed culture KB-1 (Abe *et al.*, 2009). The biotic plot had a slope 4 times higher than the one from our *cis*-DCE abiotic pattern delineating a promising new way to discriminate biodegradation and abiotic reductive dechlorination from a PRB in the field. More data is necessary, however, to show whether these initial patterns can be reproduced in future studies with different organisms and different types of ZVI.

Product-specific carbon isotope fractionation ($\epsilon_{\text{substrate} \rightarrow \text{product}}$) revealed a notable difference between the fractionation expressed in β -dichloroelimination (ethene, ethane) and in hydrogenolysis (*cis*-DCE) daughter products. The same difference (10‰) was observed in

recent work (Elsner *et al.*, 2008) suggesting that this product pattern is consistent. The pattern is indicative of abiotic transformation by ZVI, because the constant discrimination between products occurs only in the presence of β -dichloroelimination, which takes place only during abiotic transformation with ZVI. Product-related carbon isotope fractionation may therefore provide a second, independent line of evidence to distinguish biotic from abiotic degradation with ZVI.

Taken together, our study brings forward two promising approaches to distinguish biotic and abiotic transformation by ZVI and, therefore, to assess the effectiveness of ZVI treatment in field settings: (i) evidence from dual element isotope plots of chlorinated ethene parent compounds and (ii) evidence from carbon isotope ratios of their reaction products. We expect that these findings will increase the potential of carbon and chlorine isotopic data for monitoring a ZVI PRB treatment in the field.

4.11 ACKNOWLEDGEMENTS

Audí-Miró, C. and Cretnik, S., contributed equally to this work. This study was funded by the Spanish Government CICYT projects CGL2008-06373-C03-01/03-BTE and CGL2011-29975-C04-01 and by the Catalan Government project 2009 SGR 103. The authors would like to thank the Valles Business Park enterprise for providing the zero-valent iron, the Catalan Water Agency for their support and the “Centres Científics i Tecnològics” of the “Universitat de Barcelona” for the chemical analyses.

4.12 REFERENCES

- Abe, Y., Aravena, R., Zopfi, J., Shouakar-Stash, O., Cox, E., Roberts, J.D., Hunkeler, D., 2009. Carbon and chlorine isotope fractionation during aerobic oxidation and reductive dechlorination of vinyl chloride and cis-1,2-dichloroethene. *Environ. Sci. Technol.* 43, 101–107.
- Arnold, W.A., Roberts, A.L., 2000. Pathways and kinetics of chlorinated ethylene and chlorinated acetylene reaction with Fe(0) particles. *Environ. Sci. Technol.* 34, 1794-1805
- Bernstein, A., Shouakar-Stash, O., Ebert, K., Laskov, C., Hunkeler, D., Jeannotat, S., Sakaguchi-Söder, K., Laaks, J., Jochmann, M.A., Cretnik, S., Jager, J., Haderlein, S.B., Schmidt, T.C., Aravena, R., Elsner, M., 2011. Compound-specific chlorine isotope analysis: a comparison of gas chromatography/isotope ratio mass spectrometry and gas chromatography/quadrupole mass spectrometry methods in an interlaboratory study. *Anal. Chem.* 83, 7624–7634
- Brunauer, S., Emmet, P.H., Teller, E., 1938. Adsorption of gases on multimolecular layers. *J. Am. Chem. Soc.* 60, 309–319.
- Burris, D.R., Campbell, T.J., Manoranjan, V.S., 1995. Sorption of trichloroethylene and tetrachloroethylene in a batch reactive metallic iron-water system. *Environ. Sci. Technol.* 29, 2850-2855
- Clark, C.J., Rao, P.S.C., Annable, M.D., 2003. Degradation of perchloroethylene in cosolvent solutions by zero-valent iron. *J. Hazard. Mater.* B96, 65–78
- Dayan, H., Abrajano, T., Sturchio, N.C., Winsor, L., 1999. Carbon isotopic fractionation during reductive dehalogenation of chlorinated ethenes by metallic iron. *Org. Geochem.* 30, 755-763
- Dridi, L., Pollet, I., Razakarisoa, O., Schäfer, G., 2009. Characterisation of a DNAPL source zone in a porous aquifer using the partitioning interwell tracer test and an inverse modelling approach. *J. Contam. Hydrol.* 107, 22-44
- Dries, J., Bastiens, L., Springael, D., Agathos, S.N., Diels, L., 2005. Combined removal of chlorinated ethenes and heavy metals by zerovalent iron in batch and continuous flow column systems. *Environ. Sci. Technol.* 39, 8460-8465

Dybala-Defratyka, A., Rostkowski, M., Matsson, O., Westaway, K.C., Paneth, P., 2004. A new interpretation of chlorine leaving group kinetic isotope effects; a theoretical approach. *J. Org. Chem.* 69, 4900-4905

Dybala-Defratyka, A., Szatkowski, L., Kaminski, R., Wujec, M., Siwek, A., Paneth, P., 2008. Kinetic isotope effects on dehalogenations at an aromatic carbon. *Environ. Sci. Technol.* 42, 7744-7750

Elsner, M., Chartrand, M., Vanstone, N., Lacrampe-Couloume, G., Sherwood Lollar, B., 2008. Identifying abiotic chlorinated ethene degradation: characteristic isotope patterns in reaction products with nanoscale zero-valent iron. *Environ. Sci. Technol.* 42, 5963-5970

Elsner, M., Hunkeler, D., 2008. Evaluating chlorine isotope effects from isotope ratios and mass spectra of polychlorinated molecules. *Anal. Chem.* 80, 4731-4740

Elsner, M., Jochmann, M.A., Hofstetter, T.B., Hunkeler, D., Bernstein, A., Schmidt, T.C., Schimmelmann, A., 2012. Current challenges in compound-specific stable isotope analysis of environmental organic contaminants. *Anal. Bioanal. Chem.* In press.

Elsner, M., Lacrampe Coulome, G., Mancini, S.A., Burns, L., Sherwood Lollar, B., 2010. Carbon isotope analysis to evaluate nanoscale Fe(0) treatment at a chlorohydrocarbon contaminated site. *Ground Water Monit. Rem.* 30, 79-85.

Elsner, M., Lacrampe-Coulome, G., Sherwood Lollar, B., 2006. Freezing to preserve groundwater samples and improve headspace quantification limits of water-soluble organic contaminants for carbon isotope analysis. *Anal. Chem.* 78, 7528-7534

Elsner, M., Mckelvie, J., Lacrampe-Couloume, G., Sherwood Lollar, B., 2007. Insight into methyl tert-butyl ether (MTBE) stable isotope fractionation from abiotic reference experiments. *Environ. Sci. Technol.* 41, 5693-5700

Elsner, M., Zwank, L., Hunkeler, D., Schwarzenbach, A.P., 2005. A new concept linking observable stable isotope fractionation to transformation pathways of organic pollutants. *Environ. Sci. Technol.* 39, 6896-6916

Gillham, R.W., O'Hannesin, S.F., 1994. Enhanced degradation of halogenated aliphatics by zero-valent iron. *Ground Water.* 32, 958-967

- Hofstetter, T.B., Reddy, C.M., Heraty, L.J., Berg, M., Sturchio, N.C., 2007. Carbon and chlorine isotope effects during abiotic reductive dechlorination of polychlorinated ethanes. *Environ. Sci. Technol.* 41, 4662-4668
- Hunkeler, D., Abe, Y., Broholm, M.M., Jeannotat, S., Westergaard, C., Jacobsen C.S., Aravena, R., Bjerg, P.L., 2011. Assessing chlorinated ethene degradation in a large scale contaminant plume by dual carbon–chlorine isotope analysis and quantitative PCR. *J. Contam. Hydrol.* 119, 69–79
- Hunkeler, D., Meckenstock, R.U., Sherwood Lollar, B., Schmidt, T., Wilson, J., 2008. A guide for assessing biodegradation and source identification of organic ground water contaminants using Compound Specific Isotope Analysis (CSIA). US EPA. EPA 600/R-08/148, Oklahoma.
- Hunkeler, D., Van Breukelen, B.M., Elsner, M., 2009. Modeling chlorine isotope trends during sequential transformation of chlorinated ethenes. *Environ. Sci. Technol.* 43, 6750–6756
- Liu, C.-C., Tseng, D.-H., Wang, C.-Y., 2006. Effects of ferrous ions on the reductive dechlorination of trichloroethylene by zero-valent iron. *J. Hazard. Mater.* B136, 706-713.
- Liu, F., Cichocka, D., Nijenhuis, I., Richnow, H.-H., Fennell, D.E., 2010. Carbon isotope fractionation during dechlorination of 1,2,3,4-tetrachlorodibenzo-p-dioxin by a *Dehalococcoides*-containing culture. *Chemosphere.* 80, 1113–1119
- Matheson, L.J., Tratnyek, P.G., 1994. Reductive dehalogenation of chlorinated methanes by iron metal. *Environ. Sci. Technol.* 28, 2045-2053
- Palau, J., Soler, A., Teixidor, P., Aravena, R., 2007. Compound-specific carbon isotope analysis of volatile organic compounds in water using solid-phase microextraction. *J. Chromatogr. A.* 1163, 260–268
- Prommer, H., Aziz, L.H., Bolaño, N., Taubald, H., Schüth, C., 2008. Modelling of geochemical and isotopic changes in a column experiment for degradation of TCE by zero-valent iron. *J. Contam. Hydrol.* 97, 13-26.
- Scott, K.M., Lu, X., Cavanaugh, C.M., Liu, J.S., 2004. Optimal methods for estimating kinetic isotope effects from different forms of the Rayleigh distillation equation. *Geochim. Cosmochim. Acta.* 68, 433–442

Shouakar-Stash, O., Drimmie, R.J., Zhang, M., Frappe, S.K., 2006. Compound-specific chlorine isotope ratios of TCE, PCE and DCE isomers by direct injection using CF-IRMS. *Appl. Geochem.* 21, 766-781.

Slater, G.F., Lollar, B.S., King, A., O'Hannesin, S., 2002. Isotopic fractionation during reductive dechlorination of trichloroethene by zero-valent iron: influence of surface treatment. *Chemosphere.* 49, 587–596

U.S. Environmental Protection Agency's Technology Innovation Office, 2003. Engineered approaches to in situ bioremediation of chlorinated solvents: fundamentals and field applications. EPA 542-R-00-008

Vanstone, N.A., Focht, R.M., Mabury, S.A., Sherwood Lollar, B., 2004. Effect of iron type on kinetics and carbon isotopic enrichment of chlorinated ethylenes during abiotic reduction on Fe(0). *Ground Water.* 42, 268-276

Wolfsberg, M., Van Hook, W.A., Paneth, P., 2010. Isotope effects in the chemical, geological and bio sciences. Dordrecht, Heidelberg, London, New York

5

GENERAL CONCLUSIONS

Dechlorination reactions in the environment are highly relevant processes, and there are clear research needs for a better understanding of the underlying chemical mechanisms. This dissertation elucidates the potential of novel analytical methods to measure carbon and chlorine isotope effects as an innovative technique to approach the present knowledge gap.

Before this work started, a theoretical basis to evaluate isotope ratios and to quantify isotope fractionation was established for chloroethenes as starting materials. But it was unclear how isotope effects of chlorine are manifested in the respective products during stepwise reductive dechlorination. Such information can be essential for a conclusive interpretation when chlorine isotope measurements are applied for field assessments. Moreover, this study shows that a careful interpretation of the experimental data of product isotope signatures contains even more fundamental information towards position specific chlorine isotope effects of chloroethenes and mechanistic attributes directly in biotic dechlorination reactions. The developed mathematical framework retains the potential for even more stringent mechanistical interpretations, for instance when additional information of chlorine isotope signatures on individual positions of a starting material is available.

Furthermore, this dissertation presents a new approach to combine carbon and chlorine isotope effects. An exciting feature of the created dual isotope is the possibility to directly compare transformation mechanisms of environmental processes, biotic transformations, and their putative chemical model systems. In a first application of this approach, this work shows that that different microbial strains, as well as *in vitro* reactions with cobalamin, all share a common initial reaction step of TCE degradation and suggests that the same mechanism are active in these transformations. Furthermore, the results point out differences in the rate-determining step of reductive dehalogenation of TCE when comparing the model system cobaloxime with cobalamin or biodegradation. The study demonstrates the great potential of dual element isotope analysis of carbon and chlorine as a robust indicator to compare underlying mechanisms of different reaction systems. Therefore it opens the perspective to

investigate further reactions with known initial mechanisms and to understand the authenticity of mimicking reagents for the actual system.

The two dimensional isotope assessments have already been applied for other elements (e.g. ^2H , ^{14}N ^{16}O) in contaminant hydrology to identify natural transformation and different reaction pathways in the environment. Now that such dual isotope studies are possible for carbon and chlorine in chloroethenes, it can also be established as a geochemical tool. Chapter 4 of this thesis provides the first reference experiments to use this approach for the common remediation strategy in permeable reactive barriers (PRBs) with zero valent iron (ZVI). Dechlorination reactions were first conducted in batch experiments with the same zero valent material applied in field. Carbon and chlorine isotope effects were then measured for substrates and residues of chlorinated ethylenes. Two discrete approaches were explored here to distinguish the effectiveness of transformation by ZVI as opposed to natural biodegradation, with the dual isotope approach and product related carbon isotope fractionation. These findings can now be applied to trace the sustainable removal of contaminants at installations of PRBs with ZVI in the field.

Overall, the presented work demonstrates the potential of compound-specific isotope analysis of carbon and chlorine as a versatile tool for field assessments and emphasizes its applicability to approach fundamental questions regarding chemical mechanisms of chlorinated organic compounds. At the moment, the new method of chlorine isotope analysis with GC-IRMS is limited to a narrow range of masses of target compounds. However, it allows similar investigations other important chlorinated pollutants, such as chloroethanes. Furthermore this high-precision technique sets a first benchmark to assign chlorine isotope analysis with the GC-qMS methods for a broad variety of chlorinated compounds of interest.

A1

Appendix A1: Compound-specific chlorine isotope analysis: A comparison of GC-IRMS and GC-qMS methods in an interlaboratory Study

Compound-Specific Chlorine Isotope Analysis: A Comparison of Gas Chromatography/Isotope Ratio Mass Spectrometry and Gas Chromatography/Quadrupole Mass Spectrometry Methods in an Interlaboratory Study

Anat Bernstein,^{†,∇} Orfan Shouakar-Stash,[‡] Karin Ebert,[§] Christine Laskov,[§] Daniel Hunkeler,^{||} Simon Jeannotat,^{||} Kaori Sakaguchi-Söder,[⊥] Jens Laaks,[#] Maik A. Jochmann,[#] Stefan Cretnik,[†] Johannes Jäger,[⊥] Stefan B. Haderlein,[§] Torsten C. Schmidt,[#] Ramon Aravena,[‡] and Martin Elsner^{†,*}

[†]Helmholtz Zentrum München, German Research Center for Environmental Health (GmbH), Ingolstädter Landstr. 1, 85764 Neuherberg, Germany


[‡]Department of Earth and Environmental Sciences, University of Waterloo, 200 University Avenue, West Waterloo, Ontario, Canada

[§]Center for Applied Geoscience (ZAG), Eberhard Karls University Tübingen, Sigwartstr. 10, D-72076 Tübingen, Germany

^{||}Centre for Hydrogeology and Geothermics (CHYN), University of Neuchâtel, Rue Emile Argand 11, CH-2009 Neuchâtel, Switzerland

[⊥]Technische Universität Darmstadt, Institut WAR, Fachgebiet Abfalltechnik, Petersenstrasse 13, 64287 Darmstadt, Germany

[#]Instrumental Analytical Chemistry, University Duisburg-Essen, Universitätsstr. 5, D-45141 Essen, Germany

 Supporting Information

ABSTRACT: Chlorine isotope analysis of chlorinated hydrocarbons like trichloroethylene (TCE) is of emerging demand because these species are important environmental pollutants. Continuous flow analysis of noncombusted TCE molecules, either by gas chromatography/isotope ratio mass spectrometry (GC/IRMS) or by GC/quadrupole mass spectrometry (GC/qMS), was recently brought forward as innovative analytical solution. Despite early implementations, a benchmark for routine applications has been missing. This study systematically compared the performance of GC/qMS versus GC/IRMS in six laboratories involving eight different instruments (GC/IRMS, Isoprime and Thermo MAT-253; GC/qMS, Agilent 5973N, two Agilent 5975C, two Thermo DSQII, and one Thermo DSQI). Calibrations of ³⁷Cl/³⁵Cl instrument data against the international SMOC scale (Standard Mean Ocean Chloride) deviated between instruments and over time. Therefore, at least two calibration standards are required to obtain true differences between samples. Amount dependency of $\delta^{37}\text{Cl}$ was pronounced for some instruments, but could be eliminated by corrections, or by adjusting amplitudes of standards and samples. Precision decreased in the order GC/IRMS ($1\sigma \approx 0.1\%$), to GC/qMS ($1\sigma \approx 0.2\text{--}0.5\%$ for Agilent GC/qMS and $1\sigma \approx 0.2\text{--}0.9\%$ for Thermo GC/qMS). Nonetheless, $\delta^{37}\text{Cl}$ values between laboratories showed good agreement when the same external standards were used. These results lend confidence to the methods and may serve as a benchmark for future applications.

Over the past 15 years, the study of stable isotopes in environmental pollutants has increased enormously, triggered by the development of continuous flow analytical techniques for isotopes such as ¹³C/¹²C, ¹⁵N/¹⁴N, ²H/¹H. Target compounds are isolated from interfering sample components through chromatographic separation, either by gas or by liquid chromatography (GC or LC). Then, they are combusted (or pyrolyzed) online to simple analyte gases (e.g., CO₂, N₂, H₂) which are directly transferred in the continuous helium carrier stream to an isotope-ratio mass spectrometer (IRMS). Following this scheme, suitable analytical techniques for measurement of carbon, nitrogen, and hydrogen isotopes are by now quite well established for an increasing number of environmental pollutants.

It has been demonstrated that such compound-specific isotope analysis is particularly insightful when isotopes are analyzed for two or more elements in environmental contaminants because of enhanced isotopic information. Multiple isotope

analysis may provide unique mechanistic insight into contaminant degradation pathways,^{1–8} and may also distinguish between different contamination sources.^{9,10} However, such multielement isotope information has not been available for many priority pollutants, most prominently chlorinated ethylenes. For these prevalent organic groundwater contaminants online isotope analysis has until recently been limited to carbon raising the need for compound specific chlorine isotope analysis.

Continuous flow chlorine isotope analysis has been prevented by the necessity of converting compounds into analytes such as methyl chloride¹¹ or cesium chloride¹² which cannot be generated online in a carrier gas flow. Offline analysis, on the other hand, is carried out on bulk samples, which requires tedious separation of compounds from interfering components.

Received: February 28, 2011

Accepted: August 18, 2011

Published: August 18, 2011

Therefore, previous chlorine isotope studies have focused mainly on pure compounds, either on the determination of chlorine isotope composition of chlorinated ethylenes of different manufactures^{10,13–16} or on the measurement of chlorine isotope fractionation during evaporation of pure chlorinated ethylenes.^{17,18} Studies involving mixtures of chlorinated ethylenes, either from field studies or from laboratory degradation experiments, have been limited.^{19–25}

Recently, innovative approaches were brought forward for online isotope analysis of chlorinated ethylenes. The first approach²⁶ is unique for GC/IRMS because it does not include a combustion/pyrolysis step, as is typically the case for isotope analysis of C, N, and H. Instead, intact noncombusted chlorinated ethylene molecules are directly transferred within the He carrier stream into the IRMS ion source. There, they are ionized and fragmented, and selected isotopologue ions, or isotopologue ion fragments, are recorded simultaneously in dedicated collector cup configurations. In order to correct for instrument drifts, values are measured in comparison to reference/monitoring peaks which are introduced via a dual inlet system and consist of the same target analyte [e.g., trichloroethylene (TCE) pulses when TCE is measured]. Resultant machine delta values are converted into delta values relative to the international SMOC (Standard Mean Ocean Chloride) standard²⁷ by external calibration with independently characterized secondary standards, again of the same target analyte (i.e., a TCE standard calibrated to SMOC when TCE is measured).

An alternative approach²⁴ has been brought forward by Sakaguchi-Söder et al. with gas chromatography coupled to conventional quadrupole mass spectrometry (GC/qMS). Also, here analysis is conducted on noncombusted molecules. In contrast to the IRMS method, however, compound-specific standards were not available so that isotope ratios were calculated from ion multiplet intensities of molecular and fragment ions.²⁴ A theoretical justification for both approaches (GC/IRMS and GC/qMS) was subsequently given by Elsner and Hunkeler.²⁸ Very recently, the GC/qMS approach was further tested and modified by Aeppli et al.³⁰ In contrast to Sakaguchi-Söder et al.,²⁴ Aeppli et al.³⁰ considered only molecular ions for their calculations, and they performed a calibration with external standards to obtain δ values on the SMOC scale.

These two new analytical concepts are promising, and each has its specific advantages: Whereas the GC/IRMS provides high precision for a narrow range of compounds, GC/qMS instruments are shown to be not as precise, yet universal with respect to target analytes. Although both approaches have been spearheaded to a point where compound-specific values on the SMOC scale can be obtained, a systematic comparison between the performances of the two techniques has not yet been carried out. In particular, to ensure that the results derived by both concepts and in different laboratories are indeed reliable, the following fundamental aspects remain to be investigated experimentally.

Precision. To date, the precision of the two different methods (GC/IRMS versus GC/qMS) has not yet been systematically compared with the same substance on different instruments and in different laboratories to obtain a representative performance overview.

Amount Dependency. Stable isotope measurements are known to show an amount dependency. On the one hand, precision deteriorates with smaller sample amounts when approaching the shot-noise limit of the detector.^{31,32} On the other hand, space-charge effects in the ion source of the IRMS may

cause a nonlinear ionization efficiency at higher molecule abundance. These effects must be corrected to obtain accurate values. Alternatively, a strict standard bracketing strategy may be adopted where standard peak amplitudes are in the same range as the analyte peaks (within 20% difference³⁰). These observations demand a comprehensive survey for the case of continuous flow chlorine isotope analysis.

Referencing and Standardization. Ideally, peaks of the target analyte are introduced at the beginning and at the end of each gas chromatographic run in order to correct for instrument drift (monitoring/“reference” gas). This option is implemented in IRMS, but typically not in qMS instruments. In addition, when using either GC/IRMS or GC/qMS, samples should be bracketed by external standards which have been characterized relative to SMOC by an independent method beforehand. Online chlorine isotope analysis conducts the measurements on noncombusted target molecules. Therefore, monitoring gas and standards must have the same molecular structure as the target compound.

For both GC/IRMS and GC/qMS, calibrations with two external compound-specific standards may be difficult to implement in routine practice, however, so that it could be an attractive shortcut to use just one external standard. Occasionally, the absolute scale is not even of importance, for example in laboratory experiments where kinetic isotope effects are determined from the relative difference between samples. Are external standards even required in such a case? A systematic investigation is needed to explore how calibration is best accomplished for online chlorine isotope analysis and whether standard bracketing is necessary.

Accuracy³⁴. Even if a two-point calibration is performed it remains to be investigated whether the same result is indeed obtained when the same standards are used (a) with the same method but different instruments in different laboratories and (b) with different methods (GC/IRMS versus GC/qMS).

Therefore, in this study the performance of the two chlorine isotope techniques was examined by analyzing TCE standards in six different laboratories by eight different instruments. Six GC/qMS instruments were used: one Agilent 5973N, two Agilent 5975C, one Thermo DSQI, and two Thermo DSQII quadrupole mass selective detectors (in Darmstadt, Tübingen, Neuchâtel, Duisburg-Essen, Neuchâtel, and Duisburg-Essen, respectively). The other two laboratories used GC/IRMS instrumentation: one (Waterloo) an Isoprime Limited instrument (previously known as Micromass, U.K.) and the other (München) a Thermo Fisher Finnigan MAT 253 device. Both of them have a dedicated detector cup configuration to acquire the mass-to-charge ratios m/z of 95 and 97 (single dechlorinated fragment ion of TCE).

The first major objective of this work was to test for the precision and the quantification limit of the method. To this end, an aliquot of pure TCE was sent out to the participating laboratories, and they were asked to perform quintuplicate analyses of increasingly smaller amounts to span a range of concentrations typical of their method. Also, it was our aim to test the effect of amount dependency, that is, to compare nonlinearity effects of different instruments, and to test whether they can be eliminated by proper protocols.

The second major objective was to evaluate how instrument data should be calibrated to the international SMOC scale. It was our aim to examine how much the GC/qMS “raw” R ratios changed over time, how values improved after calibration with

external standards, and whether none, one, or two external standards are required in routine applications.

The third major objective was, finally, to evaluate the accuracy of results obtained in different laboratories, as well as the total uncertainty of the measurement. To this end, five pure unknown TCE samples were sent out along with two pure TCE standards (EIL-1, $\delta^{37}\text{Cl} = +3.05\text{‰}$; EIL-2, $\delta^{37}\text{Cl} = -2.70\text{‰}$) that had been characterized beforehand at the University of Waterloo. Laboratories were asked to analyze these samples relative to their in-house standards (monitoring gas peaks for GC/IRMS, external standards for GC/qMS) and to report their instrument data (machine δ values for GC/IRMS, calculated “raw” R ratios for GC/qMS).

This round robin test differs from a proficiency test in two aspects. (1) Absolute trueness of $\delta^{37}\text{Cl}$ values was not a primary objective. Although the TCE calibration standards (EIL-1 and EIL-2) are calibrated to SMOC at the University of Waterloo using secondary TCE standards (see Experimental Section), we did not attempt to characterize associated measurement errors. Instead, our focus was on internal consistency of measurements following a study design of Brand and Coplen:³⁵ it was tested whether the same results were obtained in different laboratories when the same standards were used as anchors for calibration, irrespective of their absolute trueness on the SMOC scale. (2) This study had the objective to test different methods, rather than ranking different laboratories. We therefore did not suppress information exchange between participating laboratories, but rather catalyzed a consistent measurement approach (Table 1). For this reason, six out of eight instrument setups in this study used headspace analysis, since this injection technique is known to be associated with minimal carbon isotope fractionation effects.³³ For the same reason (to obtain a “best case” result as a benchmark for further studies) a reductionist approach was chosen where samples contained pure TCE rather than complex substance mixtures.

■ EXPERIMENTAL SECTION

Chemicals. TCE was purchased from different manufacturers. The source and purity of the different products are summarized in Table S1 (Supporting Information). The pure TCE products were divided into 1.8 mL glass vials using a 50 mL glass syringe, to ensure homogeneity. Vials were filled without headspace and sealed immediately with Teflon lined caps, to avoid volatilization. These vials were shipped to all participating laboratories. Neither evaporation from closed vials nor decomposition was observed during the time of this interlaboratory test. The secondary standards EIL-1 and EIL-2 were calibrated to the SMOC scale ($n = 15$) against defined standards using a GC/IRMS in Waterloo²⁶ where the calibration at equal peak amplitudes so that no correction for amount dependency was necessary. The standard deviation replicate of measurements of the TCE standards were 0.07‰ and 0.11‰, respectively ($n = 15$). Standards were kept in 2.0 mL vials sealed with Teflon/silicone (PTFE/silicone) septa caps and stored in the dark. Analysis of the stored standards along a period of two years indicated no shift in their isotopic composition.

Chlorine Isotope Measurements. Chlorine isotope composition was measured in each laboratory either by GC/qMS or GC/IRMS. The following instruments were used (detailed

analytical methods are provided in the Supporting Information, as well as briefly summarized in Table 1).

Tübingen. An Agilent 7890A GC coupled to an Agilent 5975C quadrupole mass selective detector (Santa Clara, CA) was used for measurements. Headspace injections were performed using an automatic multipurpose sampler (Gerstel, Mülheim an der Ruhr, Germany). This instrument setup will be referred to in the following text as qMS-Agilent-1.

Darmstadt. A 6890N GC coupled to an Agilent 5973N quadrupole mass selective detector (Santa Clara, CA) was used. Samples were preconcentrated by a purge and trap system PTA 3000 from IMT (Moosbach, Germany). This instrument setup will be referred to in the following text as qMS-Agilent-2.

Neuchâtel. A Thermo Trace GC–DSQII MS (Thermo Fisher Scientific, Waltham, MA) was used for measurements. Headspace injections were performed using a CombiPal autosampler (CTC Analytics, Zwingen, Switzerland). This instrument will be referred to in the following text as qMS-Thermo-1.

Additionally, an Agilent 7890A GC coupled to an Agilent 5975C quadrupole mass selective detector (Santa Clara, CA) was tested in Neuchâtel. Headspace injections were performed using a CombiPal autosampler (CTC Analytics, Zwingen, Switzerland). This instrument will be referred to in the following text as qMS-Agilent-3.

Waterloo. An Agilent 6890 GC coupled to a continuous flow-IRMS (IsoPrime, Micromass, currently elementar) was used for measurements. Injections were carried out using a CombiPal (CTC Analytics, Zwingen, Switzerland) solid-phase microextraction (SPME) autosampler. This instrument will be referred to in the following text as IRMS-IsoPrime.

Duisburg-Essen. A Thermo Trace GC–DSQII MS (Thermo Fisher Scientific, Waltham, MA) and a Thermo Trace GC–DSQI MS (Thermo Fisher Scientific, Waltham, MA) were used for measurements. Both instruments were equipped with a CombiPal autosampler (CTC Analytics, Zwingen, Switzerland) for headspace injections. These instruments will be referred to in the following text as qMS-Thermo-2 and qMS-Thermo-3, respectively.

München. A Trace GC (Thermo Fisher Scientific, Milan, Italy) directly coupled to a Finnigan MAT 253 IRMS (Thermo Fisher Scientific, Bremen, Germany) was used for measurements. Headspace injections were carried out using a Concept autosampler (PAS Technologies, Magdala, Germany). This instrument will be referred to in the following text as IRMS-Thermo.

Each laboratory was allowed to analyze the samples according to their optimized methods with regard to recorded masses, peak integration, dwell time, etc.

Calculations, GC/qMS. Raw isotope ratios were calculated from the ion abundance of the mass spectrum. According to Sakaguchi-Söder et al.,²⁴ chlorine isotope ratios of the target compounds can be calculated as a weighted average from isotopologue ion multiplets according to the general expression

$$R_X = a \times R_m + b \times R_1 + c \times R_2 \dots + n \times R_{n-2} \quad (1)$$

where a, b, \dots, n are the normalized intensities of the various peak groups and where R is the isotope ratio derived from the respective peak group. Using this basic concept, Sakaguchi-Söder proposed a series of mathematical equations to determine chlorine isotope ratios for six chlorinated ethenes, three chlorinated ethanes, atrazine, and two dioxin congeners.²⁹ For the

Table 1. Technical Parameters and Summary of Main Results Obtained on the Different Instruments

instrument code	GC/IRMS	GC/IRMS	GC/qMS	GC/qMS	GC/qMS	GC/qMS	GC/qMS	GC/qMS	GC/qMS
laboratory	IRMS-Thermo München	IRMS-Isoprime Waterloo	GC/qMS Tübingen	GC/qMS Darmstadt	GC/qMS Neuchâtel	GC/qMS Neuchâtel	GC/qMS Thermo	GC/qMS Duisburg-Essen	GC/qMS Duisburg-Essen
instrument manufacturer	Thermo	IsoPrime	Agilent	Agilent	Agilent	Thermo	Thermo	Thermo	Thermo
qMS or IRMS	Finnigan MAT 253	IsoPrime, Micromass	Agilent 5975C	Agilent 5973N	Agilent 5975C	DSQII	DSQII	qMS-Thermo-2	qMS-Thermo-3
m/z	95, 97	95, 97	60, 62, 95, 97, 130, 132	60, 62, 95, 97, 130, 132	130, 132	60, 62, 95, 97, 130, 132	60, 62, 95, 97, 130, 132	Duisburg-Essen	Duisburg-Essen
dwell time	∞	∞	30 ms	100 ms	50 ms	30 ms	10 ms		
GC	Thermo Trace GC	Agilent 6890	Agilent 7890A	Agilent 6890N	Agilent 7890A	Thermo Trace GC	Thermo Trace GC		
flow	1.4 mL min ⁻¹	1.8 mL min ⁻¹	1.0 mL min ⁻¹	1.0–2.0 mL min ⁻¹	1.2 mL min ⁻¹	1.5 mL min ⁻¹	1.0 mL min ⁻¹		1.0 mL min ⁻¹
split	1:15	splitless	1:10–1:100	splitless	1:10	1:10	1:10		1:10
column	DB-5 (30 m × 0.25 mm × 0.25 μm, Agilent J&W) + a wax column (60 m × 1 μm, Agilent J&W)	DB-5 (60 m × 0.320 mm × 0.25 μm, Agilent J&W)	RTX-VM5 (60 m × 0.25 mm × 1.4 μm, Restek)	DB-624 (60 m × 0.25 mm × 1.4 μm, Agilent J&W)	DB-5 (30 m × 0.25 mm × 0.25 μm, Agilent J&W)	DB-VRX (60 m × 0.25 mm × 1.4 μm, Agilent J&W)	RTX-VM5 capillary column (60 m × 0.32 mm, 1 μm, Restek)	StabilwaxDA (60 m × 0.32 mm, 1 μm, Restek)	
injection technique	automated HS	SPME	automated HS	purge and trap	automated HS	automated HS	automated HS	automated HS	automated HS
peak integration	Isodat version 2.5	MassLynx Inorganic version 4017	ChemStation software, version E.01.01.355; RTE integrator	ChemStation version D.02.00.237; ChemStation Integrator	ChemStation version E.02.01.1177	Excibur version 1.4	Excibur version 1.4	Excibur version 1.4	Excibur version 1.4
software	Supelcowax 10)								
typical precision (1σ)	<0.1% ^a	0.09 ± 0.03% ^b	0.18–0.50% ^a	0.15–0.57% ^a	0.16–0.49% ^a	0.37–0.92% ^a	0.35–0.84% ^{a,d}	0.63 ± 0.09% ^{b,d}	0.35 ± 0.11% ^{b,e}
detection limit	5.3 ng for 1σ<0.15% ^b	not determined	0.26 ± 0.05% ^b	0.27 ± 0.06% ^b	0.37 ± 0.11% ^b	0.71 ± 0.11% ^b	0.35% ± 0.33% ^e	not determined	not determined
mass dependency	1% over 0.8–53 ng	high (not determined in this study)	20 ng for 1σ<0.5% ^b	10 ng for 1σ<0.5% ^b	>36 ng for 1σ<0.5% ^b	12.5 ng for 1σ<1.0% ^b	0.4 ng for 1σ<0.85% ^e	20% over 1.0–200 ng ^e	not determined
two-point calibration	1.08 ± 0.02		1.20 ± 0.05	0.72 ± 0.03	1.09 ± 0.06	1.24 ± 0.22	0.91 ± 0.14 ^e	1.31 ± 0.12 ^e	1.33 ± 0.10 ^d
curve slope							1.35 ± 0.22 ^d		
av uncertainty of calibrated SMOC	0.040 ± 0.003% ^b		0.11 ± 0.02% ^b	0.08 ± 0.01% ^b	0.10 ± 0.01% ^b	0.47 ± 0.22% ^b	0.53 ± 0.13% ^b and	0.39 ± 0.02% ^b and	0.21 ± 0.03% ^{b,d}
values ± standard deviation for replicate measurement of different TCE compounds ^e	(n = 10, m = 20)		(n = 10, m = 20)	(n = 10, m = 20)	(n = 10, m = 20)	(n = 5, m = 10)	(n = 5, m = 10),	(n = 5, m = 10),	(n = 5, m = 10),
range of z-scores ^f	0.50–1.05		0.06–1.58	0.08–2.37	0.26–0.79	0.09–1.23	0.13–1.44 ^e	0.13–0.69 ^f	0.68–3.45 ^d

^a Values obtained in the linearity test of Figure 1 (TCE repeatedly injected at varying amount). ^b Values obtained in the accuracy test of Figure 3b (TCE repeatedly injected at same amount). ^c Default peak integration settings. ^d Modified peak integration settings. ^e Values obtained in the accuracy test of Figure 3c. ^f Absolute value of z-score, calculated for accuracy test.

specific case of TCE this gives

$$\begin{aligned}
 R_{\text{TCE}} &= \frac{I_{130}}{I_{130} + I_{95} + I_{60}} \times \left(\frac{1}{3} \cdot \frac{I_{132}}{I_{130}} \right) \\
 &+ \frac{I_{95}}{I_{130} + I_{95} + I_{60}} \times \left(\frac{1}{2} \cdot \frac{I_{97}}{I_{95}} \right) \\
 &+ \frac{I_{60}}{I_{130} + I_{95} + I_{60}} \times \left(\frac{I_{62}}{I_{60}} \right) \\
 &= \frac{1}{3} \cdot \frac{I_{132}}{I_{130} + I_{95} + I_{60}} + \frac{1}{2} \cdot \frac{I_{97}}{I_{130} + I_{95} + I_{60}} \\
 &+ \frac{I_{62}}{I_{130} + I_{95} + I_{60}} \quad (2)
 \end{aligned}$$

where I_{132} and I_{130} are peak intensities of the most abundant peaks in the molecular ion group, I_{97} and I_{95} in the group of the single dechlorinated fragment ion, and I_{62} and I_{60} in the group of the double dechlorinated fragment. The binomial coefficients account for the fact that ^{37}Cl can sit in either of three positions in the molecular ion, in either of two positions in the single dechlorinated fragment, and in only one position in the double dechlorinated fragment.

Alternatively, as validated theoretically by Elsner and Hunkeler,²⁸ isotope ratios should be directly attainable from any pair of isotopologues, either of the parent ion, or of any fragment ion. For the specific case of TCE this gives

$$R_{\text{TCE}} = \frac{1}{3} \cdot \frac{I_{132}}{I_{130}} = \frac{1}{2} \cdot \frac{I_{97}}{I_{95}} = \frac{I_{62}}{I_{60}} \quad (3)$$

R_{TCE} ratios calculated according to eqs 2 or 3 are subsequently converted to an internal δ scale by referencing against an external laboratory standard, R_{std} , measurements of which bracketed those of the samples:

$$\delta = [(R_{\text{sample}}/R_{\text{std}}) - 1] \times 1000 \quad (4)$$

Choice of Ions. Consequently, isotope values may be derived from GC/qMS measurements in different ways. Calculations may consider only molecular ions,³⁰ also fragment ions (eqs 1 and 2), only the most abundant two peaks³⁰ (eqs 1 and 2), or also the less abundant peaks of a given multiplet. In our study, laboratories were allowed to analyze the samples according to their optimized methods. The different calculation approaches were recently compared experimentally.³⁶ It was found that considering only molecular ions resulted in less precise raw isotope ratios than considering the two most abundant ions of each fragment group (for TCE: 60, 62, 95, 97, 130, 132). On the other hand, including all nine ions of TCE resulted in less precise raw isotope ratios again, since analyzing too many ions conflicted with maintaining a sufficient dwell time and scan rate. Although significant, the magnitude of the differences reported in ref 36 suggests that different calculation schemes are not a likely reason for the systematic differences observed in this study.

Peak Integration Parameters. Most participating laboratories relied on default peak integration settings of their software. In one case (qMS-Thermo-2 and qMS-Thermo-3 in Duisburg-Essen) evaluation was performed in two ways: (1) with default peak parameters; (2) with parameters such that the peak start and end points were as similar as possible for each fragment ion. (A defined adjustment proved difficult, since the software

“Excalibur” treated every ion as an independent compound.) Unless mentioned otherwise, results of the optimized evaluation method 2 are presented.

Calculations, GC/IRMS. In the GC/IRMS method, target peaks were automatically evaluated against monitoring peaks that were introduced through a dual inlet system during each sample run using the respective software (Isodat 2.0, Thermo Electron Corporation, and MassLynx Inorganic, V. 4017, GV Instruments, currently Isoprime Limited, U.K., in München and Waterloo, respectively).

External Calibration. For both analytical techniques (GC/qMS and GC/IRMS), these “raw” δ values were subsequently converted to the international SMOC scale using two previously characterized TCE standards, EIL-1 and EIL-2, which are 5.75‰ apart on the $\delta^{37}\text{Cl}_{\text{SMOC}}$ scale. Internal values were transformed according to a two-point linear regression trend line. The slope’s error of the calibration curve, as it appears in the following sections, was calculated as 95% confidence interval (slope’s standard error multiplied by the student t for $\alpha = 0.05$). The performance of the different laboratories in terms of accuracy was tested by z -score,⁴⁰ defined as $z = (x - X)/\sigma$, where x is the average value obtained in the respective laboratory, X is the assigned value (or “consensus value”), and σ is the standard deviation of the measured value in the laboratory. The assigned value, X , was set as the results obtained by IRMS-Isoprime from Waterloo, following the long experience that has been gained in this laboratory over the years. The uncertainty of SMOC values derived from multiple measurements of the same sample and following the uncertainty of the calibration curve was calculated as

$$S_m = \left(\frac{S_r}{|M|} \right) \sqrt{\frac{1}{m} + \frac{1}{n} + \frac{(y_m - y_{\text{avg}})^2}{M^2 \sum (x_i - x_{\text{avg}})^2}} \quad (5)$$

where S_m is the standard deviation of a reported x value derived from its associated instrument value y through calibration, S_r is the standard deviation of the calibration’s regression, M is the slope of the calibration curve, m is the number of x - y pairs of the calibration curve, n is the number of replicate measurements of the unknown, y_m is the measured y value to be calibrated, y_{avg} is the average y value of the calibration curve, x_i is the concentration of the standards, and x_{avg} is the average concentration of the standards.

The S_m value can be further used to calculate the 95% confidence interval, Δ , of the value on the SMOC scale by student’s t as

$$\Delta = t \frac{S_m}{\sqrt{n}} \quad (6)$$

RESULTS AND DISCUSSION

Precision and Amount Dependency (“Linearity”). To test for the precision and linearity of the different analytical approaches, two aspects were addressed: (1) How precise are replicate measurements at a given injected amount? (2) How precise are measurements at a range of varying injected amounts? Figure 1 presents these two aspects for replicate TCE measurements over a wide range of amounts. Typically, 1σ ($n = 5$, unless specified otherwise) values obtained for replicate injections of the same amount of TCE were higher on GC/qMS instruments than on GC/IRMS. One standard deviation (1σ) of GC/qMS

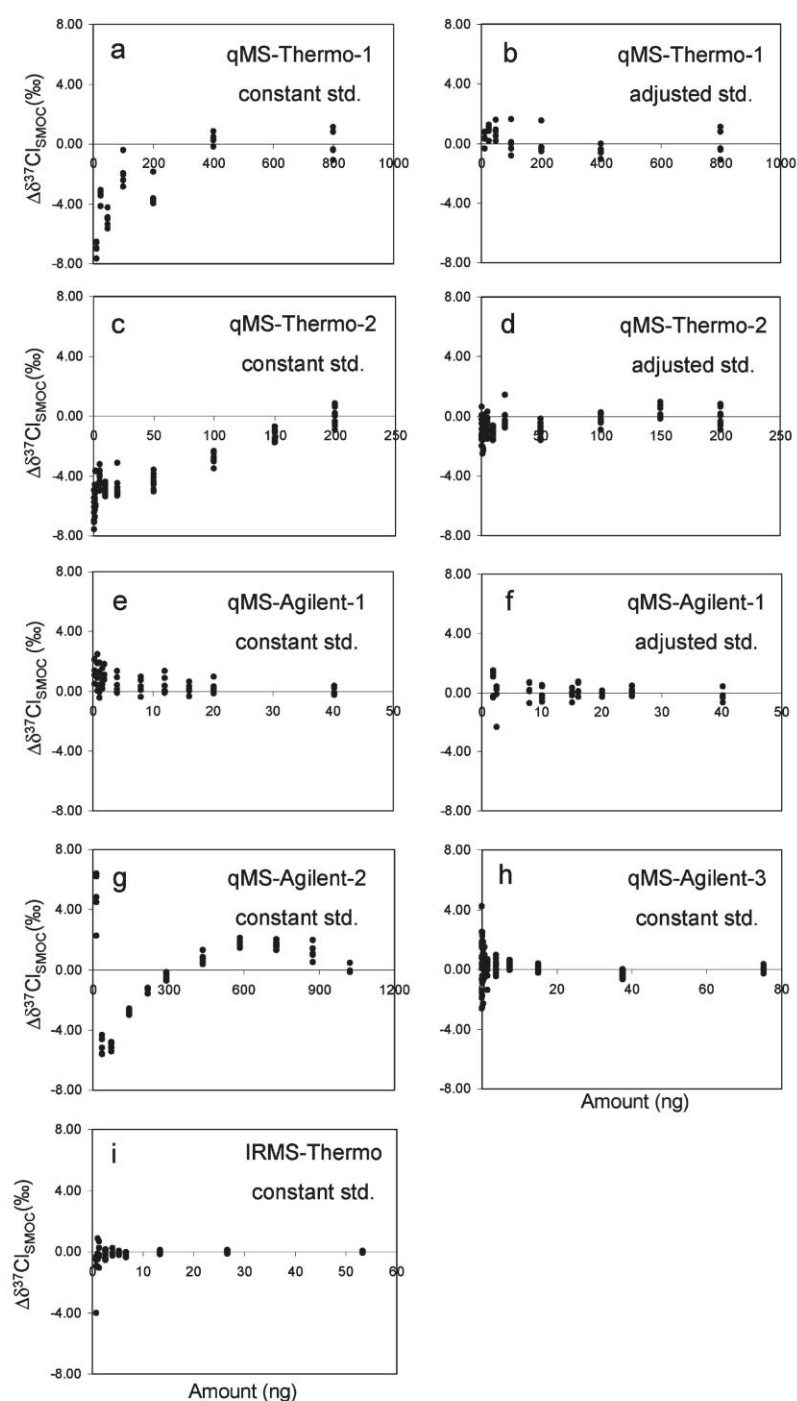


Figure 1. Measured $\delta^{37}\text{Cl}$ depending on the on-column amount of TCE. Values are presented as the difference from the average of the replicates in the highest on-column amount. (a) qMS-Thermo-1 (automated headspace injections, amplitude of standards along the sequence was held constant). (b) qMS-Thermo-1 (automated headspace injections, standards were adapted to the amplitude of target peaks). (c) qMS-Thermo-2 (automated headspace injections, amplitude of standards along the sequence was held constant). (d) qMS-Thermo-2 (automated headspace injections, standards were adapted to the amplitude of target peaks). (e) qMS-Agilent-1 (automated headspace injections, amplitude of standards along the sequence was held constant). (f) qMS-Agilent-1 (automated headspace injections, standards were adapted to the amplitude of target peaks). (g) qMS-Agilent-2, (purge-and-trap injection, amplitude of standards along the sequence was held constant). (h) qMS-Agilent-3 (automated headspace injections, amplitude of standards along the sequence was held constant). (i) IRMS-Thermo, automated headspace injections where reference peaks were introduced at the beginning and end of each GC run (amount was held constant).

instruments was in the following range (on-column amounts and corresponding figure panels are given in brackets): 0.18–0.50‰ on the qMS-Agilent-1 (0.4–40 ng; Figure 1e), 0.15–0.57‰ on the qMS-Agilent-2 (37–1000 ng; Figure 1g), and 0.16–0.49‰ on the qMS-Agilent-3 (0.75–75 ng; Figure 1h; $n = 15$ for each amount). On the Thermo instruments, lower precisions were observed with typical 1σ in the range 0.37–0.92‰ on the qMS-Thermo-1 (13–800 ng; Figure 1a), and 0.35–0.84‰ on the qMS-Thermo-2 (0.4–200 ng; Figure 1c; up to $n = 10$ for each amount). In GC/IRMS measurements, in contrast, much higher precisions were observed, with $1\sigma = 0.06\%$ at 53 ng on the IRMS-Thermo (Figure 1i). A similar precision was obtained earlier on the IRMS-Isoprime,²⁶ but was not evaluated again in this study. At 1.1 ng TCE the value for 1σ was still 0.6‰ at the IRMS-Thermo, representing the lower limit for precise chlorine isotope analysis (Figure 1i). The better performance of GC/IRMS likely reflects the ability to simultaneously acquire different ions in a dedicated cup configuration, as well as to introduce monitoring gas peaks during each gas chromatographic run.

Amount Dependency. The second aspect of precision is the “linearity”: How precise are measurements in a range of varying injected amounts (i.e., are the measured values amount dependent)? Here, our study clearly shows that amount dependency (“non-linearity”) effects can be very substantial, and where they occur appropriate correction is mandatory, such as brought forward by Shouakar-Stash et al., in 2006.²⁶ Surprisingly, similar analytical concepts did not necessarily entail an identical pattern of amount dependency. For example, on the IRMS-Thermo linearity was significantly better than on the IRMS-Isoprime.²⁶ Even instruments of similar construction such as qMS-Thermo-1 and 2, or qMS-Agilent-1, 2, and 3 gave different amount dependency trends. It should be noted, however, that results from different instruments do not necessarily reflect identical ranges of injected amounts; hence, the data evaluation must be performed individually by each laboratory for the analyzed concentration range.

Importantly, our results demonstrate that a proper standardization scheme, as brought forward by Aeppli et al.,³⁰ may eliminate the need for an amount dependency correction. Here, samples are bracketed by known external standards along the sequence of measurements. Our data clearly shows that amount dependency effects are pronounced if standards have a constant amplitude whereas amplitudes of the samples vary (Figure 1e,a,c for qMS-Agilent-1, qMS-Thermo-1, and qMS-Thermo-2, respectively). In contrast, they become negligible if the amount of the standard is adapted to the sample (Figures 1f, 1b, and 1d for qMS-Agilent-1, qMS-Thermo-1, and qMS-Thermo-2, respectively). This strategy of adjusting samples and standards to the same concentration is clearly advantageous when samples with known concentrations are analyzed. Alternatively, good linearity is desirable (e.g., as observed on the IRMS-Thermo, or on the qMS-Agilent-3). If linearity is not as good, however, and if sample concentrations are not known beforehand, an amount dependency correction may have to be performed on the basis of amount dependency trends that are defined by running additional standards with differing amounts along the sequence.

Besides processes in the ion source, also the injection technique may be of importance since isotope discrimination during injection might contribute to the amount dependency effects. To test this hypothesis a comparison of manual headspace injection versus purge-and-trap was performed at the qMS-Agilent-2, and a

comparison between automated headspace injections versus SPME injections was performed at the qMS-Agilent-1 (Figure S1 in the Supporting Information). The comparison shows that the injection technique alone cannot explain the strong amount dependency on the qMS-Agilent-2. It remains to be investigated whether there is potential for improvement by a specific tuning for enhanced linearity as is well-known from GC/IRMS applications.³⁷

Calibration of Data to the SMOC δ Scale. Calibration by external standards (1) corrects for instability of the instrument; (2) projects instrument values on the international SMOC scale through correction for an offset; (3) corrects for distortion relative to the SMOC scale (e.g., if two standards that are 5‰ apart differ by only 4‰ on the instrument scale).

Instability of the Instrument. The variability of “raw” instrument values R calculated from mass spectra according to eq 2 was investigated on the qMS-Agilent-1 instrument (Figure 2a). Figure 2a shows that large differences in the R values were obtained at different dates and with different filaments (differences of 0.004 corresponding to 12‰ on the δ scale; eq 4). However, these differences could be corrected when standards were analyzed in the same sequence (Figure 2b). Thus, temporal variations in the instrument largely cancel out when standards are exposed to the same conditions as the samples. These results emphasize the need for standardization in GC/qMS when determination of absolute values is of concern or when a set of samples is not analyzed in the same sequence: Although in theory calculated R values are directly related to the ³⁵Cl/³⁷Cl ratio of the bulk material²⁴ (see eq 2), our results show that these R values are influenced by instrumental factors and require proper correction.

Slopes of Two-Point Calibrations. To obtain absolute values on the international SMOC scale, a two-point calibration was performed in each of the participating laboratories using the EIL-1 and EIL-2 standards. Although such two-point isotopic calibrations are well established in dual inlet-IRMS and EA-IRMS measurements (see, e.g., refs 35,38), they are rare in compound specific isotope analysis by GC/IRMS. Figure 2c presents the resultant calibration curves of the different laboratories. The comparison reveals that curves were different between laboratories, giving slopes for GC/qMS instruments of 1.20 ± 0.05 (qMS-Agilent-1), 0.72 ± 0.03 (qMS-Agilent-2), 1.09 ± 0.06 (qMS-Agilent-2), 1.24 ± 0.22 (qMS-Thermo-1), 0.91 ± 0.14 (qMS-Thermo-2 with default peak integration), 1.35 ± 0.22 (qMS-Thermo-2 after peak reintegration), 1.31 ± 0.12 (qMS-Thermo-3 with default peak integration), and 1.33 ± 0.10 (qMS-Thermo-3 after peak reintegration), and for GC/IRMS of 1.08 ± 0.02 (IRMS-Thermo). The given uncertainty corresponds to 95% confidence intervals that were calculated from the slope's standard error multiplied by the appropriate student t factor for $\alpha = 0.05$.

Calibration slopes did not only differ between instruments, but also may change over time. Whereas calibration slopes of the IRMS-Thermo ranged between 0.98 ± 0.04 and 1.09 ± 0.04 in five different measurement series within a three month period, slopes of the qMS-Agilent-1 in Tübingen ranged between 1.14 ± 0.12 and 1.25 ± 0.10 in nine different measurement series within a similar time period. A longer period of observation was recorded on the IRMS-Isoprime in Waterloo over the years 2008–2010, where slopes of almost 150 distinct measurement sequences ranged from 0.90 to 1.23 (Figure 2d).

Since finding and characterizing two sufficiently different standards for every new target compound is difficult and labor intensive, at the beginning of this paper we raised the question

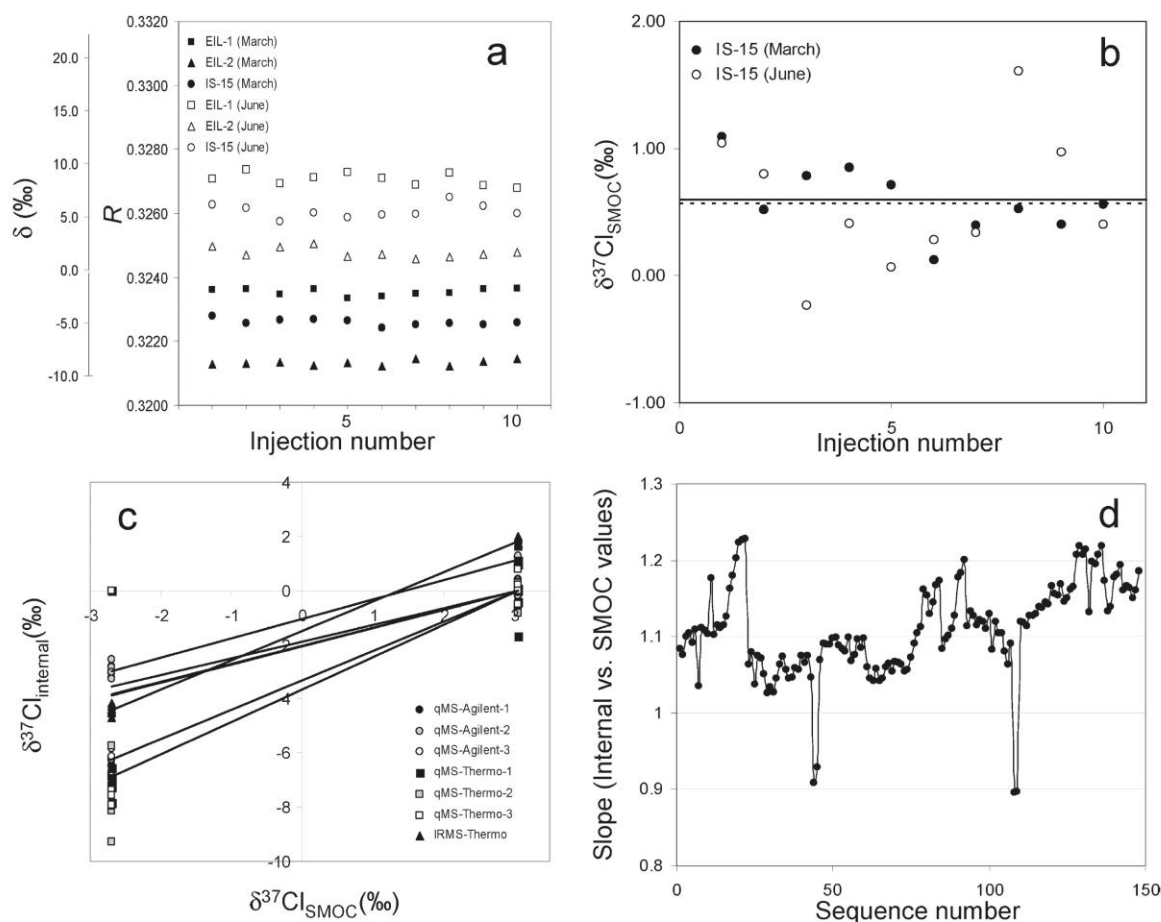


Figure 2. (a) Nominal R and corresponding δ values calculated according to eq 2 for three different types of TCE using data from qMS-Agilent-1 analysis in March and June 2010 with different filaments (constant amount injected). The R and δ values are referred to a relative scale. (b) The corresponding $\delta^{37}\text{Cl}_{\text{SMOC}}$ (‰) values of the TCE product IS-15, obtained from the same qMS-Agilent-1 measurements after external calibration with EIL-1 and EIL-2. Average values for the measurements of March and of June are indicated as solid and dashed lines, respectively. (c) Calibration curves for converting the internal values to the SMOC scale in different laboratories. (d) Slopes of calibration curves measured by IRMS-Isoprime for almost 150 distinct measurement sequences during the years 2008–2010.

whether calibration with two standards is necessary if the primary focus is on differences in isotope ratios rather than on absolute numbers, and if all samples are analyzed on the same day. Would calculation of isotope ratios from isotopologue ions (e.g., according to eq 3) still give useful, internally consistent data sets, even if the numbers were not correct on an absolute scale? Our results strongly discourage such a practice. The calibration slopes clearly document a significant, nonsystematic distortion of instrument scales relative to the SMOC scale. Therefore, even differences between isotope values (e.g., changes in isotope ratios relative to an initial value or to an undefined internal standard) would be inaccurate without proper calibration, and would, for example, give wrong fractionation factors in a degradation experiment.

Accuracy Test. The need for a multipoint calibration is further supported by the results of the accuracy test, as shown in Figure 3. Five TCE products of different producers were analyzed in the different laboratories, using either one or two TCE standards for calibration to the SMOC scale (Figure 3; the figure's raw data is provided in the Supporting Information,

Table S2). When results were projected on the SMOC scale using one standard only, large differences were obtained (Figure 3a). In contrast, when using two calibration anchor points, dramatically better agreement was accomplished between laboratories (Figure 3b,c). Excellent agreement was observed between the two laboratories that used GC/IRMS, where values of all five products were identical within 0.2‰. Good agreement was observed with GC/qMS values where more significant differences were observed, yet generally in the range of 1σ ($n = 10$).

Accuracy and Total Uncertainty. For defining the accuracy and total uncertainty of the measurements, different strategies may be taken: (1) When asking what the uncertainty of an average value on the SMOC scale is, based on n replicates and a calibration curve with a defined uncertainty, eqs 5 and 6 should be applied. (2) When asking whether a single measurement belongs to, or differs from, an average value of n replicates, the standard deviation of the replicates should be considered, with 2σ indicating the 95% confidence interval. (3) When asking

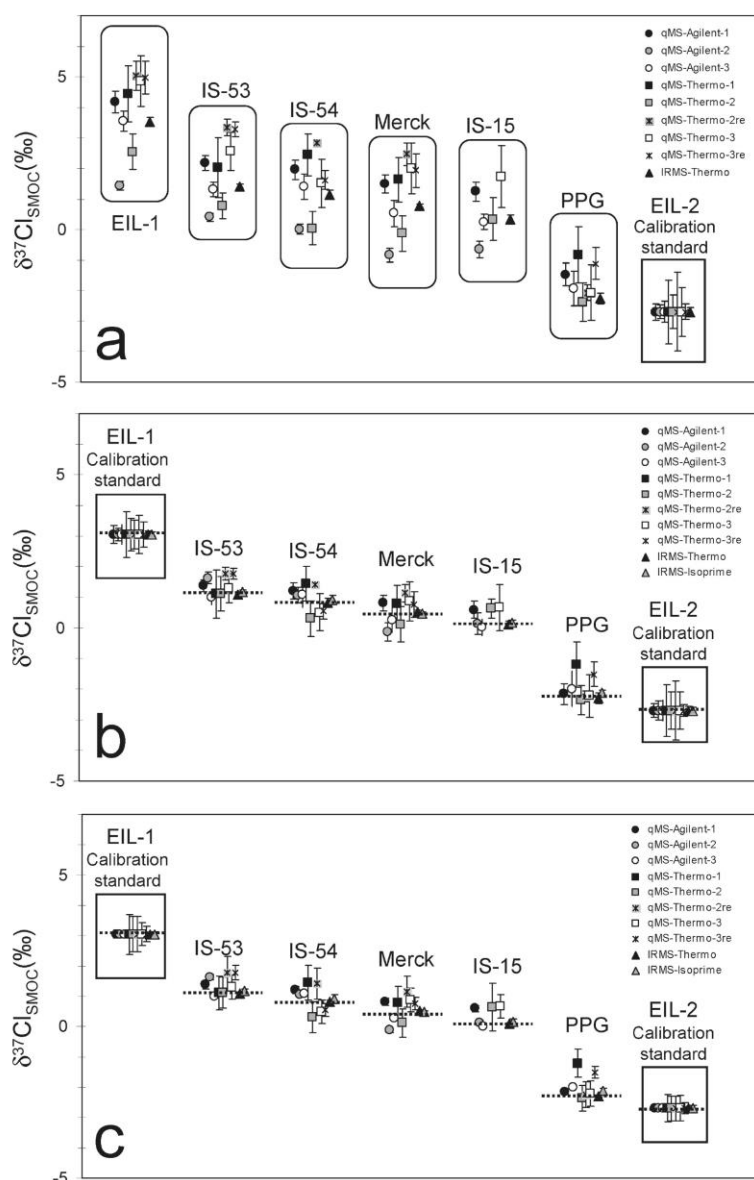


Figure 3. Measured $\delta^{37}\text{Cl}$ of 5 different TCE products in different laboratories. (a) Calibration to the SMOC scale was carried out using a single standard; error bars indicate 1σ on the internal instrument scale (y axis of Figure 2c). (b) Calibration to the SMOC scale was carried out using two standards; error bars indicate 1σ converted to the SMOC scale (x axis of Figure 2c, relevant for the z-score). (c) Calibration to the SMOC scale was carried out using two standards; error bars indicate the total uncertainty of each data point (95% confidence interval) calculated according to eqs 5–6 (error that would be reported in an interlaboratory exercise). Horizontal dashed lines represent the consensus value (i.e., the measurements on the IRMS-Isoprime in Waterloo).

whether an average value from a single laboratory is similar to a consensus value, z-scores may be calculated.

In the first case, average SMOC values are associated with (a) the uncertainty of n replicate measurements and (b) the uncertainty of the calibration curve which converts instrument values on the SMOC scale (eqs 5 and 6). Both uncertainties depend on the number of measurements, that is, n (the measurements of the unknown) and m (the number of data points in the calibration). The average uncertainty of the calibrated SMOC values are in the range 0.08–0.11‰ for the Agilent qMS instruments, 0.21–0.47‰ for the Thermo qMS instruments (note that $n = 5$, $m = 10$), and

0.04‰ for GC/IRMS-Thermo instrument ($n = 10$, $m = 20$). Values for each individual instrument are provided in Table 1.

Alternatively, in the second case (i.e., for differentiating between samples that are run in a single sequence and are therefore associated with the same uncertainty of the same calibration curve), one may consider the standard deviation of replicate injections to differentiate between samples. For 95% confidence intervals in this case, at least two standard deviations should be allowed. Therefore, if two samples, e.g., at a field site, are to be different on the 95% confidence level, they should differ at least by four standard deviations. With the data summarized in

Table 1, this amounts to about 2‰ for the Agilent GC/qMS instruments, up to 4‰ for the Thermo GC/qMS instruments, and about 0.4‰ for the GC/IRMS instruments (Table 1), depending on the number of replicate measurements. Such ranges would be in line with current guidelines for carbon isotope analysis which recommend as a rule of thumb that samples be 2‰ apart when the total uncertainty of the measurement is 0.5‰.³⁹

In the third case, the data of this interlaboratory comparison allows a rough estimate of the accuracy of the different methods relative to a consensus value. If the IRMS-Isoprime results are taken as the consensus values of the unknown samples,⁴⁰ and if the averages measured by the other instruments are compared to these consensus values, the most extreme difference between each instrument and the consensus value may provide an error estimate of the instrument. Doing so, the following intervals were obtained for the GC/qMS instruments: 0.43‰ (qMS-Agilent-1), 0.60‰ (qMS-Agilent-2), 0.21‰ (qMS-Agilent-3), 0.92‰ (qMS-Thermo-1), 0.50‰ and 0.62‰ (qMS-Thermo-2, with default and modified peak integration settings, respectively), and 0.61‰ and 0.66‰ (qMS-Thermo-3, with default and modified peak integration settings, respectively). For the GC/IRMS instrument, the interval was 0.17‰ (IRMS-Thermo). In most cases, the calculated *z*-scores⁴⁰ for these differences were lower than 2.0 (Table 1), indicating that the specified precision agrees with deviations from the consensus value. Exceptional are IS-15 in qMS-Agilent-2, with a *z*-score of 2.37, and various measurements of qMS-Thermo-2 and qMS-Thermo-3 after changing its peak integration settings. Whereas the >2.0 value by qMS-Agilent-2 is exceptional for this instrument, and may stem from inadvertent sample handling, the values of the two qMS-Thermo instruments indicate a systematic bias in the estimated precision. Thus, although the change in the peak integration setting improved the precision of the qMS-Thermo-2 and qMS-Thermo-3 measurements, the accuracy test indicates that the stated precision underestimated the true uncertainty. Overall, however, deviations in the accuracy tests were in good agreement with the precision of the respective instruments indicating the absence of additional systematic errors.

Finally, we caution that in reality errors may be greater than reported in this study because samples are typically not pure and are not determined in 10-fold replicate. Also, our set of five unknown samples is small, and larger deviations may occur if a greater set of samples is analyzed. Finally, calibration in all laboratories was conducted with the same secondary standards eliminating a possible systematic bias from different standard sets.

CONCLUSIONS

Chlorine isotope methods are at their initial stages of application, and it is therefore crucial to systematically evaluate instrumental behavior and to define proper protocols of analytical and standardization schemes for future routine applications. This study investigated precision and accuracy, as well as different schemes of standardization, for continuous flow GC/IRMS and GC/qMS methods. Different instruments were found to present individual amount dependency trends and variable calibration slopes against the SMOC scale. The different amount dependency trends could be eliminated by standard bracketing when the amplitude of the external standard was adapted to that of the respective sample, consistent with Aeppli et al.³⁰ The different calibration slopes against the SMOC scale, on the other hand, emphasized the need for a careful standardization and calibration scheme in each laboratory and on each measurement day.

In particular, we found that it is mandatory to include a minimum of two compound-specific calibration standards with defined $\delta^{37}\text{Cl}_{\text{SMOC}}$ in any sequence of samples in order to obtain true differences between samples and to convert internal values to the international SMOC scale. In practice, this may be a challenge since for chlorine isotope analysis a universal standard is not as easily obtainable as, e.g., for carbon, where CO_2 can be used for all analyzed compounds.

Our study also gives the first comprehensive comparison of the precision and the total uncertainty associated with the analytical techniques. Our results suggest that isotope values can be confidently assessed to be different, if they differ at least by 0.4‰ in GC/IRMS measurements (either Isoprime or Thermo MAT-253), by 2‰ in most GC/qMS instruments measurements, and up to 4‰ in GC/qMS measurements on one of the Thermo instruments tested in this study.

On the other hand, despite lower precision, GC/qMS applications have considerable advantages over GC/IRMS. First, whereas we are aware of only two GC/IRMS instruments worldwide (München and Waterloo) that are configured to analyze $\delta^{37}\text{Cl}$ in TCE directly, without prior offline separation and conversion to methyl chloride or CsCl , a vast number of laboratories are equipped with GC/qMS instruments. Second, whereas GC/IRMS instruments are limited to analysis of C_2 chlorinated compounds, GC/qMS can be applied for $\delta^{37}\text{Cl}$ analysis in a variety of compounds, as well as in specific fragments of such compounds. This enables the introduction of chlorine isotope analysis for new compounds of interest.

Finally, our study demonstrated good to excellent agreement of $\delta^{37}\text{Cl}$ values measured with GC/IRMS and GC/qMS in different laboratories/instruments if the same external standards were used. This general agreement is very encouraging and lends confidence to both methods. The results of this interlaboratory test may, therefore, serve as a benchmark for future applications of compound-specific chlorine isotope analysis.

ASSOCIATED CONTENT

S Supporting Information. Methods of chlorine isotope measurements, Table S1 listing the TCE products used in this study, Table S2 summarizing $\delta^{37}\text{Cl}$ values of TCE products measured at different laboratories, and Figure S1 showing measured $\delta^{37}\text{Cl}$ in GC/qMS-Darmstadt and GC/qMS-Tübingen depending on the amount on-column using different injection methods. This material is available free of charge via the Internet at <http://pubs.acs.org>.

AUTHOR INFORMATION

Corresponding Author

*Phone: +49(0)89 3187 2565. Fax: +49(0)89 3187 3361. E-mail: martin.elsner@helmholtz-muenchen.de.

Present Addresses

[†]Zuckerberg Institute for Water Research, Department of Environmental Hydrology and Microbiology, Ben-Gurion University of the Negev, Sede Boqer Campus, 84990, Israel.

ACKNOWLEDGMENT

This work was supported by a postdoctoral fellowship of the Minerva Foundation, Max-Planck-Gesellschaft to A.B. and funding by the Helmholtz Initiative and Networking Fund to M.E.

K.E. received financial support by the Landesgraduiertenförderung (LGFG) Baden Württemberg (D) and acknowledges the advice and support of Biao Jin. K.S.-S. acknowledges the technical support of Prof. Christoph Schüth and Dr. Matthias Piepenbrink. This work was also supported by the National Science and Engineering Research Council of Canada (NSERC) funding to O.S.-S. and the Swiss National Science Foundation funding S.J. and D.H.

REFERENCES

- (1) Elsner, M.; McKelvie, J.; Couloume, G. L.; Sherwood Lollar, B. *Environ. Sci. Technol.* **2007**, *41*, 5693–5700.
- (2) Elsner, M. J. *Environ. Monit.* **2010**, *12*, 2005–2031.
- (3) Kuder, T.; Wilson, J. T.; Kaiser, P.; Kolhatkar, R.; Philp, P.; Allen, J. *Environ. Sci. Technol.* **2005**, *39*, 213–220.
- (4) Meyer, A. H.; Penning, H.; Elsner, M. *Environ. Sci. Technol.* **2009**, *43*, 8079–8085.
- (5) Penning, H.; Sorensen, S. R.; Meyer, A. H.; Aamand, J.; Elsner, M. *Environ. Sci. Technol.* **2010**, *44*, 2372–2378.
- (6) Zwank, L.; Berg, M.; Elsner, M.; Schmidt, T. C.; Schwarzenbach, R. P.; Haderlein, S. B. *Environ. Sci. Technol.* **2005**, *39*, 1018–1029.
- (7) Hofstetter, T. B.; Bernasconi, S. M.; Schwarzenbach, R. P. *Environ. Sci. Technol.* **2008**, *42*, 7737–7743.
- (8) Vogt, C.; Cyrus, E.; Herklotz, I.; Herrmann, S.; Bahr, A.; Richnow, H. H.; Fischer, A. *Environ. Sci. Technol.* **2008**, *42*, 7793–7800.
- (9) Schmidt, T. C.; Zwank, L.; Elsner, M.; Berg, M.; Meckenstock, R. U.; Haderlein, S. B. *Anal. Bioanal. Chem.* **2004**, *378*, 283–300.
- (10) Shouakar-Stash, O.; Drimmie, R. J.; Frape, S. K. *J. Contam. Hydrol.* **2003**, *60*, 211–228.
- (11) Holt, B. D.; Sturchio, N. C.; Abrajano, T. A.; Heraty, L. J. *Anal. Chem.* **1997**, *69*, 2727–2733.
- (12) Holmstrand, H.; Andersson, P.; Gustafsson, O. *Anal. Chem.* **2004**, *76*, 2336–2342.
- (13) Beneteau, K. M.; Aravena, R.; Frape, S. K. *Org. Geochem.* **1999**, *30*, 739–753.
- (14) Drenzek, N. J.; Tarr, C. H.; Eglinton, T. I.; Heraty, L. J.; Sturchio, N. C.; Shiner, V. J.; Reddy, C. M. *Org. Geochem.* **2002**, *33*, 437–444.
- (15) Jendrzewski, N.; Eggenkamp, H. G. H.; Coleman, M. L. *Appl. Geochem.* **2001**, *16*, 1021–1031.
- (16) Van Warmerdam, E. M.; Frape, S. K.; Drimmie, R. J.; Flatt, H.; Cherry, J. A. *Appl. Geochem.* **1995**, *10*, 547–552.
- (17) Huang, L.; Sturchio, N. C.; Abrajano, T.; Heraty, L. J.; Holt, B. D. *Org. Geochem.* **1999**, *30*, 777–785.
- (18) Poulson, S. R.; Drever, J. I. *Environ. Sci. Technol.* **1999**, *33*, 3689–3694.
- (19) Abe, Y.; Aravena, R.; Zopfi, J.; Shouakar-Stash, O.; Cox, E.; Roberts, J. D.; Hunkeler, D. *Environ. Sci. Technol.* **2009**, *43*, 101–107.
- (20) Hofstetter, T. B.; Reddy, C. M.; Heraty, L. J.; Berg, M.; Sturchio, N. C. *Environ. Sci. Technol.* **2007**, *41*, 4662–4668.
- (21) Holmstrand, H.; Mandalakis, M.; Zencak, Z.; Andersson, P.; Gustafsson, O. *Chemosphere* **2007**, *69*, 1533–1539.
- (22) Numata, M.; Nakamura, N.; Koshikawa, H.; Terashima, Y. *Environ. Sci. Technol.* **2002**, *36*, 4389–4394.
- (23) Reddy, C. M.; Xu, L.; Drenzek, N. J.; Sturchio, N. C.; Heraty, L. J.; Kimblin, C.; Butler, A. J. *Am. Chem. Soc.* **2002**, *124*, 14526–14527.
- (24) Sakaguchi-Söder, K.; Jäger, J.; Grund, H.; Matthäus, F.; Schüth, C. *Rapid Commun. Mass Spectrom.* **2007**, *21*, 3077–3084.
- (25) Sturchio, N. C.; Clausen, J. L.; Heraty, L. J.; Huang, L.; Holt, B. D.; Abrajano, T. A. *Environ. Sci. Technol.* **1998**, *32*, 3037–3042.
- (26) Shouakar-Stash, O.; Drimmie, R. J.; Zhang, M.; Frape, S. K. *Appl. Geochem.* **2006**, *21*, 766–781.
- (27) Kaufmann, R.; Long, A.; Bentley, H.; Davis, S. *Nature* **1984**, *309*, 338–340.
- (28) Elsner, M.; Hunkeler, D. *Anal. Chem.* **2008**, *80*, 4731–4740.
- (29) Sakaguchi-Söder, K. A New Method for Compound-Specific Stable Chlorine Isotope Analysis: Basics and Application. Ph.D. Thesis, Technische Universität, Darmstadt, Germany, 2010.
- (30) Aeppli, C.; Holmstrand, H.; Andersson, P.; Gustafsson, O. *Anal. Chem.* **2010**, *82*, 420–426.
- (31) Merritt, D. A.; Freeman, K. H.; Ricci, M. P.; Studley, S. A.; Hayes, J. M. *Anal. Chem.* **1995**, *67*, 2461–2473.
- (32) Sherwood Lollar, B.; Hirschorn, S. K.; Chartrand, M. M. G.; Lacrampe-Couloume, G. *Anal. Chem.* **2007**, *79*, 3469–3475.
- (33) Slater, G. F.; Dempster, H.; Sherwood Lollar, B.; Ahad, J. *Environ. Sci. Technol.* **1999**, *33*, 190–194.
- (34) International Standardization Organization. *Accuracy (Trueness and Precision) of Measurement Methods and Results, Part 1: General Principles and Definitions. ISO 5. 5725–1*; Geneva, 1994.
- (35) Brand, W. A.; Coplen, T. B. *J. Anal. Chem.* **2001**, *370*, 358–362.
- (36) Jin, B.; Laskov, C.; Rolle, M.; Haderlein, S. B. *Environ. Sci. Technol.* **2011**, *45*, 5279–5286.
- (37) Brand, W. A. In *Handbook of Stable Isotope Analytical Techniques*; de Groot, P. A., Ed.; Elsevier: Amsterdam, 2004; Vol. I, pp 835–858.
- (38) Schimmelmann, A.; Albertino, A.; Sauer, P. E.; Qi, H.; Molinie, R.; Mesnard, F. *Rapid Commun. Mass Spectrom.* **2009**, *23*, 3513–3521.
- (39) Hunkeler, D.; Meckenstock, R. U.; Sherwood Lollar, B.; Schmidt, T. C.; Wilson, J. T. A *Guide for Assessing Biodegradation and Source Identification of Organic Ground Water Contaminants using Compound Specific Isotope Analysis (CSIA)*; U.S. EPA: OK, 2008.
- (40) International Standardization Organization. *Statistical Methods for Use in Proficiency Testing by Interlaboratory Comparisons; Text in German and English. DIN ISO 13528*; Berlin, 2009.

A2

Appendix A2: Supporting information of Chapter 2

A2.1 MATERIALS AND METHODS

Biodegradation of PCE with *Desulfitobacterium* Strain Viet-1

Biodegradation experiments of PCE were carried out using the microbial strain *Desulfitobacterium* strain VIET-1, which reductively dechlorinates PCE to the final product TCE. It was gratefully provided by Frank Loeffler and his collection of Microorganisms at University of Tennessee and it was cultured according to DSMZ instructions, medium 720, with PCE as the electron acceptor. The growth medium for the experiment was prepared in glass bottles (250 ml), equipped with Mininert valves (Supelco, Bellefonte, Pennsylvania, USA), and filled with 150 ml of medium, leaving a headspace of 40%. The bottles were amended with 10 µl of neat PCE and constantly shaken on a horizontal shaker at 120 rpm for four days. Inoculation was carried out by adding 20 ml of active culture, which was previously grown in a similar medium. To eliminate carry-over of the degradation product (TCE) to the fresh medium, the media with the culture that was used for inoculation was flushed with N₂/CO₂ gas stream (80/20%) for 5 hours prior transferring to the fresh medium. A complete removal of chloroethenes after degassing was controlled by GC-FID measurements. This procedure was followed for three biological replicates. Abiotic control batches were prepared similarly, but without inoculation of the active culture. Sampling was carried out 20 min after inoculation for the initial sample, and at given time points along the degradation. A total sample volume of 7 ml was taken with a glass syringe (Hamilton), which was distributed in portions of 1 ml each into 7 amber vials with an active volume of 1.6 ml. In order to stop biological activity, the vials were spiked with 50 µl of NaOH (1M) and closed with PTFE-lined screw caps. All vials were frozen upside down for subsequent isotope analysis, except one vial, which was used immediately for concentration analysis.

Biodegradation of TCE with *Geobacter lovleyi* Strain SZ

Biodegradation experiments of TCE were carried out using the microbial strain *Geobacter lovleyi* strain SZ, purchased from the German Collection of Microorganisms and Cell Cultures (DSMZ, Germany). This strain reductively dechlorinates TCE to the final product *cis*-DCE. A growth medium was prepared according to DSMZ instructions, medium 732, with the exception that neither hexadecane nor perchloroethylene was added to the medium. The growth medium for the experiment was prepared in glass bottles (250 ml), equipped with Mininert valves (Supelco, Bellefonte, Pennsylvania, USA), and filled with 150 ml of medium,

leaving a headspace of 40%. The bottles were amended with 10 μ l of neat TCE and constantly shaken on a horizontal shaker at 120 rpm for four days. Inoculation was carried out by adding 14 ml of active culture, which was previously grown in a similar medium. To eliminate carry-over of the degradation product (*cis*-DCE) to the fresh medium, the media with the culture that was used for inoculation was flushed with N₂/CO₂ gas stream (80/20%) for 5 hours prior transferring to the fresh medium. A complete removal of chloroethenes after degassing was controlled by GC-FID measurements. This procedure was followed for three biological replicates. Abiotic control batches were prepared similarly, but without inoculation of the active culture. Sampling was carried out 20 min after inoculation for the initial sample, and at given time points along the degradation. A total sample volume of 7 ml was taken with a glass syringe (Hamilton), which was distributed in portions of 1 ml each into 7 amber vials with an active volume of 1.6 ml. In order to stop biological activity, the vials were spiked with 50 μ l of NaOH (1M) and closed with PTFE-lined screw caps. All vials were frozen upside down for subsequent isotope analysis, except one vial, which was used immediately for concentration analysis.

Concentration measurements

PCE, TCE and *cis*-DCE concentrations in the biodegradation experiments were measured by a gas chromatograph equipped with flame ionization detector (GC-FID, Hewlett Packard 5890 Series II) equipped with a 30 m VOCOL column (Supelco, Bellefonte, Pennsylvania, USA) 0.25 mm inner diameter, with a film thickness of 1.5 μ m and operated with nitrogen as carrier gas at 1.6 ml/min. Automated headspace injections of 1 ml from 10 ml headspace vials were carried out using a Pal™ autosampler (CTC Analytics), and an injector temperature on the GC of 200 °C. Calibrations were performed along each measurement using solutions of the chloroethenes with concentrations between 4.0 and 383.9 mg/l. The resulting total relative error in concentrations was estimated as $\pm 10\%$.

Stable Carbon Isotope Analysis

Compound Specific Isotope Analysis (CSIA) for carbon was conducted by injection of headspace samples on a GC-IRMS system (Thermo Fisher Scientific, Waltham, Massachusetts, USA) consisting of a Trace GC with a Pal™ autosampler (CTC Analytics), coupled to a MAT 253 IRMS through a GC/C III combustion interface. The gas chromatograph was equipped with a 30 m VOCOL column (Supelco, Bellefonte, Pennsylvania, USA), 0.25 mm inner diameter, with a film thickness of 1.5 μ m and operated with He carrier gas at 1.4 ml/min. The GC program started at 85 °C (8 min) and increased at

60 °C/min to 205 °C (1 min). Internal standards of PCE, TCE and *cis*-DCE were used along the measurements. The analytical uncertainty 2σ of carbon isotope analysis was $\pm 0.5\%$.

Stable Chlorine Isotope Analysis

Chlorine isotope analysis of TCE was performed according to a method adapted from Shouakar-Stash et al. (2006).²³ PCE, TCE, and *cis*-DCE are transferred from a Trace-GC (Thermo Scientific, Waltham, Massachusetts, USA) to the MAT 253 IRMS through the He carrier stream, where the chloroethenes are ionized and fragmented for isotope ratio measurements. The measurements were conducted at masses $m/z = 94, 96$ for PCE, $m/z = 95, 97$ for TCE, $m/z = 96, 98$ for *cis*-DCE. The gas chromatograph was equipped with a 30 m VOCOL column (Supelco, Bellefonte, Pennsylvania, USA) with 0.25 mm inner diameter, a film thickness of 1.5 μm and operated with a He carrier gas at 1.4 ml/min. The GC program used started at 50 °C (7 min), increasing at 60 °C/min to 70 °C (2.70 min) and at 80 °C/min to 140 °C (0.10 min). External standards were measured daily for calibration of $\delta^{37}\text{Cl}$ values according to Bernstein *et al.*²⁹

Briefly, a reference gas of each target analyte is introduced via a dual inlet system. In order to enable isotope measurements of two chloroethenes in one run, the chloroethene with the shorter retention time was introduced at the beginning of each run from one bellow of the dual inlet, while at the end of each run the chloroethene with the longer retention time was introduced from the other bellow. The conversion to delta values relative to the international reference Standard Mean Ocean Chloride (SMOC) was performed by an external two-point calibration analysing chloroethene-standards as previously characterized in the Department of Earth Sciences, University of Waterloo.²³ Each of these standards was added in triplicates before, during and at the end of each sequence, in order to calibrate the obtained values of the samples with respect to SMOC. The analytical uncertainty 2σ of chlorine isotopic measurements was $\pm 0.2\%$.

A2.2 EQUATIONS

The following considerations are based on the one hand on Rayleigh equation, as it is well established to express enrichment factors ε for a certain element E in a substrate along a certain progress of reaction f according to equation (9) in the manuscript with

$$\delta^h E = \delta^h E_0 + \varepsilon \cdot \ln f \quad (\text{S1})$$

On the other hand, an isotopic mass balance can be performed for any reaction in a closed system. Here, the reactant contains m_S atoms of element E in its structure. $\delta^h E_0$ is the original reactant isotope ratio, whereas $\delta^h E$ is the ratio when reaction has occurred so that only a fraction f of reactant remains. A fraction of $(1-f)$ has then been converted to one or more (up to n) products; m_i is the number of atoms of E inside the structure of product i , $\delta^h E_{P,i}$ is the respective product's isotope value. In the Manuscript, the respective relationship is given with equation (11) with

$$\sum_{i=1}^n m_i \cdot \delta^h E_{P,i} = \frac{m_S \cdot \delta^h E_0 - m_S \cdot f \cdot \delta^h E}{(1-f)} \quad (\text{S2})$$

Dechlorination reactions with PCE

In the case of PCE, molecular positions are chemically equivalent so that the same chlorine atoms may potentially end up in TCE or Cl^- . Isotopes then partition according to the kinetic isotope effects associated with the formation of either product, $\alpha_i = 1/\text{KIE}_i$. As a consequence, in both cases their isotope ratios relate according to

$$\frac{R_{P_1}}{R_{P_2}} = \frac{\alpha_1}{\alpha_2} \quad (\text{S3})$$

This can be expressed in the delta notation as

$$\frac{\delta^{37}\text{Cl}_{P_1} + 1}{\delta^{37}\text{Cl}_{P_2} + 1} = \frac{\alpha_1}{\alpha_2} = \alpha_{\text{Diff}} \quad (\text{S4})$$

with α_{Diff} expressing the ratio between the primary isotope effect (in the formation of Cl^-) and the average secondary isotope effects (in the three molecular positions which become TCE).

This equation can be rearranged and simplified according to

$$\delta^{37}\text{Cl}_{P_1} + 1 = \alpha_{\text{Diff}} (\delta^{37}\text{Cl}_{P_2} + 1) \quad \rightarrow \quad \delta^{37}\text{Cl}_{P_1} - \underbrace{\alpha_{\text{Diff}}}_{\approx 1} \cdot \delta^{37}\text{Cl}_{P_2} = \alpha_{\text{Diff}} - 1 \quad (\text{S5})$$

$$\rightarrow \quad \delta^{37}\text{Cl}_{P_1} - \delta^{37}\text{Cl}_{P_2} = \alpha_{\text{Diff}} - 1 = \varepsilon_{\text{Diff}} \quad (\text{S6})$$

This means the difference between primary and secondary isotope effects ε_{Diff} is directly obtained from product isotope values, because chlorine isotope ratios of Cl^- and TCE are always by ε_{Diff} apart.

This can be combined with the isotopic mass balance for the case of PCE degradation to TCE according to

$$\rightarrow \delta^{37}Cl_{0,PCE} = f \cdot \delta^{37}Cl_{PCE} + \frac{1}{4}(1-f)\delta^{37}Cl_{Cl^-} + \frac{3}{4}(1-f) \cdot \delta^{37}Cl_{TCE} \quad (S7)$$

Equation (17) in the manuscript is here expressed in (S8) with

$$\begin{aligned} \delta^{37}Cl_{TCE} - \delta^{37}Cl_{Cl^-} &= \varepsilon_{Diff} \\ \rightarrow \delta^{37}Cl_{TCE} &= \varepsilon_{Diff} + \delta^{37}Cl_{Cl^-} \quad \text{and} \quad \delta^{37}Cl_{Cl^-} = \delta^{37}Cl_{TCE} - \varepsilon_{Diff} \end{aligned} \quad (S8)$$

When (S7) and (S8) is combined, we can resolve the isotope signatures individually for chloride according to

$$\delta^{37}Cl_{0,PCE} = f \cdot \delta^{37}Cl_{PCE} + \frac{1}{4}(1-f)\delta^{37}Cl_{Cl^-} + \frac{3}{4}(1-f) \cdot \varepsilon_{Diff} + \frac{3}{4}(1-f) \cdot \delta^{37}Cl_{Cl^-}$$

Together with the Rayleigh enrichment trend for PCE, the isotope trends of the formed chloride can be expressed with

$$\rightarrow \delta^{37}Cl_{Cl^-} = \underbrace{\delta^{37}Cl_{0,PCE} - \frac{3}{4}\varepsilon_{Diff}}_{\text{constant: } K_{Cl^-}} - \varepsilon_{chlorine} \cdot \frac{f \cdot \ln f}{(1-f)} \quad (S9)$$

A similar procedure can be followed in order to resolve equations (S7) and (S8) towards TCE, and we obtain an expression to model the enrichment trend of TCE with

$$\rightarrow \delta^{37}Cl_{TCE} = \underbrace{\delta^{37}Cl_{0,PCE} + \frac{1}{4}\varepsilon_{Diff}}_{\text{constant: } K_{TCE}} - \varepsilon_{chlorine} \cdot \frac{f \cdot \ln f}{(1-f)} \quad (S10)$$

The equations to equations (S9) and (S10) are equal to equations (18) and (19) from the manuscript, which were used for mathematical modeling of product isotope enrichment of PCE.

Dechlorination reactions with TCE

In the case of TCE, molecular positions are chemically distinguishable, and a structural preference is present in the α -position according to the selective formation of *cis*-DCE so that the same chlorine atoms may potentially end up in TCE or Cl^- . It is, then, of interest to which percentage of $Cl_{\alpha,E}$ and $Cl_{\alpha,Z}$ react to form the cleaved chloride. A factor x can be introduced to express this as

x = percentage that reacts from $Cl_{\alpha,E}$ to $Cl_{\alpha,2}$

$(1-x)$ = percentage that reacts from $Cl_{\alpha,Z}$ to $Cl_{\alpha,2}$

With an $x=1$ the reaction would follow a position-specific cleavage, while any $1 > x > 0$ would reflect a case where two positions are involved. For each of the three chlorinated positions the mass balance can be raised individually in an extension of the equations describing the isotopic mass balance

$$\delta^{37}Cl_{0,\alpha,E} = f \cdot \delta^{37}Cl_{\alpha,E} + x \cdot (1-f) \cdot \delta^{37}Cl_{Cl_{\alpha,2}}^{from\alpha,E} + (1-x)(1-f) \cdot \delta^{37}Cl_{cDCE,\alpha,1}^{from\alpha,E} \quad (S11)$$

$$\delta^{37}Cl_{0,\alpha,Z} = f \cdot \delta^{37}Cl_{\alpha,Z} + (1-x) \cdot (1-f) \cdot \delta^{37}Cl_{Cl_{\alpha,2}}^{from\alpha,Z} + x \cdot (1-f) \cdot \delta^{37}Cl_{cDCE,\alpha,1}^{from\alpha,Z} \quad (S12)$$

$$\delta^{37}Cl_{0,\beta} = f \cdot \delta^{37}Cl_{\beta} + (1-f) \cdot \delta^{37}Cl_{cDCE,\beta} \quad (S13)$$

For the two individual reacting positions, the difference in their isotope signatures reflect the difference of position specific enrichment factors for the case of a primary isotope effect with the formation of chloride, or a secondary isotope effect with the formation of cis-DCE. This difference of enrichment factors have to be treated separately for $Cl_{\alpha,E}$ and $Cl_{\alpha,Z}$, according to

$$\delta^{37}Cl_{Cl_{\alpha,2}}^{from\alpha,E} - \delta^{37}Cl_{cDCE,\alpha,1}^{from\alpha,E} = \varepsilon_{Diff,\alpha,E} \quad (S14)$$

$$\delta^{37}Cl_{Cl_{\alpha,2}}^{from\alpha,Z} - \delta^{37}Cl_{cDCE,\alpha,1}^{from\alpha,Z} = \varepsilon_{Diff,\alpha,Z} \quad (S15)$$

These differences in fractionation factors can be included in the position specific mass balance to give

$$\delta^{37}Cl_{Cl_{\alpha,2}}^{from\alpha,E} = \delta^{37}Cl_{0,\alpha,E} + (1-x) \cdot \varepsilon_{Diff,\alpha,E} - \varepsilon_{\alpha,E} \frac{f \ln f}{(1-f)} \quad (S16)$$

$$\delta^{37}Cl_{Cl_{\alpha,2}}^{from\alpha,Z} = \delta^{37}Cl_{0,\alpha,Z} + x \cdot \varepsilon_{Diff,\alpha,Z} - \varepsilon_{\alpha,Z} \frac{f \ln f}{(1-f)} \quad (S17)$$

$$\delta^{37}Cl_{cDCE,\alpha,1}^{from\alpha,E} = \delta^{37}Cl_{0,\alpha,E} - x \cdot \varepsilon_{Diff,\alpha,E} - \varepsilon_{\alpha,E} \frac{f \ln f}{(1-f)} \quad (S18)$$

$$\delta^{37}Cl_{cDCE,\alpha,1}^{from\alpha,Z} = \delta^{37}Cl_{0,\alpha,Z} - (1-x) \cdot \varepsilon_{Diff,\alpha,Z} - \varepsilon_{\alpha,Z} \frac{f \ln f}{(1-f)} \quad (S19)$$

$$\delta^{37}Cl_{cDCE,\beta} = \delta^{37}Cl_{0,\beta} - \varepsilon_{\beta} \frac{f \ln f}{(1-f)} \quad (S20)$$

The isotopic mass balance can now be set up for the cleaved chloride according to

$$\begin{aligned} \delta^{37}Cl_{Cl_{\alpha,2}^-} &= \left(x \cdot \delta^{37}Cl_{Cl_{\alpha,2}^-}^{from\alpha,E} + (1-x) \cdot \delta^{37}Cl_{Cl_{\alpha,2}^-}^{from\alpha,Z} \right) \quad (S21) \\ &= \left(x \cdot \delta^{37}Cl_{0,\alpha,E} + x(1-x) \cdot \varepsilon_{Diff,\alpha,E} - x\varepsilon_{\alpha,E} \frac{f \ln f}{(1-f)} + (1-x)\delta^{37}Cl_{0,\alpha,Z} + (1-x) \cdot x \cdot \varepsilon_{Diff,\alpha,Z} - (1-x) \cdot \varepsilon_{\alpha,Z} \frac{f \ln f}{(1-f)} \right) \\ &= \underbrace{\left(x \cdot \delta^{37}Cl_{0,\alpha,E} + (1-x)\delta^{37}Cl_{0,\alpha,Z} + x(1-x) \cdot [\varepsilon_{Diff,\alpha,E} + \varepsilon_{Diff,\alpha,Z}] \right)}_{constant: K_{Cl^-}} - \underbrace{\left[x \cdot (\varepsilon_{\alpha,E} - \varepsilon_{\alpha,Z}) + \varepsilon_{\alpha,Z} \right]}_{\varepsilon_{TCE \rightarrow chloride}} \frac{f \ln f}{(1-f)} \end{aligned}$$

The enrichment factor can be extracted here in order to reflect equation (22) from the manuscript

$$\varepsilon_{TCE \rightarrow chloride} = \left(x \cdot \varepsilon_{\alpha,E} + (1-x) \cdot \varepsilon_{\alpha,Z} \right) \quad (S22)$$

In the interpretation of our experiments, isotope data of chloride was therefore modeled with

$$\delta^{37}Cl_{Cl^-} = K_{Cl^-} - \varepsilon_{TCE \rightarrow chloride} \frac{f \ln f}{(1-f)} \quad (S23)$$

Also in the case of *cis*-DCE, an isotopic mass balance could be set up according to

$$\begin{aligned} \delta^{37}Cl_{TCE \rightarrow cis-DCE} &= \frac{1}{2} \delta^{37}Cl_{\beta} + \frac{1}{2} \left[(1-x) \cdot \delta^{37}Cl_{cDCE,\alpha,1}^{from\alpha,E} + x \cdot \delta^{37}Cl_{cDCE,\alpha,1}^{from\alpha,Z} \right] \quad (S24) \\ &= \frac{1}{2} \left(\delta^{37}Cl_{0,\beta} - \varepsilon_{\beta} \frac{f \ln f}{(1-f)} \right) \\ &+ \frac{1}{2} \left[(1-x) \left(\delta^{37}Cl_{0,\alpha,E} - x \cdot \varepsilon_{Diff,\alpha,E} - \varepsilon_{\alpha,E} \frac{f \ln f}{(1-f)} \right) + x \left(\delta^{37}Cl_{0,\alpha,Z} - (1-x) \cdot \varepsilon_{Diff,\alpha,Z} - \varepsilon_{\alpha,Z} \frac{f \ln f}{(1-f)} \right) \right] \\ &= \frac{1}{2} \left(\delta^{37}Cl_{0,\beta} + \frac{(1-x) \cdot \delta^{37}Cl_{0,\alpha,E} + x \cdot \delta^{37}Cl_{0,\alpha,Z}}{2} \right) + \frac{1}{2} x \cdot (1-x) [\varepsilon_{Diff,\alpha,E} - \varepsilon_{Diff,\alpha,Z}] - \frac{1}{2} [\varepsilon_{\beta} + x(\varepsilon_{\alpha,Z} - \varepsilon_{\alpha,E}) + \varepsilon_{\alpha,E}] \frac{f \ln f}{(1-f)} \\ &\quad \underbrace{\hspace{10em}}_{constant: K_{cDCE}} \quad \underbrace{\hspace{10em}}_{\varepsilon_{TCE \rightarrow cis-DCE}} \end{aligned}$$

The enrichment factor can be extracted here in order to reflect equation (23) from the manuscript

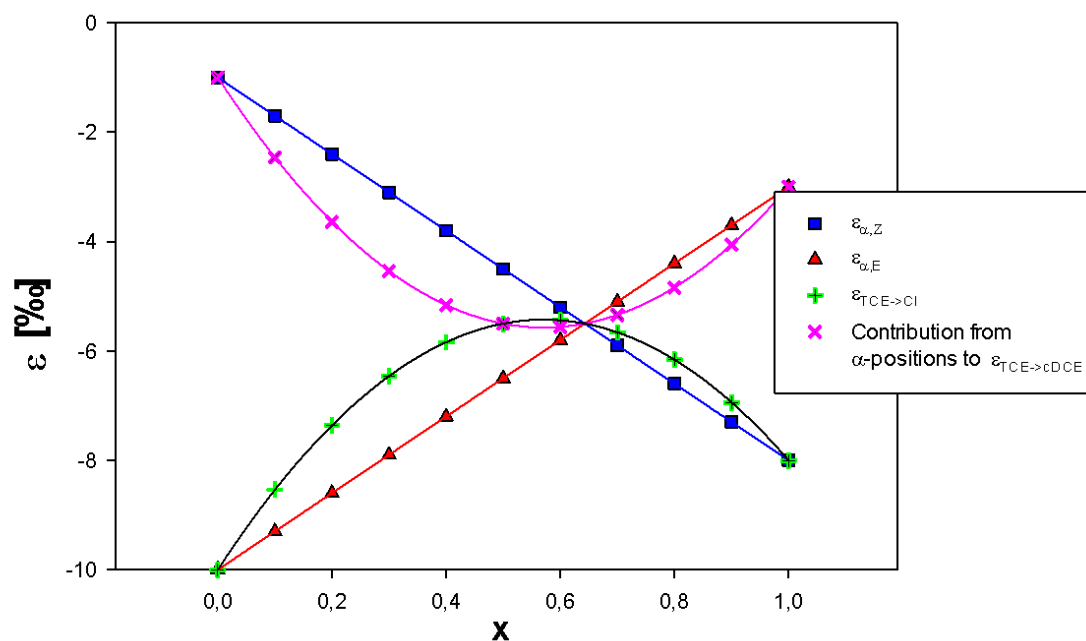
$$\varepsilon_{TCE \rightarrow cis-DCE} = \frac{1}{2} [\varepsilon_{\beta} + (x \cdot (\varepsilon_{\alpha,Z} - \varepsilon_{\alpha,E}) + \varepsilon_{\alpha,E})] = \frac{1}{2} [\varepsilon_{\beta} + (x \cdot \varepsilon_{\alpha,Z} + (1-x)\varepsilon_{\alpha,E})] \quad (S25)$$

Modeling of the obtained isotope data of *cis*-DCE from our experiments was therefore possible with

$$\delta^{37}Cl_{cDCE} = K_{cDCE} - \varepsilon_{TCE \rightarrow cis-DCE} \frac{f \ln f}{(1-f)} \quad (S26)$$

A2.3 VISUALISATION OF FIGURE 4 WITH DIFFERENT CONTRIBUTIONS OF PRIMARY AND SECONDARY ISOTOPE EFFECTS

A different numerical scenario is visualized here, in order to show how different contributions in the α -positions depend on x , by accounting for different primary and secondary chlorine isotope effects for the individual positions. The exemplary numeric values here were $\epsilon_{\alpha,E,primary} = -10\text{‰}$; $\epsilon_{\alpha,E,secondary} = -3\text{‰}$; $\epsilon_{\alpha,Z,primary} = -8\text{‰}$; $\epsilon_{\alpha,Z,secondary} = -1\text{‰}$. The representation shows a similar qualitative trend, where (i) ϵ_{α} is stronger in the position from which more chloride is formed, and (ii) in addition, more atoms of this position are passed on to chloride so that product curve of chloride more strongly reflects this higher enrichment trend. The opposite trend can be observed in the product curve of *cis*-DCE.



A3

Appendix A3: Supporting information of Chapter 3

Individual data from experimental replicates

Concentrations: Concentration data over time for trichloroethene (TCE) degradation in experimental replicates (crosses) and controls (diamonds) at given time points.

Rayleigh plots: Evaluation of enrichment factors ϵ_{Cl} and ϵ_{C} by regression of $\ln [(\delta^{13}\text{C}+1)/(\delta^{13}\text{C}_0+1)]$ versus $\ln(\text{conc.}/\text{conc.}_0)$ data (Rayleigh plots) for each individual experimental replicate. Respective error ranges are smaller than the displayed symbols. $\delta^{13}\text{C}$ are carbon isotope ratios, conc. are concentrations, the subscript “0” indicates values at the beginning of the reaction and analogous regressions apply for chlorine. Note that the expression

$$\ln [(\delta^{13}\text{C}+1)/(\delta^{13}\text{C}_0+1)] = \epsilon_{\text{C}} \cdot \ln(\text{conc.}/\text{conc.}_0) = \epsilon_{\text{C}} \cdot \ln(f)$$

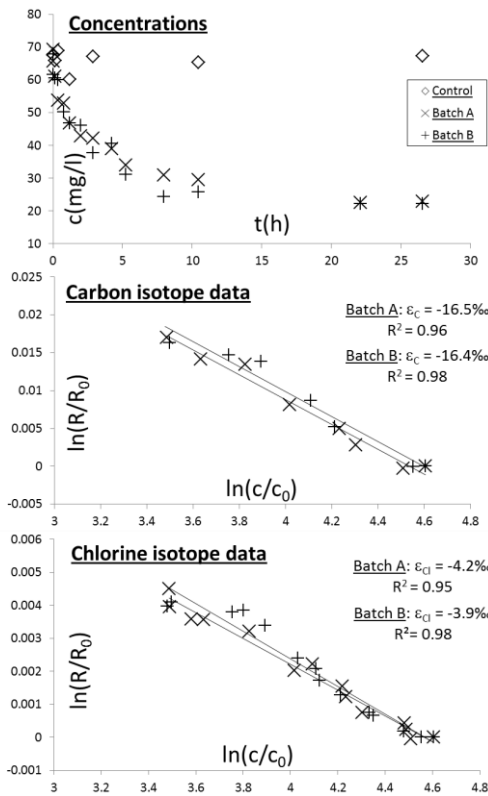
is analogous to the expression

$$\ln (\delta^{13}\text{C}+1) = \epsilon_{\text{C}} \cdot \ln(f) + \ln(\delta^{13}\text{C}_0+1)$$

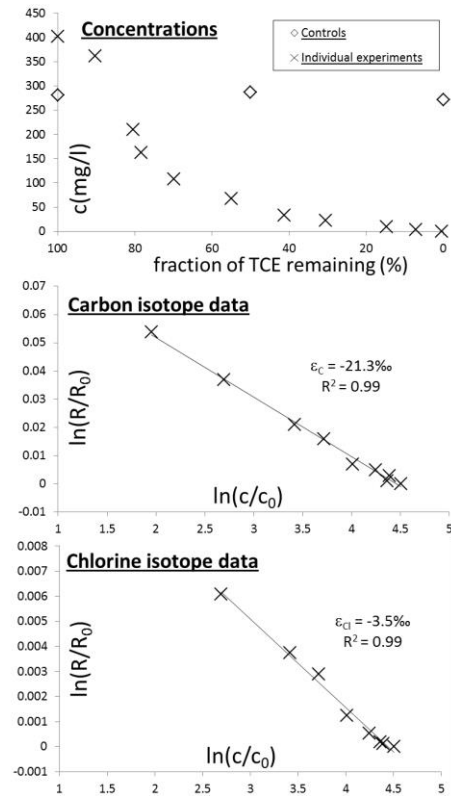
for which equation (1) of the manuscript is an approximation with $\ln (\delta^{13}\text{C}+1) \approx \delta^{13}\text{C}$:

$$\delta^{13}\text{C} = \epsilon_{\text{C}} \cdot \ln(f) + \delta^{13}\text{C}_0$$

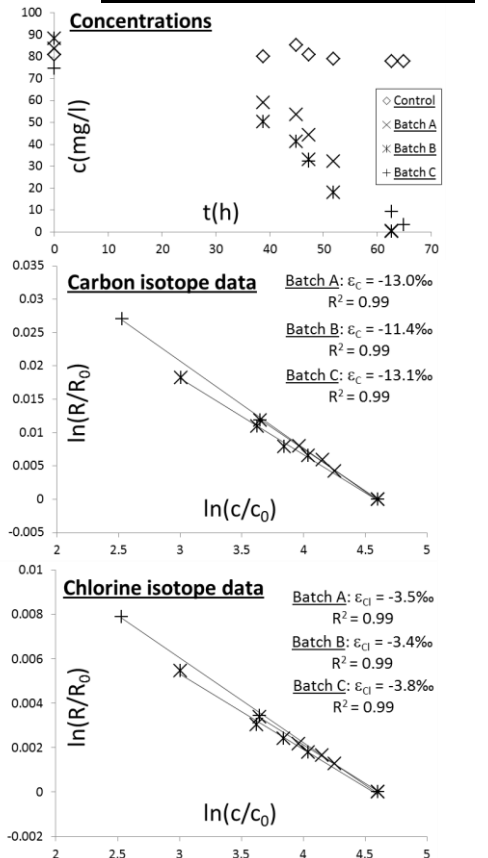
Cyanocobalamin:



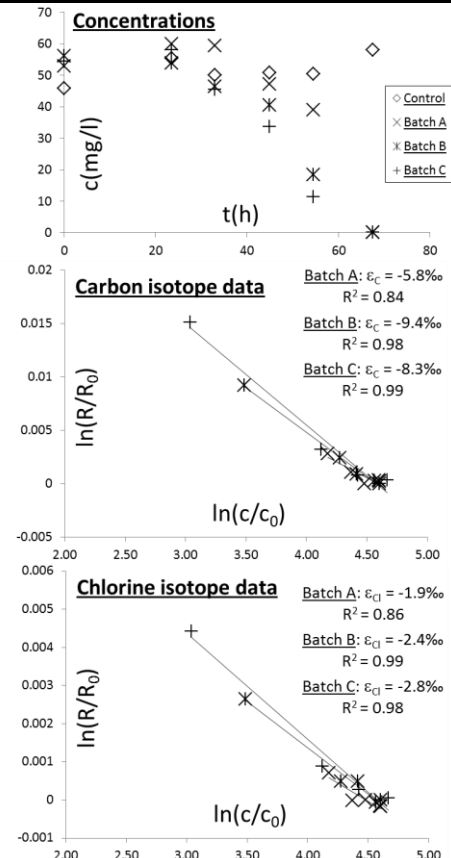
Cobaloxime:



***Geobacter lovleyi* strain SZ:**



***Desulfitobacter hafniense* strain Y51:**



A4

Appendix A4: Supporting information of Chapter 4

Considering TCE, cis-DCE and VC reduction kinetics by cast ZVI pseudo-first order reactions (Arnold and Roberts, 2000), a k_{obs} was estimated for each experiment, and, according to this value, half lives were calculated. Data from TCE, cis-DCE and VC Dual Element experiments and from TCE and cis-DCE preliminary experiments are shown in Table S1. Moreover, it shows reported K_{obs} values of TCE and cis-DCE degradation by ZVI from previous studies (Dayan et al., 1999 and Slater et al., 2002) obtained for cast and electrolytic iron with different specific surface area, different treatment conditions and different ratios iron/solution. Degradation rates are influenced by the iron specific surface area, therefore, surface normalized rate constant (K_{SA} , $K_{SA} = (k_{obs}/a_s \cdot \rho_m)$, where a_s is the specific surface area of ZVI (m^2/g) and ρ_m is the mass concentration of ZVI ($g \cdot L^{-1}$)), is used for comparisons between different studies (Johnson et al. 1996).

TABLE S.1. Summary of observed pseudo first order rate constants (K_{obs}) for dechlorination experiments of TCE, cis-DCE and VC experiments^a, including literature data by different ZVI types and surface treatments.

	Substrate	Concentration (μM)	Iron type	Surface treatment	a_s^c (m^2/g)	ρ_m^d (g/L)	K_{obs} (d^{-1})	95% CI ^b	R^2	K_{obs} (d^{-1}) Combined exp.	95% CI ^b	K_{SA}^e ($h^{-1} \cdot m^{-2} \cdot L$)	95% CI ^b	HalfLife (d)
TCE Dual Element experiment	TCE	441	Cast	Acid cleaned	0.70	200	0.28	± 0.015	0.98	0.24	± 0.018	1.7E-03	$\pm 1.3E-04$	2.5
		503	Cast	Acid cleaned	0.70	200	0.21	± 0.011	0.98					3.3
TCE Preliminar Experiment	TCE	50	Cast	Acid cleaned	0.70	100	0.15	± 0.051	0.94	0.15	± 0.044	2.1E-03	$\pm 6.2E-04$	4.5
		50	Cast	Acid cleaned	0.70	100	0.15	± 0.060	0.91					4.6
cis-DCE Dual Element experiment	cis-DCE	787	Cast	Acid cleaned	0.70	200	0.013	± 0.001	0.99	0.01	± 0.001	7.1E-05	$\pm 8.8E-06$	51.7
		852	Cast	Acid cleaned	0.70	200	0.012	± 0.001	0.99					57.8
cis-DCE Preliminar Experiment	cis-DCE	186	Cast	Acid cleaned	0.70	100	0.25	± 0.043	0.97	0.28	± 0.028	4.0E-03	$\pm 3.4E-04$	2.7
		186	Cast	Acid cleaned	0.70	100	0.31	± 0.034	0.98					2.2
VC Dual Element experiment	VC	185	Cast	Acid cleaned	0.70	200	0.009	± 0.005	0.64	0.007	± 0.003	5.0E-05	$\pm 2.1E-05$	80.6
		185	Cast	Acid cleaned	0.70	200	0.003	± 0.004	0.42					195.3
Slater et al., 2002	TCE	152	Cast	Autoclaved	-	100	0.09	-	0.94	-	-	-	-	7.6
	TCE	152	Cast	Autoclaved	-	50	0.07	-	0.86	-	-	-	-	10.3
	TCE	152	Cast	Autoclaved	-	25	0.05	-	0.98	-	-	-	-	13.8
	TCE	152	Cast	Acid cleaned	0.38	100	0.22	-	0.96	-	5.8E-03	-	-	3.2
	TCE	152	Cast	Autoclaved	0.35	100	0.03	-	0.96	-	8.2E-04	-	-	24.1
	TCE	152	Electrolytic 1	Acid cleaned	0.06	250	2.88	-	0.82	-	2.0E-01	-	-	0.2
	TCE	152	Electrolytic 1	Autoclaved	0.24	250	10.80	-	0.99	-	1.8E-01	-	-	0.1
	TCE	152	Electrolytic 2	Acid cleaned	-	250	2.64	-	0.95	-	-	-	-	0.3
TCE	152	Electrolytic 2	Autoclaved	-	250	0.07	-	0.99	-	-	-	-	10.3	
Dayan et al., 1999	TCE	91	Electrolytic	Acid cleaned	4.17	80	0.21	-	-	-	6.2E-04	-	-	3.4
	cis-DCE	784	Electrolytic	Acid cleaned	4.17	80	0.13	-	-	-	1.3E-05	-	-	5.45

^aNote that duplicates are listed separately so that each entry represents one experimental batch. ^b95% confidence interval. ^c a_s : specific surface area. ^d ρ_m : mass concentration of ZVI in solution. ^e K_{SA} : surface normalized rate constant

